

Jeans mass-radius relation of self-gravitating Bose-Einstein condensates and typical parameters of the dark matter particle

Pierre-Henri Chavanis

Laboratoire de Physique Théorique, Université de Toulouse, CNRS, UPS, Toulouse, France



(Received 2 November 2020; accepted 11 May 2021; published 30 June 2021)

We study the Jeans mass-radius relation of Bose-Einstein condensate dark matter in Newtonian gravity. We show at a general level that it is similar to the core mass-radius relation of Bose-Einstein condensate dark matter halos [P. H. Chavanis, *Phys. Rev. D* **84**, 043531 (2011)]. Bosons with a repulsive self-interaction generically evolve from the Thomas-Fermi regime to the noninteracting regime as the Universe expands. In the Thomas-Fermi regime, the Jeans radius remains approximately constant while the Jeans mass decreases. In the noninteracting regime, the Jeans radius increases while the Jeans mass decreases. Bosons with an attractive self-interaction generically evolve from the nongravitational regime to the noninteracting regime as the Universe expands. In the nongravitational regime, the Jeans radius and the Jeans mass increase. In the noninteracting regime, the Jeans radius increases while the Jeans mass decreases. The transition occurs at a maximum Jeans mass which is similar to the maximum core mass of Bose-Einstein condensate dark matter halos with an attractive self-interaction. We use the core mass-radius relation of dark matter halos and the observational evidence of a “minimum halo” (with typical radius $R \sim 1$ kpc and typical mass $M \sim 10^8 M_\odot$) to constrain the mass m and the scattering length a_s of the dark matter particle. For noninteracting bosons, m is of the order of 2.92×10^{-22} eV/ c^2 . The mass of bosons with an attractive self-interaction can be only slightly smaller (2.19×10^{-22} eV/ c^2 $< m < 2.92 \times 10^{-22}$ eV/ c^2 and -1.11×10^{-62} fm $\leq a_s \leq 0$); otherwise, the minimum halo would be unstable. Constraints from particle physics and cosmology imply $m = 2.92 \times 10^{-22}$ eV/ c^2 and $a_s = -3.18 \times 10^{-68}$ fm for ultralight axions, and it is then found that attractive self-interactions can be neglected in both the linear and the nonlinear regimes of structure formation. The mass of bosons with a repulsive self-interaction can be larger by 18 orders of magnitude (2.92×10^{-22} eV/ c^2 $< m < 1.10 \times 10^{-3}$ eV/ c^2 and $0 \leq a_s \leq 4.41 \times 10^{-6}$ fm). The maximum allowed mass ($m = 1.10 \times 10^{-3}$ eV/ c^2 and $a_s = 4.41 \times 10^{-6}$ fm) is determined by the Bullet Cluster constraint while the transition between the noninteracting limit and the Thomas-Fermi limit corresponds to $m = 2.92 \times 10^{-22}$ eV/ c^2 and $a_s = 8.13 \times 10^{-62}$ fm. For each of these models, we calculate the Jeans length and the Jeans mass at the epoch of radiation-matter equality and at the present epoch.

DOI: [10.1103/PhysRevD.103.123551](https://doi.org/10.1103/PhysRevD.103.123551)

I. INTRODUCTION

Even after 100 years of research, the nature of dark matter (DM) is still elusive. The standard cold dark matter (CDM) model, in which DM is represented by a classical pressureless fluid at zero temperature ($T = 0$) or by a collisionless N -body system of classical particles, works extremely well at large (cosmological) scales and can account for precise measurements of the cosmic microwave background (CMB) from WMAP [1] and Planck missions [2,3]. However, in addition to the lack of evidence for any CDM particle such as a weakly interacting massive particle (WIMP) with a mass in the GeV–TeV range, the CDM model faces serious problems at small (galactic) scales that are known as the “core-cusp” problem [4], the “missing satellites” problem [5–7], and the “too big to fail” problem

[8]. This “small-scale crisis of CDM” [9] is somehow related to the assumption that DM is pressureless, implying that gravitational collapse takes place at all scales. A possibility to solve these problems is to consider self-interacting dark matter (SIDM) [10], warm dark matter (WDM) [11], or the feedback of baryons that can transform cusps into cores [12–14]. Another promising possibility to solve the CDM crisis is to take into account the quantum (or wave) nature of the DM particle. Indeed, in quantum mechanics, an effective pressure is present even at $T = 0$. This quantum pressure may balance the gravitational attraction at small scales and solve the CDM crisis.

In this paper, we shall consider the possibility that the DM particle is a boson, e.g., an ultralight axion

(ULA) [15].¹ At $T = 0$, bosons form Bose-Einstein condensates (BECs), and they are described by a single wave function $\psi(\mathbf{r}, t)$ called the condensate wave function. They can therefore be interpreted as a scalar field (SF). The bosons may be noninteracting or may have a repulsive or an attractive self-interaction (for example, the QCD axion has an attractive self-interaction). On astrophysical scales, one must generally take into account gravitational interactions between the bosons. The evolution of the wave function of self-gravitating BECs is then governed by the Schrödinger-Poisson equations when the bosons are noninteracting or by the Gross-Pitaevskii-Poisson (GPP) equations when the bosons are self-interacting. BECDM halos can thus be viewed as gigantic bosonic atoms where the bosonic particles are condensed in a single macroscopic quantum state. The wave properties of the SF are negligible at large (cosmological) scales where the SF behaves as CDM, but they become important at small (galactic) scales where they can prevent gravitational collapse, providing halo cores and suppressing small-scale structures. This model has been given several names such as wave DM, fuzzy dark matter (FDM), BECDM, ψ DM, or SFDM [75–190] (see the Introduction of [107] and Ref. [191] for an early history of this model and Refs. [15,192–196] for reviews). Here, we shall use the name BECDM. In the BECDM model, gravitational collapse is prevented by the quantum pressure arising from the Heisenberg uncertainty principle or from the scattering of the bosons (when the self-interaction is repulsive).² Therefore, quantum mechanics (or a repulsive self-interaction) may solve the small-scale problems of the CDM model mentioned above.

It is usually considered that large-scale structures such as galaxies or dark matter halos form in a homogeneous universe by Jeans instability [237]. For a cold classical gas, the Jeans length vanishes or is extremely small ($\lambda_J \simeq 0$), implying that structures can form at all scales. This is not what we observe and this leads to the CDM crisis. By contrast, when quantum mechanics (or a repulsive self-interaction) is taken into account, the Jeans length is nonzero, implying the absence of structures below a minimum scale in agreement with the observations. The Jeans instability of a self-gravitating BEC with repulsive or attractive self-interaction was first considered by Khlopov

et al. [76] and Bianchi *et al.* [79] in a general relativistic framework based on the Klein-Gordon-Einstein (KGE) equations. The Jeans instability of a noninteracting self-gravitating BEC in Newtonian gravity described by the Schrödinger-Poisson equations was studied by Hu *et al.* [87] and Sikivie and Yang [102]. Finally, the Jeans instability of a Newtonian self-gravitating BEC with repulsive or attractive self-interactions described by the GPP equations was studied by Chavanis [107]. These results were extended in general relativity by Suárez and Chavanis [153] going beyond some of the approximations made by Khlopov *et al.* [76] (see footnote 7 of [153]). More recently, Harko [180] considered the Jeans instability of rotating Newtonian BECs in the Thomas-Fermi (TF) limit (previous results are recovered when $\Omega = 0$). In these different studies, the authors determined the Jeans length and the Jeans mass of the BECs and used them to obtain an estimate of the minimum size and minimum mass of BECDM halos.³ We refer to [190] for a review about the Jeans instability of nonrelativistic self-gravitating BECs.

The Jeans instability study is valid only in the linear regime of structure formation. It describes the initiation of the large-scale structures of the Universe. The Jeans instability leads to a growth of the perturbations and the formation of condensations (clumps). When the density contrast reaches a sufficiently large value, the condensations experience a free fall, followed by a complicated process of gravitational cooling [267] and violent relaxation [268]. They can also undergo merging and accretion. This corresponds to the nonlinear regime of structure formation leading to the DM halos that we observe today. BECDM halos result from the balance between the gravitational attraction and the quantum pressure due to the Heisenberg principle and the self-interaction of the bosons. Observations reveal that, contrary to the prediction of the CDM model, there are no halos with a mass smaller than $M \sim 10^8 M_\odot$ and with a size smaller than $R \sim 1$ kpc. These ultracompact DM halos correspond typically to dwarf spheroidal galaxies (dSphs) like Fornax. To be specific, we shall assume that Fornax is the smallest halo observed in the Universe. In the BECDM model, this “minimum halo” is interpreted as the ground state of the self-gravitating BEC at $T = 0$. Bigger halos have a core-halo structure with a quantum core (ground state)

¹Some authors have considered the case where the DM particle is a fermion such as a massive neutrino [16–74]. In this model, gravitational collapse is prevented by the quantum pressure arising from the Pauli exclusion principle.

²A repulsive self-interaction ($a_s > 0$) stabilizes the quantum core. By contrast, an attractive self-interaction (as for the axion) destabilizes the quantum core above a maximum mass $M_{\max} = 1.012\hbar/\sqrt{Gm|a_s|}$ first identified in [107] (see Refs. [107,108,145,156,163,179,181,189,197–227] for recent works on axion stars [228–230] and Ref. [231] for a review). This maximum mass has a nonrelativistic origin. It is physically different from the maximum mass of fermion stars [232] and boson stars [233–236] that is due to general relativity.

³These studies were performed in a static Universe. The Jeans instability of an infinite homogeneous self-gravitating BEC in an expanding universe has been studied by Bianchi *et al.* [79], Suárez and Matos [113], and Suárez and Chavanis [133] in general relativity and by Sikivie and Yang [102] and Chavanis [114] in Newtonian gravity. These studies are valid for a complex SF describing the wave function of a BEC. They rely on a hydrodynamical representation of the wave equation. The Jeans instability of a real SF has been studied by numerous authors in Refs. [15,99,101,117,141,238–266].

surrounded by an approximately isothermal atmosphere which results from the quantum interferences of the excited states. This core-halo structure is observed in numerical simulations of BECDM [125,126,142,151,154,155,178,185]. The quantum core may solve the small-scale problems of the CDM model such as the cusp problem and the missing satellite problem. The approximately isothermal atmosphere is consistent with the classical Navarro-Frenk-White (NFW) profile and accounts for the flat rotation curves of the galaxies at large distances. The mass-radius relation of BECDM halos at $T = 0$ (ground state) representing the minimum halo or the quantum core of larger halos has been determined in Refs. [107,108] for bosons with vanishing, repulsive, or attractive self-interactions. It can be obtained either numerically [108] by solving the GPP equations or analytically [107] by using a Gaussian ansatz for the wave function.⁴ The quantum core mass–halo mass relation $M_c(M_h)$ was first obtained by Shive *et al.* [126] in the case of noninteracting bosons from direct numerical simulations and heuristic arguments. This relation was later derived in Refs. [169,179,181] from an effective thermodynamic approach by maximizing the Lynden-Bell [268] entropy at fixed mass and energy. It was also extended in these papers to the case of self-interacting bosons (with a repulsive or an attractive self-interaction) and to the case of fermions.

It was noticed in Ref. [107] that the Jeans mass–radius relation obtained from the dispersion relation of self-gravitating homogeneous BECs is similar to the core mass–radius relation of BECDM halos obtained by solving the equation of quantum hydrostatic equilibrium with a Gaussian ansatz. This agreement is surprising because the two relations apply to very different regimes of structure formation: linear versus nonlinear. It results, however, essentially from dimensional analysis. The aim of the present paper is to further develop this analogy and study its consequences. In Sec. II, we recall the basic equations describing self-gravitating BECs. Using the Madelung [269] transformation, we write the GPP equations in the form of hydrodynamic equations. We then consider spatially inhomogeneous solutions of these equations describing the core of BECDM halos. They correspond to stationary solutions of the GPP equations or to stationary solutions of the quantum Euler-Poisson equations satisfying the condition of hydrostatic equilibrium. Stable equilibrium states follow a minimum energy principle. We also consider the Jeans instability of an infinite homogeneous self-gravitating BEC. We recall the general dispersion relation and the general Jeans wave number obtained in Ref. [107] from which we can obtain the Jeans length and the Jeans mass. We briefly discuss the Jeans instability in

an expanding universe. In Sec. III, we derive the analytical core mass–radius relation of BECDM halos from a general ansatz on the wave function (f -ansatz). We determine the parameters of this relation by comparing its asymptotic limits with the exact results obtained by solving the GPP equations numerically [108]. In this manner, the analytical mass–radius relation that we obtain provides a very good agreement with the exact mass–radius relation obtained numerically. In Sec. IV, we use the fact that this mass–radius relation applies to the minimum halo (with $R \sim 1$ kpc and $M \sim 10^8 M_\odot$) to obtain the dark matter particle mass–scattering length relation. This is a constraint that the parameters of the DM particle must satisfy in order to reproduce the characteristics of the minimum halo (assumed to correspond to the ground state of the BECDM model). Using additional constraints such as the Bullet Cluster constraint, or constraints from particle physics and cosmology, we can put some bounds on the possible values of m and a_s . We consider specific models of physical interest that we call BECNI, BECTF, BECt, BECcrit and BECth. Once the values of m and a_s have been determined from the previous considerations, we study in Sec. V the core mass–halo mass relation and conclude (in line with our previous investigations [179,181]) that the quantum cores of DM halos are stable in all cases of astrophysical interest. In Sec. VI, we study the evolution of the Jeans radius and Jeans mass as a function of the cosmic density as the Universe expands. We confirm that the Jeans mass–radius relation is similar to the core mass–radius relation of DM halos, the density of the universe playing in this analogy the role of the average core density of DM halos. We characterize different regimes (noninteracting, TF, nongravitational) for bosons with repulsive or attractive self-interaction. Finally, we explain how our results can be extended to more general forms of self-interaction.

II. SELF-GRAVITATING BOSE-EINSTEIN CONDENSATES

A. Gross-Pitaevskii-Poisson equations

We assume that DM is made of bosons (such as the axion) in the form of BECs at $T = 0$. We use a non-relativistic approach based on Newtonian gravity. The evolution of the wave function $\psi(\mathbf{r}, t)$ of a self-gravitating BEC is governed by the GPP equations (see, e.g., [107])

$$i\hbar \frac{\partial \psi}{\partial t} = -\frac{\hbar^2}{2m} \Delta \psi + m \frac{dV}{d|\psi|^2} \psi + m\Phi\psi, \quad (1)$$

$$\Delta \Phi = 4\pi G |\psi|^2, \quad (2)$$

where $\Phi(\mathbf{r}, t)$ is the gravitational potential and m is the mass of the bosons. The first term in Eq. (1) is the kinetic term which accounts for the Heisenberg uncertainty

⁴A Gaussian density profile usually provides a fair approximation of the exact density profile up to a few halo radii (see, e.g., Fig. 2 of [169] in the case of noninteracting bosons).

principle. The second term takes into account the self-interaction of the bosons via a potential $V(|\psi|^2)$. The third term accounts for the self-gravity of the BEC. The mass density of the BEC is $\rho(\mathbf{r}, t) = |\psi|^2$.

For the standard BEC, we have

$$V(|\psi|^2) = \frac{2\pi a_s \hbar^2}{m^3} |\psi|^4, \quad (3)$$

where a_s is the scattering length of the bosons. The interaction between the bosons is repulsive when $a_s > 0$ and attractive when $a_s < 0$. This potential is valid provided that the gas is sufficiently dilute. It corresponds to a power-law potential of the form

$$V(|\psi|^2) = \frac{K}{\gamma - 1} |\psi|^{2\gamma} \quad (4)$$

with

$$\gamma = 2 \quad \text{and} \quad K = \frac{2\pi a_s \hbar^2}{m^3}. \quad (5)$$

The GPP equations conserve the mass

$$M = \int |\psi|^2 d\mathbf{r} \quad (6)$$

and the energy

$$E_{\text{tot}} = \frac{\hbar^2}{2m^2} \int |\nabla\psi|^2 d\mathbf{r} + \int V(|\psi|^2) d\mathbf{r} + \frac{1}{2} \int |\psi|^2 \Phi d\mathbf{r}, \quad (7)$$

which is the sum of the kinetic energy Θ , the internal energy U , and the gravitational energy W (i.e., $E_{\text{tot}} = \Theta + U + W$).

Remark:—The GPP equations (1) and (2) may be obtained in the nonrelativistic limit $c \rightarrow +\infty$ of the KGE equations describing a SF interacting via a potential $V_R(\varphi)$ (see, e.g., [134,146] for a complex SF and [156,189] for a real SF).

B. The Madelung transformation

Writing the wave function as

$$\psi(\mathbf{r}, t) = \sqrt{\rho(\mathbf{r}, t)} e^{iS(\mathbf{r}, t)/\hbar}, \quad (8)$$

where $\rho(\mathbf{r}, t)$ is the mass density and $S(\mathbf{r}, t)$ is the action, and making the Madelung [269] transformation

$$\rho(\mathbf{r}, t) = |\psi|^2 \quad \text{and} \quad \mathbf{u} = \frac{\nabla S}{m}, \quad (9)$$

where $\mathbf{u}(\mathbf{r}, t)$ is the velocity field, the GPP equations (1) and (2) can be written under the form of hydrodynamic equations

$$\frac{\partial \rho}{\partial t} + \nabla \cdot (\rho \mathbf{u}) = 0, \quad (10)$$

$$\frac{\partial S}{\partial t} + \frac{(\nabla S)^2}{2m} + m[\Phi + V'(\rho)] + Q = 0, \quad (11)$$

$$\frac{\partial \mathbf{u}}{\partial t} + (\mathbf{u} \cdot \nabla) \mathbf{u} = -\frac{1}{m} \nabla Q - \frac{1}{\rho} \nabla P - \nabla \Phi, \quad (12)$$

$$\Delta \Phi = 4\pi G \rho, \quad (13)$$

where

$$Q = -\frac{\hbar^2}{2m} \frac{\Delta \sqrt{\rho}}{\sqrt{\rho}} = -\frac{\hbar^2}{4m} \left[\frac{\Delta \rho}{\rho} - \frac{1}{2} \frac{(\nabla \rho)^2}{\rho^2} \right] \quad (14)$$

is the quantum potential taking into account the Heisenberg uncertainty principle. The pressure P is a function $P(\mathbf{r}, t) = P[\rho(\mathbf{r}, t)]$ of the density (the fluid is barotropic) which is determined by the potential $V(\rho)$ through the relation

$$P'(\rho) = \rho V''(\rho) \quad (15)$$

implying⁵

$$P(\rho) = \rho V'(\rho) - V(\rho) = \rho^2 \left[\frac{V(\rho)}{\rho} \right]'. \quad (16)$$

Equation (16) determines the equation of state $P(\rho)$ for a given potential $V(\rho)$. Inversely, for a given equation of state, the potential is given by

$$V(\rho) = \rho \int \frac{P(\rho)}{\rho^2} d\rho. \quad (17)$$

We can add a term of the form $A\rho$ in the potential without changing the pressure. The squared speed of sound c_s is given by

$$c_s^2 = P'(\rho) = \rho V''(\rho). \quad (18)$$

For a power-law potential of the form of Eq. (4), we get a polytropic equation of state

$$\begin{aligned} V(\rho) = \frac{K}{\gamma - 1} \rho^\gamma &\Rightarrow P = K\rho^\gamma \\ &\Rightarrow c_s^2 = K\gamma\rho^{\gamma-1}. \end{aligned} \quad (19)$$

In particular, for the standard BEC, we obtain

⁵This relation is consistent with the first principle of thermodynamics for a barotropic gas at $T = 0$ (see Appendix H). It shows that $V(\rho)$ represents the density of internal energy ($u = V$). Then, the enthalpy is given by $h = (P + V)/\rho = V'(\rho)$, and it satisfies the identity $h'(\rho) = P'(\rho)/\rho$. This allows us to replace $(1/\rho)\nabla P$ by ∇h in Eq. (12) [107].

$$V(\rho) = \frac{2\pi a_s \hbar^2}{m^3} \rho^2 \Rightarrow P = \frac{2\pi a_s \hbar^2}{m^3} \rho^2$$

$$\Rightarrow c_s^2 = \frac{4\pi a_s \hbar^2}{m^3} \rho. \quad (20)$$

In that case, the equation of state is quadratic. The hydrodynamic equations (10)–(13) are called the quantum Euler-Poisson equations [107]. Equation (10) is the continuity equation, and Eq. (11) is the quantum Hamilton-Jacobi (or Bernoulli) equation. In the TF limit where the quantum potential can be neglected (formally $\hbar = 0$),⁶ they become equivalent to the classical Euler-Poisson equations of a barotropic gas [270].⁷

The quantum Euler equations conserve the mass

$$M = \int \rho d\mathbf{r} \quad (21)$$

and the energy (see, e.g., [107])

$$E_{\text{tot}} = \Theta_c + \Theta_Q + U + W, \quad (22)$$

which is the sum of the classical kinetic energy

$$\Theta_c = \int \rho \frac{\mathbf{u}^2}{2} d\mathbf{r}, \quad (23)$$

the quantum kinetic energy

$$\Theta_Q = \frac{\hbar^2}{8m^2} \int \frac{(\nabla\rho)^2}{\rho} d\mathbf{r} = \frac{1}{m} \int \rho Q d\mathbf{r}, \quad (24)$$

the internal energy

$$U = \int V(\rho) d\mathbf{r} = \int \rho \int^\rho \frac{P(\rho')}{\rho'^2} d\rho' d\mathbf{r}, \quad (25)$$

and the gravitational energy

$$W = \frac{1}{2} \int \rho \Phi d\mathbf{r}. \quad (26)$$

At equilibrium, the classical (macroscopic) kinetic energy vanishes and we get

⁶We note that \hbar appears in the quantum potential Q and in the self-interaction constant $g = 4\pi a_s \hbar^2 / m^3$. The TF limit (formally $\hbar \rightarrow 0$ with $4\pi a_s \hbar^2 / m^3$ finite) amounts to neglecting Q but not g . A precise criterion for the validity of the TF regime is given in Sec. III B.

⁷In the classical limit $\hbar = 0$ and for $P = 0$, the quantum Euler-Poisson equations (10)–(13) reduce to the pressureless hydrodynamic equations of the CDM model.

$$E_{\text{tot}} = \Theta_Q + U + W. \quad (27)$$

The quantum virial theorem writes (see, e.g., [107,149])

$$\frac{1}{2} \ddot{I} = 2(\Theta_c + \Theta_Q) + 3 \int P d\mathbf{r} + W, \quad (28)$$

where

$$I = \int \rho r^2 d\mathbf{r} \quad (29)$$

is the moment of inertia. At equilibrium, it reduces to

$$2\Theta_Q + 3 \int P d\mathbf{r} + W = 0. \quad (30)$$

For a polytropic equation of state $P = K\rho^\gamma$, we have the relation $\int P d\mathbf{r} = (\gamma - 1)U$ and the equilibrium virial theorem may be written as $2\Theta_Q + 3(\gamma - 1)U + W = 0$. In particular, for the standard BEC for which $\gamma = 2$, we get $\int P d\mathbf{r} = U$ and the equilibrium virial theorem reduces to $2\Theta_Q + 3U + W = 0$.

By using the Madelung transformation, the GPP equations (1) and (2) have been written in the form of hydrodynamic equations involving a quantum potential taking into account the Heisenberg uncertainty principle and a pressure force arising from the self-interaction of the bosons. This transformation allows us to treat the BEC as a quantum fluid (superfluid) and to apply standard methods developed in astrophysics as discussed below.

Remark:—The GPP equations (1) and (2) and the quantum Euler-Poisson equations (10)–(13) can be written in terms of the functional derivative of the total energy E_{tot} (see Sec. 3.6 of [149]). They can also be obtained from a least action principle and a Lagrangian (see Appendix B of [145] and Appendix F of [149]).

C. Spatially inhomogeneous equilibrium states in the nonlinear regime: BECDM halos

We first apply the GPP equations (1) and (2), or equivalently the quantum Euler-Poisson equations (10)–(13), to BECDM halos that appear in the nonlinear regime of structure formation in cosmology.

A stationary solution of GPP equations is of the form

$$\psi(\mathbf{r}, t) = \phi(\mathbf{r}) e^{-iEt/\hbar}, \quad (31)$$

where $\phi(\mathbf{r}) = \sqrt{\rho(\mathbf{r})}$ and E are real. Substituting Eq. (31) into Eqs. (1) and (2), we obtain the eigenvalue problem

$$-\frac{\hbar^2}{2m} \Delta\phi + m \frac{dV}{d\phi^2} \phi + m\Phi\phi = E\phi, \quad (32)$$

$$\Delta\phi = 4\pi G\phi^2, \quad (33)$$

determining the eigenfunctions $\phi(\mathbf{r})$ and the eigenvalues E . For the fundamental mode (the one with the lowest energy) the wave function $\phi(r)$ is spherically symmetric and has no node so that the density profile decreases monotonically with the radial distance. Dividing Eq. (32) by ϕ and using $\rho = \phi^2$, we obtain the identity

$$Q + mV'(\rho) + m\Phi = E, \quad (34)$$

which can also be obtained from the quantum Hamilton-Jacobi (or Bernoulli) equation (11) with $S = -Et$. Multiplying Eq. (34) by ρ/m and integrating over the system we get

$$NE = \Theta_Q + \int \rho V'(\rho) d\mathbf{r} + 2W. \quad (35)$$

For a polytropic equation of state $P = K\rho^\gamma$, we have the relation $\int \rho V'(\rho) d\mathbf{r} = \gamma U$ and Eq. (35) may be written as $NE = \Theta_Q + \gamma U + 2W$. In particular, for the standard BEC for which $\gamma = 2$, we get $\int \rho V'(\rho) d\mathbf{r} = 2U$ and Eq. (35) reduces to $NE = \Theta_Q + 2U + 2W$.

Equivalent results can be obtained from the hydrodynamic equations (10)–(13). Indeed, the condition of quantum hydrostatic equilibrium, corresponding to a steady state of the quantum Euler equation (12), writes

$$\frac{\rho}{m} \nabla Q + \nabla P + \rho \nabla \Phi = \mathbf{0}. \quad (36)$$

Dividing Eq. (36) by ρ and integrating the resulting expression with the help of Eq. (15), we recover Eq. (34) where E appears as a constant of integration. On the other hand, combining Eq. (36) with the Poisson equation (13), we obtain the fundamental differential equation of quantum hydrostatic equilibrium

$$\frac{\hbar^2}{2m^2} \Delta \left(\frac{\Delta \sqrt{\rho}}{\sqrt{\rho}} \right) - \nabla \cdot \left(\frac{\nabla P}{\rho} \right) = 4\pi G\rho. \quad (37)$$

This equation describes the balance between the quantum potential taking into account the Heisenberg uncertainty principle, the pressure due to the self-interaction of the bosons, and the self-gravity. For the standard BEC, using Eq. (20), it takes the form

$$\frac{\hbar^2}{2m^2} \Delta \left(\frac{\Delta \sqrt{\rho}}{\sqrt{\rho}} \right) - \frac{4\pi a_s \hbar^2}{m^3} \Delta \rho = 4\pi G\rho. \quad (38)$$

These results can also be obtained from an energy principle (see Appendix B). Indeed, one can show that an equilibrium state of the GPP equations is an extremum of energy E_{tot} at fixed mass M and that an equilibrium state is stable if, and only if, it is a minimum of energy at fixed mass. We are led therefore to considering the minimization problem

$$\min \{E_{\text{tot}} | M \text{ fixed}\}. \quad (39)$$

Writing the variational problem for the first variations (extremization problem) as

$$\delta E_{\text{tot}} - \frac{\mu}{m} \delta M = 0, \quad (40)$$

where μ (global chemical potential) is a Lagrange multiplier taking into account the mass constraint, we obtain $\mathbf{u} = \mathbf{0}$ and

$$Q + mV'(\rho) + m\Phi = \mu. \quad (41)$$

This relation is equivalent to Eq. (34) provided that we make the identification $E = \mu$.⁸ Therefore, the eigenenergy E coincides with the global chemical potential μ . Equation (41) is also equivalent to the condition of quantum hydrostatic equilibrium (36). Therefore, an extremum of energy at fixed mass is an equilibrium state of the GPP equations. Furthermore, as shown in Appendix B, among all possible equilibria, only minima of energy at fixed mass are dynamically stable with respect to the GPP equations (maxima or saddle points are linearly unstable). The stability of an equilibrium state can be settled by studying the sign of $\delta^2 E_{\text{tot}}$ or, equivalently, by linearizing the equations of motion about the equilibrium state and investigating the sign of the squared pulsation ω^2 (see Appendix B). In each case, these methods require one to solve a rather complicated eigenvalue equation. Alternatively, the stability of an equilibrium state can be settled more directly by plotting the series of equilibria and using the Poincaré-Katz [271,272] turning point criterion applied to the curve $\mu(M)$ or the Wheeler [273] theorem applied to the curve $M(R)$ (see [107,108,156] for a specific application of these methods to the case of axion stars). It may also be useful to plot the curve $E_{\text{tot}}(M)$ in order to compare the energy of different equilibrium states with the same mass M . Since $\delta M = 0 \Leftrightarrow \delta E_{\text{tot}} = 0$ according to Eq. (40), the extrema of mass coincide with the extrema of energy in the series of equilibria. As a result, the curve $E_{\text{tot}}(M)$ presents cusps at these critical points (see, e.g., Fig. 11 of [108] for illustration).

The fundamental equation of hydrostatic equilibrium of BECDM halos, Eq. (38), has been solved analytically (approximately) by using a Gaussian ansatz in [107], and numerically (exactly) in [108], for an arbitrary self-interaction (repulsive or attractive). It describes a compact quantum object (soliton/BEC). Because of quantum effects, the central density is finite instead of diverging as in the CDM model. Therefore, quantum mechanics is able to solve the cusp-core problem.

⁸Using the results of Appendix H, Eq. (41) can be interpreted as a quantum Gibbs condition $Q + mh + m\Phi = \mu$ expressing the fact that the quantum potential Q/m plus the enthalpy $h = V'(\rho)$ [equal to the local chemical potential $\mu_{\text{loc}}(\rho)/m$] plus the gravitational potential Φ is a constant equal to the global chemical potential μ/m .

For noninteracting bosons ($a_s = 0$), Eq. (38) reduces to

$$\frac{\hbar^2}{2m^2} \Delta \left(\frac{\Delta \sqrt{\rho}}{\sqrt{\rho}} \right) = 4\pi G \rho. \quad (42)$$

The solution of this equation is usually called a soliton. The density profile is plotted in Fig. 2 of [179] using the results of [108]. The density has not a compact support: it decreases to zero at infinity exponentially rapidly. The mass-radius relation is given by [77,108]

$$M = 9.95 \frac{\hbar^2}{Gm^2 R_{99}}, \quad (43)$$

where R_{99} represents the radius containing 99% of the mass. The mass decreases as the radius increases. The equilibrium states are all stable.⁹

For bosons with a repulsive self-interaction ($a_s > 0$), some density profiles are plotted in [108]. The density does not have a compact support except in the TF limit (see below). The mass-radius relation is plotted in Fig. 4 of [108] (see also Fig. 2 in Sec. III B). There is a minimum radius, given by Eq. (48) below, reached for $M \rightarrow +\infty$ (TF limit). The mass decreases as the radius increases. The equilibrium states are all stable. In the TF limit, Eq. (38) reduces to

$$\frac{4\pi a_s \hbar^2}{m^3} \Delta \rho + 4\pi G \rho = 0. \quad (46)$$

This equation is equivalent to the Lane-Emden equation for a polytrope of index $n = 1$ [274]. It has a simple analytical solution¹⁰

⁹In Appendix E of [179] we showed that the soliton is similar to a polytrope of index $n = 2$ with an effective equation of state

$$P = \left(\frac{2\pi G \hbar^2}{9m^2} \right)^{1/2} \rho^{3/2} \quad (44)$$

depending on the gravitational constant G . In that case, the density profile is determined by the Lane-Emden equation of index $n = 2$ which has to be solved numerically [274]. It has a compact support (see Fig. 2 of [179]) and the mass-radius relation is given by [179]

$$M = 5.25 \frac{\hbar^2}{Gm^2 R}. \quad (45)$$

¹⁰The Helmholtz-type equation (46) and its solution (47) have a long history. As mentioned by Chandrasekhar [274], the analytical solution (47) was first given by Ritter [275] in the context of self-gravitating polytropic spheres. Actually, this solution was already familiar to Laplace [276]. It corresponds indeed to Laplace's celebrated law of density for the earth interior [$\sin(nr)/r$] which he suggested as a consequence of supposing the earth to be a liquid globe, having pressure increasing from the surface inward in proportion to the augmentation of the square of the density.

$$\rho = \frac{\rho_0 R}{\pi r} \sin \left(\frac{\pi r}{R_{\text{TF}}} \right). \quad (47)$$

The density profile is plotted in Fig. 3 of [179]. In the TF limit, the density has a compact support: it vanishes at a finite radius R_{TF} . The equilibrium states have a unique radius given by [78,82,89,96,98,107,228]

$$R_{\text{TF}} = \pi \left(\frac{a_s \hbar^2}{Gm^3} \right)^{1/2}, \quad (48)$$

which is independent of their mass M . In the noninteracting (NI) limit $R \gg R_{\text{TF}}$, we recover Eqs. (42) and (43).

For bosons with an attractive self-interaction ($a_s < 0$), some density profiles are plotted in [108]. The density does not have a compact support. The mass-radius relation is plotted in Fig. 6 of [108] (see also Fig. 3 in Sec. III C). There is a maximum mass [107,108]

$$M_{\text{max}} = 1.012 \frac{\hbar}{\sqrt{Gm|a_s|}} \quad (49)$$

at

$$R_{99}^* = 5.5 \left(\frac{|a_s| \hbar^2}{Gm^3} \right)^{1/2}. \quad (50)$$

The density profile at the maximum mass is plotted in Fig. 1 using the results of [108]. There is no equilibrium state with $M > M_{\text{max}}$. In that case, the BEC is expected to collapse [145]. The outcome of the collapse (dense axion star, black hole, bosonova, etc.) is discussed in [145,156,201,204,207,210,211,214,215]. For $M < M_{\text{max}}$

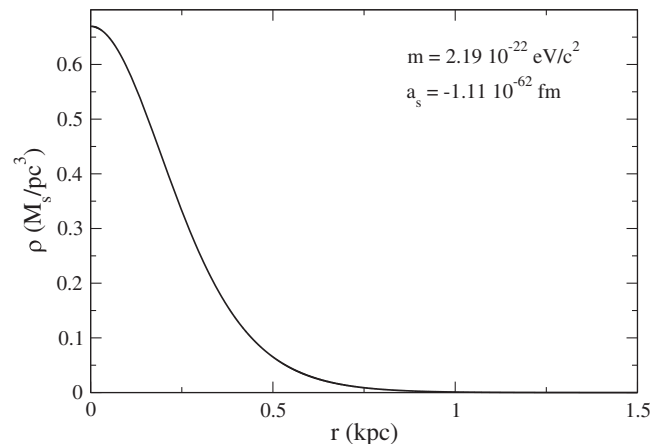


FIG. 1. Density profile of a self-gravitating BEC with an attractive self-interaction at the maximum mass M_{max} . For illustration, we have adopted the values $m = 2.19 \times 10^{-22} \text{ eV}/c^2$ and $a_s = -1.11 \times 10^{-62} \text{ fm}$ (see Sec. III C) corresponding to a DM halo of mass $M = 10^8 M_{\odot}$ and radius $R = 1 \text{ kpc}$ (minimum halo) that would be marginally stable.

the equilibrium states with $R > R_{99}^*$ are stable and the equilibrium states with $R < R_{99}^*$ are unstable.¹¹ In the nongravitational (NG) limit $R \ll R_{99}^*$, Eq. (38) can be written as

$$-\frac{\hbar^2}{2m} \frac{\Delta\sqrt{\rho}}{\sqrt{\rho}} + \frac{4\pi a_s \hbar^2}{m^2} \rho = E. \quad (51)$$

It is equivalent to the standard stationary GP equation. The mass-radius relation is given by (see, e.g., [108])

$$M = 0.275 \frac{mR_{99}}{|a_s|}. \quad (52)$$

These equilibrium states are unstable. In the NI limit $R \gg R_{99}^*$, we recover Eqs. (42) and (43). These equilibrium states are stable.

Remark:—We have seen that self-gravitating BECs with an attractive self-interaction ($a_s < 0$) can be at equilibrium only below a maximum mass given by Eq. (49). Conversely, a self-gravitating BEC of mass M can be at equilibrium only if the scattering length of the bosons is above a minimum negative value [107,108]

$$(a_s)_{\min} = -1.024 \frac{\hbar^2}{GmM^2}. \quad (53)$$

D. Infinite homogeneous BEC in the linear regime: Quantum Jeans problem

We now apply the GPP equations (1) and (2), or equivalently the quantum Euler-Poisson equations (10)–(13), to the universe as a whole in order to study the initiation of structure formation. Specifically, following [107], we study the linear dynamical stability of an infinite homogeneous self-gravitating BEC with density ρ and velocity $\mathbf{u} = \mathbf{0}$ described by the quantum Euler-Poisson equations (10)–(13). This is a generalization of the classical Jeans problem [237] to a quantum fluid.

Considering a small perturbation about an infinite homogeneous equilibrium state, making the Jeans swindle [270,277], and linearizing the hydrodynamic equations (10)–(13), we obtain¹²

$$\frac{\partial\delta}{\partial t} + \nabla \cdot \mathbf{u} = 0, \quad (54)$$

$$\frac{\partial\mathbf{u}}{\partial t} = -c_s^2 \nabla\delta - \nabla\delta\Phi + \frac{\hbar^2}{4m^2} \nabla(\Delta\delta), \quad (55)$$

¹¹This can be shown by using the Poincaré criterion, by using the Wheeler theorem, or by computing the squared pulsation [107,108,156].

¹²See Refs. [107,153,190] for a more detailed discussion and some comments about the Jeans swindle.

$$\Delta\delta\Phi = 4\pi G\rho\delta, \quad (56)$$

where $c_s^2 = P'(\rho)$ is the squared speed of sound and $\delta(\mathbf{r}, t) = \delta\rho(\mathbf{r}, t)/\rho$ is the density contrast. Taking the time derivative of Eq. (54) and the divergence of Eq. (55), and using the Poisson equation (56), we obtain a single equation for the density contrast

$$\frac{\partial^2\delta}{\partial t^2} = -\frac{\hbar^2}{4m^2} \Delta^2\delta + c_s^2 \Delta\delta + 4\pi G\rho\delta. \quad (57)$$

Expanding the solutions of this equation into plane waves of the form $\delta(\mathbf{r}, t) \propto \exp[i(\mathbf{k} \cdot \mathbf{r} - \omega t)]$, we obtain the general dispersion relation [107]

$$\omega^2 = \frac{\hbar^2 k^4}{4m^2} + c_s^2 k^2 - 4\pi G\rho. \quad (58)$$

This quantum dispersion relation may also be obtained from the gravitational Bogoliubov equations (see Appendix D of Ref. [190]). For $\hbar = 0$, we recover the classical Jeans dispersion relation. The dispersion relation (58) is studied in detail in [107,153,190]. The generalized Jeans wave number k_J , corresponding to $\omega = 0$, is determined by the quadratic equation

$$\frac{\hbar^2 k_J^4}{4m^2} + c_s^2 k_J^2 - 4\pi G\rho = 0. \quad (59)$$

It is given by [107]

$$k_J^2 = \frac{2m^2}{\hbar^2} \left(-c_s^2 + \sqrt{c_s^4 + \frac{4\pi G\rho\hbar^2}{m^2}} \right). \quad (60)$$

In the classical (or TF) limit $\hbar \rightarrow 0$ we recover the classical Jeans wave number

$$k_J^2 = \frac{4\pi G\rho}{c_s^2}. \quad (61)$$

In the noninteracting limit $c_s^2 = 0$ we obtain the quantum Jeans wave number

$$k_J^2 = \left(\frac{16\pi G\rho m^2}{\hbar^2} \right)^{1/2}. \quad (62)$$

The Jeans length is $\lambda_J = 2\pi/k_J$. The Jeans radius and the Jeans mass are defined by

$$R_J = \frac{\lambda_J}{2} = \frac{\pi}{k_J}, \quad M_J = \frac{4}{3} \pi \rho R_J^3. \quad (63)$$

They represent the minimum radius and the minimum mass of a fluctuation that can collapse at a given epoch. They are therefore expected to provide an order of magnitude of the

minimum size and minimum mass of DM halos interpreted as self-gravitating BECs.¹³

We note that when $c_s^2 < 0$, the system can be unstable even in the absence of self-gravity ($G = 0$). This is a purely hydrodynamic instability (also called tachyonic instability for a SF). In that case, the dispersion relation (58) reduces to

$$\omega^2 = \frac{\hbar^2 k^4}{4m^2} - |c_s^2| k^2. \quad (64)$$

The critical wave number of the instability is [107]

$$k_J = \left(\frac{4m^2 |c_s^2|}{\hbar^2} \right)^{1/2}. \quad (65)$$

The maximum growth rate is equal to

$$\gamma_{\max} = \frac{m |c_s^2|}{\hbar}. \quad (66)$$

It corresponds to a wave number

$$k_m = \left(\frac{2m^2 |c_s^2|}{\hbar^2} \right)^{1/2} = \frac{k_J}{\sqrt{2}}. \quad (67)$$

These results and their generalization in the presence of self-gravity are discussed in [107,153,190].

Extending the Jeans instability study for a self-gravitating BEC in an expanding universe, using the equations of Appendix I, we find that the evolution of the density contrast $\delta_{\mathbf{k}}(t)$ is determined by the equation [114]

$$\ddot{\delta} + 2 \frac{\dot{a}}{a} \dot{\delta} + \left(\frac{\hbar^2 k^4}{4m^2 a^4} + \frac{c_s^2 k^2}{a^2} - 4\pi G \rho_b \right) \delta = 0. \quad (68)$$

This equation extends the classical Bonnor equation to a quantum gas. A detailed study of this equation has been performed in Refs. [114,153]. In a static universe ($a = 1$), writing $\delta \propto e^{-i\omega t}$, we recover the dispersion relation (58). The comoving Jeans length is $\lambda_J^c = \lambda_J/a$. The Jeans instability criterion corresponds to $\lambda > \lambda_J^c$. In a static universe, the density contrast increases exponentially rapidly with time as $e^{\gamma t}$ [237]. In an expanding universe, it usually increases algebraically rapidly with time [278].

Remark:—In the CDM model for which $\hbar = 0$ and $c_s \simeq 0$, we find that $\lambda_J \simeq 0$. This implies that structures can form at all scales. This is not what is observed and this is why the BECDM model has been introduced. In that case, there is a nonzero (relatively large) Jeans length even at $T = 0$ because of quantum effects.

¹³This is only an order of magnitude because the true mass and the true size of the structures are determined by the complex evolution of the system in the nonlinear regime.

III. MASS-RADIUS RELATION OF BECDM HALOS FROM THE f -ANSATZ

In Ref. [107], using a Gaussian ansatz for the wave function, we have obtained an approximate analytical expression of the mass-radius relation of self-gravitating BECs. In Appendix G 2, we show that the form of this relation is independent of the ansatz. Indeed, it is always given by

$$M = \frac{a \frac{\hbar^2}{Gm^2 R}}{1 - b^2 \frac{a_s \hbar^2}{Gm^3 R^2}}, \quad (69)$$

where only the value of the coefficients a and b depends on the ansatz. Here, we shall determine the coefficients a and b so as to recover the exact mass-radius relation in some particular limits. Once the mass-radius relation is known, we can compute the average density of the DM halo by

$$\rho = \frac{3M}{4\pi R^3}. \quad (70)$$

Remark:—With the Gaussian ansatz, we get $a_G^* = 2\sigma_G/\nu_G = 3.76$ and $b_G^* = (6\pi\zeta_G/\nu_G)^{1/2} = 1.73$, where we have used Eq. (F4) with $\sigma_G = 3/4$, $\zeta_G = 1/(2\pi)^{3/2}$, and $\nu_G = 1/\sqrt{2\pi}$. However, below, we shall identify the radius R with R_{99} , not with the radius R of the f -ansatz defined in Eq. (G9). Since $R_{99} = 2.38167R$ for the Gaussian ansatz, we obtain $a_G = 2.38167a_G^* = 8.96$ and $b_G = 2.38167b_G^* = 4.12$ to be compared with the more exact values of a and b found below.

A. Noninteracting bosons

For noninteracting bosons ($a_s = 0$), the mass-radius relation from Eq. (69) reduces to

$$M = a \frac{\hbar^2}{Gm^2 R}. \quad (71)$$

The mass decreases as the radius increases. If we identify R with the radius R_{99} containing 99% of the mass and compare Eq. (71) with the exact mass-radius relation of noninteracting self-gravitating BECs from Eq. (43), we get $a = 9.946$.

The average density is given by

$$\rho = \frac{3a}{4\pi} \frac{\hbar^2}{Gm^2 R^4} = \frac{3}{4\pi a^3} \frac{G^3 m^6 M^4}{\hbar^6}. \quad (72)$$

The density decreases along the series of equilibria going from small radii to large radii. The equilibrium states are all stable.

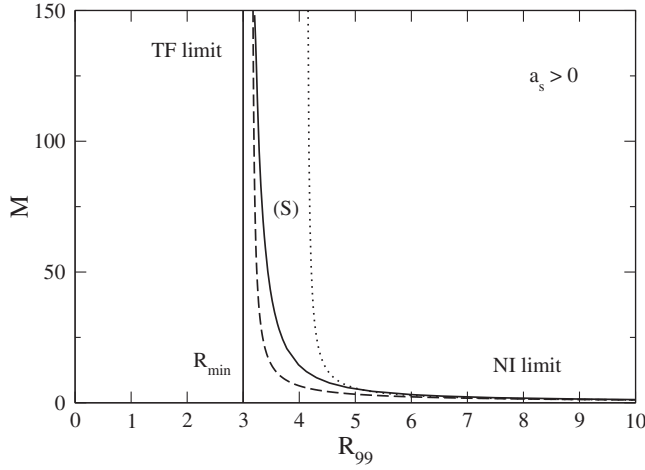


FIG. 2. Mass-radius relation of self-gravitating BECs with $a_s > 0$ (full line: exact [108]; dotted line: Gaussian ansatz [107]; dashed line: fit from Eq. (69) with $a = 9.946$ and $b = \pi$). The mass is normalized by $M_a = \hbar/\sqrt{Gma_s}$ and the radius by $R_a = (a_s \hbar^2/Gm^3)^{1/2}$.

B. Repulsive self-interaction

For bosons with a repulsive self-interaction ($a_s > 0$), the exact mass-radius relation is represented in Fig. 2. The mass decreases as the radius increases. In the TF limit ($\hbar \rightarrow 0$ with fixed $g = 4\pi a_s \hbar^2/m^3$), the mass-radius relation from Eq. (69) reduces to

$$R = b \left(\frac{a_s \hbar^2}{Gm^3} \right)^{1/2}. \quad (73)$$

The radius is independent of the mass. If we identify R with the radius at which the density vanishes and compare Eq. (73) with the exact radius of self-gravitating BECs in the TF limit from Eq. (48), we get $b = \pi$. On the other hand, in the NI limit, we recover the result from Eq. (71) leading to $a = 9.946$. We shall adopt these values of a and b in the repulsive case (see Fig. 2 for a comparison with the exact result).

The average density decreases along the series of equilibria going from small radii to large radii, i.e., from the TF regime to the NI regime. In the TF regime, the average density is given by

$$\rho = \frac{3M}{4\pi b^3} \left(\frac{Gm^3}{a_s \hbar^2} \right)^{3/2}. \quad (74)$$

In the NI regime it is given by Eq. (72). The equilibrium states are all stable.

The transition between the TF regime and the NI regime [obtained by equating Eqs. (71) and (73)] typically occurs at

$$M_t = \frac{a}{b} \frac{\hbar}{\sqrt{Gma_s}}, \quad R_t = b \left(\frac{a_s \hbar^2}{Gm^3} \right)^{1/2}, \quad \rho_t = \frac{3a}{4\pi b^4} \frac{Gm^4}{a_s^2 \hbar^2}. \quad (75)$$

The TF regime is valid when $M \gg M_t$ and $R \sim R_t$. The NI regime is valid when $M \ll M_t$ and $R \gg R_t$. Note that R_t corresponds to the minimum radius R_{\min} (i.e., the radius in the TF regime).

C. Attractive self-interaction

For bosons with an attractive self-interaction ($a_s < 0$), the exact mass-radius relation is represented in Fig. 3. The mass increases as the radius increases, reaches a maximum value

$$M_{\max} = \frac{a}{2b} \frac{\hbar}{\sqrt{Gm|a_s|}} \quad \text{at } R_* = b \left(\frac{|a_s| \hbar^2}{Gm^3} \right)^{1/2}, \quad (76)$$

and decreases. If we identify R_* with the radius (R_{*99}) containing 99% of the mass and compare Eq. (76) with the exact values of the maximum mass and of the corresponding radius from Eqs. (49) and (50), we get $b = 5.5$ and $a/2b = 1.012$, leading to $a = 11.1$. We shall adopt these values in the attractive case (see Fig. 3 for a comparison with the exact result). We note that the value $a = 11.1$ obtained from the maximum mass is relatively close to the value $a = 9.946$ obtained from the NI limit (see Sec. III A). In the NG limit, the mass-radius relation from Eq. (69) reduces to

$$M = \frac{a}{b^2} \frac{mR}{|a_s|}. \quad (77)$$

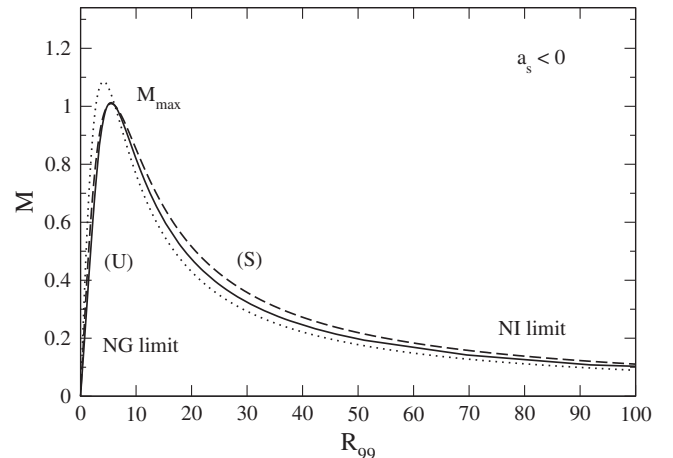


FIG. 3. Mass-radius relation of self-gravitating BECs with $a_s < 0$ [full line: exact [108]; dotted line: Gaussian ansatz [107]; dashed line: fit from Eq. (69) with $a = 11.1$ and $b = 5.5$]. The mass is normalized by $M_a = \hbar/\sqrt{Gm|a_s|}$ and the radius by $R_a = (|a_s| \hbar^2/Gm^3)^{1/2}$.

The value $a/b^2 = 0.367$ obtained from the maximum mass is relatively close to the exact value 0.275 from Eq. (52). This is a consistency check. The density decreases along the series of equilibria going from small radii to large radii, i.e., from the NG regime to the NI regime. In the NG regime, the average density is given by

$$\rho = \frac{3a}{4\pi b^2} \frac{m}{|a_s|R^2} = \frac{3a^3}{4\pi b^6} \frac{m^3}{|a_s|^3 M^2}. \quad (78)$$

In the NI regime it is given by Eq. (72). The average density at the maximum mass is

$$\rho_* = \frac{3a}{8\pi b^4} \frac{Gm^4}{a_s^2 \hbar^2}. \quad (79)$$

The equilibrium states are unstable before the turning point of mass ($R < R_*$) and stable after the turning point of mass ($R > R_*$).

The transition between the NG regime and the NI regime [obtained by equating Eqs. (71) and (77)] typically occurs at

$$M_t = \frac{a}{b} \frac{\hbar}{\sqrt{Gm|a_s|}}, \quad R_t = b \left(\frac{|a_s| \hbar^2}{Gm^3} \right)^{1/2}, \quad \rho_t = \frac{3a}{4\pi b^4} \frac{Gm^4}{a_s^2 \hbar^2}. \quad (80)$$

These scales are similar to those corresponding to the maximum mass (we have $\rho_t = 2\rho_*$, $M_t = 2M_{\max}$, and $R_t = R_*$). The NG regime is valid when $M \ll M_t$ and $R \ll R_t$ but these equilibrium states are unstable. The NI regime is valid when $M \ll M_t$ and $R \gg R_t$. There is no equilibrium state of mass $M > M_{\max}$.

Remark:—The scales (80) determining the transition between the NG regime and the NI regime in the attractive case are similar to the scales (75) determining the transition between the TF regime and the NI regime in the repulsive case provided that a_s is replaced by $|a_s|$.

IV. DARK MATTER PARTICLE MASS-SCATTERING LENGTH RELATION

As explained previously, in the BECDM model, the mass-radius relation (69) of a self-gravitating BEC at $T = 0$ (ground state) describes the smallest halos observed in the Universe.¹⁴ They correspond to dSphs like Fornax. From the observations, these ultracompact DM halos have a typical radius ~ 1 kpc and a typical mass $\sim 10^8 M_\odot$. To fix the ideas, we shall consider a minimum halo of radius and mass¹⁵

$$R = 1 \text{ kpc}, \quad M = 10^8 M_\odot \quad (\text{Fornax}). \quad (81)$$

Its average density is

$$\rho = \frac{3M}{4\pi R^3} = 1.62 \times 10^{-18} \text{ g/m}^3 \quad (\text{Fornax}). \quad (82)$$

Since R and M are prescribed by Eq. (81), we find that Eq. (69) provides a relation

$$a_s = \frac{amR}{b^2 M} \left(\frac{GMm^2 R}{a\hbar^2} - 1 \right) \quad (83)$$

between the mass m and the scattering length a_s of the bosonic DM particle. Such a relation is necessary to obtain a minimum halo consistent with the observations. The DM particle mass-scattering length relation (83) may be written as

$$\frac{a_s}{a'_*} = \left(\frac{m}{m_0} \right)^3 - \frac{m}{m_0}, \quad (84)$$

where we have introduced the scales

$$m_0 = \left(\frac{a\hbar^2}{GMR} \right)^{1/2} \quad (85)$$

and

$$a'_* = \frac{a^{3/2}}{b^2} \left(\frac{\hbar^2 R}{GM^3} \right)^{1/2}. \quad (86)$$

The relation $m(a_s)$ is plotted in Fig. 4. Taking $a = 9.946$ and $b = \pi$ (see Secs. III A and III B) adapted to bosons with

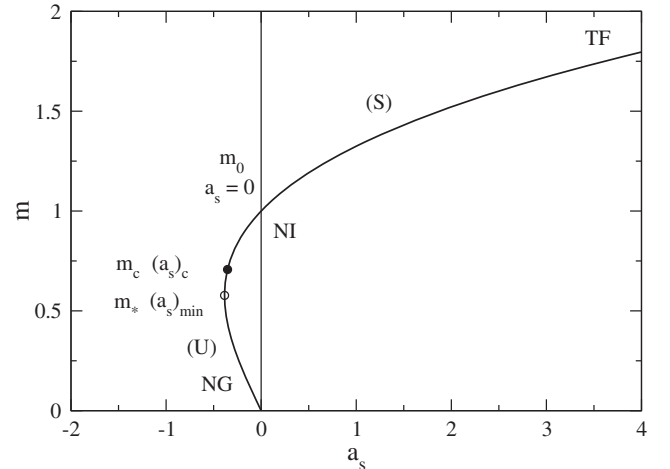


FIG. 4. Mass m of the DM particle as a function of the scattering length a_s in order to match the characteristics of the minimum halo. The mass is normalized by m_0 and the scattering length by a'_* . The stable part of the curve starts at the critical minimum halo point $[(a_s)_c, m_c]$. It differs from the minimum of the curve $a_s(m)$.

¹⁴It also describes the quantum core of larger DM halos [179].

¹⁵If more accurate values of R and M are adopted, the numerical applications of our paper would slightly change. However, the main ideas and the main results would remain substantially the same.

a repulsive self-interaction (or no interaction), we get $m_0 = 2.92 \times 10^{-22} \text{ eV}/c^2$ and $a'_* = 8.13 \times 10^{-62} \text{ fm}$. Taking $a = 11.1$ and $b = 5.5$ (see Sec. III C) adapted to bosons with an attractive self-interaction, we get $m_0 = 3.08 \times 10^{-22} \text{ eV}/c^2$ and $a'_* = 3.12 \times 10^{-62} \text{ fm}$.

A. Noninteracting bosons

For noninteracting bosons ($a_s = 0$), we get

$$m = m_0 = 2.92 \times 10^{-22} \text{ eV}/c^2 \quad (\text{BECNI}). \quad (87)$$

This is the typical mass considered in the literature when the bosons are assumed to be noninteracting.

Remark:—In the NI regime, the mass from Eq. (87) can be written as

$$m = \left(\frac{a\hbar^2}{GMR} \right)^{1/2}, \quad (88)$$

which is equivalent to Eq. (71).

B. Repulsive self-interaction

For bosons with a repulsive self-interaction ($a_s > 0$), a'_* determines the transition between the NI regime ($a_s \ll a'_*$) where $m \sim m_0$ and the TF regime ($a_s \gg a'_*$) where

$$\frac{m}{m_0} \sim \left(\frac{a_s}{a'_*} \right)^{1/3}. \quad (89)$$

When the self-interaction is repulsive, we have seen that all the equilibrium states are stable. Therefore, in principle, all the scattering lengths $a_s > 0$ and the corresponding masses $m > m_0$ are possible. In the TF regime, the mass-scattering length relation (89) can be written as

$$\frac{a_s}{m^3} \sim \frac{GR^2}{b^2\hbar^2}, \quad (90)$$

which is equivalent to Eq. (73). The minimum halo [Eq. (81)] just determines the ratio

$$\frac{a_s}{m^3} = 3.28 \times 10^3 \text{ fm}/(\text{eV}/c^2)^3. \quad (91)$$

Note that only the radius R of the minimum halo matters in this determination. In order to determine m and a_s individually, we need another equation. Observations of the Bullet Cluster give the constraint $\sigma/m \leq 1.25 \text{ cm}^2/\text{g}$ where $\sigma = 4\pi a_s^2$ is the self-interaction cross section [279]. This can be written as

$$\frac{4\pi a_s^2}{m} \leq 1.25 \text{ cm}^2/\text{g} \Leftrightarrow \frac{(a_s/a'_*)^2}{m/m_0} \leq 7.83 \times 10^{92}. \quad (92)$$

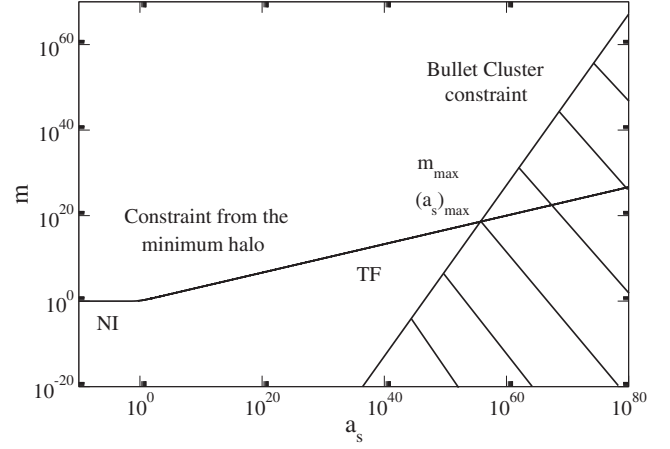


FIG. 5. The initially upper curve gives the DM particle mass versus scattering length relation in order to match the characteristics of the minimum halo [see Eq. (84)]. The mass is normalized by m_0 and the scattering length by a'_* . The initially lower curve gives the Bullet Cluster constraint from Eq. (92). Only the region above this curve is allowed by the observations. The intersection between these two curves determines the maximum DM particle mass $m_{\text{max}}/m_0 = 3.79 \times 10^{18}$ and its maximum scattering length $(a_s)_{\text{max}}/a'_* = 5.45 \times 10^{55}$, leading to the results of Eq. (93). We note that the intersection occurs in the TF regime where Eq. (84) can be approximated by Eq. (89).

If we replace the inequality by an equality, and combine Eq. (92) with Eq. (89), we find that the mass and scattering length of the DM particle are given by¹⁶

$$m_{\text{max}} = 1.10 \times 10^{-3} \text{ eV}/c^2, \quad (a_s)_{\text{max}} = 4.41 \times 10^{-6} \text{ fm} \quad (\text{BECTF}). \quad (93)$$

More generally, because of the Bullet Cluster constraint, the scattering length of the DM boson must lie in the range $0 \leq a_s \leq (a_s)_{\text{max}}$ and its mass must lie in the range $m_0 \leq m \leq m_{\text{max}}$ (see Fig. 5). Therefore, when we account for a repulsive self-interaction, the mass m of the boson required to match the observations of the minimum halo can increase by ~ 18 orders of magnitude as compared to its value m_0 in the NI case [see Eqs. (87) and (93)].

¹⁶Craciun and Harko [280] obtained a similar estimate. However, they took a larger BECDM radius $R = 10 \text{ kpc}$ instead of $R = 1 \text{ kpc}$ because they modeled large DM halos by a pure BEC at $T = 0$ in its ground state while we argue that the ground state solution leading to Eq. (48) only applies to the minimum halo with $M = 10^8 M_\odot$ and $R = 1 \text{ kpc}$ and to the quantum core of size $R_c = 1 \text{ kpc}$ of larger DM halos (recall that the quantum core of large DM halos is surrounded by an approximately isothermal atmosphere due to the quantum interferences of excited states) [169,179]. Since they applied Eq. (48) to the whole DM halo instead of just its core as we do, they found a smaller maximum mass $m_{\text{max}} = 0.1791 \text{ meV}/c^2$ instead of $m_{\text{max}} = 1.10 \text{ meV}/c^2$.

The BECTF model discussed previously corresponds to the case where the bound fixed by the Bullet Cluster is reached. For comparison, we can consider a BECt model which corresponds to the transition between the NI limit and the TF limit. It is obtained by substituting Eq. (87) into Eq. (89), or Eq. (88) into Eq. (90), giving

$$m_t = 2.92 \times 10^{-22} \text{ eV}/c^2, \quad (a_s)_t = 8.13 \times 10^{-62} \text{ fm} \quad (\text{BECt}). \quad (94)$$

This corresponds to the scales m_0 and a'_* defined by Eqs. (85) and (86).

C. Attractive self-interaction

For bosons with an attractive self-interaction ($a_s < 0$), the relation (84) reveals the existence of a minimum scattering length

$$\frac{(a_s)_{\min}}{a'_*} = -\frac{2}{3\sqrt{3}} \quad \text{at which} \quad \frac{m_*}{m_0} = \frac{1}{\sqrt{3}}. \quad (95)$$

We find $(a_s)_{\min} = -1.20 \times 10^{-62} \text{ fm}$ and $m_* = 1.78 \times 10^{-22} \text{ eV}/c^2$. The NI regime corresponds to $|a_s| \ll a'_*$ and $m \sim m_0$. The NG regime corresponds to $|a_s| \ll a'_*$ and $m \ll m_0$ such that

$$\frac{m}{m_0} \sim \frac{|a_s|}{a'_*}. \quad (96)$$

In the NG regime, the mass-scattering length relation (96) can be written as

$$\frac{|a_s|}{m} = \frac{aR}{b^2 M} = 1.01 \times 10^{-40} \text{ fm}/(\text{eV}/c^2), \quad (97)$$

which is equivalent to Eq. (77). It is important to note that the minimum scattering length $(a_s)_{\min}$ does *not* correspond to the critical point (associated with the maximum mass M_{\max}) separating stable from unstable equilibrium states. This latter is located at

$$\frac{(a_s)_c}{a'_*} = -\frac{1}{2\sqrt{2}}, \quad \frac{m_c}{m_0} = \frac{1}{\sqrt{2}}. \quad (98)$$

The equilibrium states with $m < m_c$ are unstable (they correspond to configurations with $R < R_*$) so that only the equilibrium states with $m_c < m < m_0$ are stable (they correspond to configurations with $R > R_*$). Therefore, in the attractive case, the scattering length of the DM boson must lie in the range $(a_s)_c < a_s < 0$ and its mass must lie in the range $m_c < m < m_0$, with

$$m_c = 2.19 \times 10^{-22} \text{ eV}/c^2, \quad (a_s)_c = -1.11 \times 10^{-62} \text{ fm} \quad (\text{BECcrit}). \quad (99)$$

There is no equilibrium state with $a_s < (a_s)_{\min}$. On the other hand, the equilibrium states with $(a_s)_{\min} < a_s < (a_s)_c$ are unstable. We note that, in the attractive case, the mass m does not change substantially from its value m_0 in the NI limit. The BECcrit model from Eq. (99) corresponds to the case where the minimum halo is critical (i.e., its mass $M = 10^8 M_\odot$ is equal to M_{\max}).

D. Constraints from particle physics and cosmology

For bosons with an attractive self-interaction, such as the axion [15], it is more convenient to express the results in terms of the decay constant f instead of the scattering length a_s . They are related by (see, e.g., [156])

$$f = \left(\frac{\hbar c^3 m}{32\pi |a_s|} \right)^{1/2}. \quad (100)$$

Particle physics and cosmology lead to the following relation between f and m [147]:

$$\Omega_{\text{axion}} \sim 0.1 \left(\frac{f}{10^{17} \text{ GeV}} \right)^2 \left(\frac{m}{10^{-22} \text{ eV}/c^2} \right)^{1/2}, \quad (101)$$

where Ω_{axion} is the present fraction of axions in the universe. Taking $\Omega_{\text{axion}} \sim \Omega_{\text{m},0} = 0.3089$ (assuming that DM is exclusively made of axions), this relation can be rewritten as

$$\frac{m^{3/2}}{|a_s|} = 1.57 \times 10^{35} (\text{eV}/c^2)^{3/2}/\text{fm} \quad (102)$$

or, in dimensionless form, as

$$\frac{(m/m_0)^{3/2}}{|a_s|/a'_*} = 9.06 \times 10^5. \quad (103)$$

Considering the intersection between the curves defined by Eqs. (84) and (103), we find that $m \simeq m_0$. Then, taking $m = m_0 = 2.92 \times 10^{-22} \text{ eV}/c^2$ [see Eq. (87)] and using Eq. (102) we get $a_s = -3.18 \times 10^{-68} \text{ fm}$. Therefore, we can determine a_s and m *individually*. We find

$$m_{\text{th}} = 2.92 \times 10^{-22} \text{ eV}/c^2, \quad (a_s)_{\text{th}} = -3.18 \times 10^{-68} \text{ fm} \quad (\text{BECth}). \quad (104)$$

We note that m has approximately the same value as in the noninteracting model while a_s has a nonzero value. It corresponds to a decay constant $f_{\text{th}} = 1.34 \times 10^{17} \text{ GeV}$. Interestingly, f lies in the range $10^{16} \text{ GeV} \leq f \leq 10^{18} \text{ GeV}$ expected in particle physics (f is bounded above by the reduced Planck mass and below by the grand unified scale

of particle physics) [147]. We note that $|a_s|_{\text{th}} \ll a'_*$ so we are essentially in the NI regime. This is confirmed by the discussion of Sec. V C.

E. QCD axions

In the previous sections, we have determined some constraints that the mass m and the scattering length a_s of the bosons possibly composing DM must satisfy so that they are able to form giant BECs of mass $M \sim 10^8 M_\odot$ and radius $R \sim 1$ kpc comparable to dSphs like Fornax. This leads to ULAs with a very small mass that are allowed by particle physics (in connection to string theory) but that have not been fully characterized yet [15]. On the other hand, the characteristics of the QCD axion are precisely known from cosmology and particle physics, and we can see how they enter into the problem.

QCD axions have a mass $m = 10^{-4}$ eV/ c^2 and a negative scattering length $a_s = -5.8 \times 10^{-53}$ m [281], corresponding to a dimensionless self-interaction constant $\lambda = -7.39 \times 10^{-49}$ and a decay constant $f = 5.82 \times 10^{19}$ eV (see Appendix C). The maximum mass of QCD axion stars is $M_{\text{max}}^{\text{exact}} = 6.46 \times 10^{-14} M_\odot$ and their minimum stable radius is $(R_{99}^*)^{\text{exact}} = 227$ km (their average maximum density is $\bar{\rho} = 2.62 \times 10^3$ g/ m^3 and the maximum number of axions in an axion star is $N_{\text{max}} = M_{\text{max}}/m = 7.21 \times 10^{56}$).

These values of M_{max} and R_{99}^* correspond to the typical size of asteroids. Obviously, QCD axions cannot form giant BECs with the dimension of DM halos like Fornax. However, they can form mini boson stars (mini axion stars or dark matter stars) of very low mass—asteroids—that could be the constituents of DM halos under the form of mini massive compact halo objects (mini MACHOs) [145,156]. These mini axion stars are Newtonian self-gravitating BECs of QCD axions with an attractive self-interaction stabilized by the quantum pressure (Heisenberg uncertainty principle). They may cluster into structures similar to standard CDM halos. They might play a role as DM components (i.e., DM halos could be made of mini axion stars interpreted as MACHOs instead of WIMPs) if they exist in the Universe in abundance. However, mini axion stars (MACHOs) behave essentially as CDM and do not solve the small-scale crisis of CDM.

Remark:—The collapse of axion stars above the limiting mass M_{max} [107] has been discussed by several authors [145,156,201,204,207,210,211,214,215]. The collapse may lead to the formation of a dense axion star or a black hole. It may also be accompanied by an explosion with an ejection of relativistic axions (bosenova).

V. CORE MASS–HALO MASS RELATION

The results of Secs. II–IV describe the ground state of a self-gravitating BEC [107]. They apply to the minimum halo [see Eq. (81)] which is a purely condensed object without atmosphere. Larger DM halos have a core-halo

structure with a quantum core (soliton) in its ground state and an approximately isothermal atmosphere due to quantum interferences of excited states [149]. The results of Secs. II–IV also apply to the quantum core of these objects. The mass M_c of the quantum core increases with the halo mass M_h . For noninteracting bosons and for bosons with a repulsive self-interaction we may wonder if the core mass can reach the maximum mass $M_{\text{max}}^{\text{GR}}$ set by general relativity and collapse toward a supermassive black hole (SMBH). For bosons with an attractive self-interaction we may wonder if the core mass can reach the maximum mass found in [107] and collapse. The outcome of the collapse in that case would be a dense axion star (soliton), a black hole, or a bosenova [145,156,201,204,207,210,211,214,215]. These questions have been addressed in [169,179,181], and we recall below the main results of these studies.

In Refs. [169,179,181], we have derived the core mass–halo mass relation of DM halos (without or with the presence of a central black hole) from a thermodynamic approach. We have obtained a general relation $M_c(M_h)$ valid for noninteracting bosons as well as for bosons with a repulsive or an attractive self-interaction and for fermions. To obtain this relation we have first shown [169,179] that the maximization of the Lynden-Bell entropy at fixed mass and energy leads to the “velocity dispersion tracing” relation according to which the velocity dispersion in the core $v_c^2 \sim GM_c/R_c$ is of the same order as the velocity dispersion in the halo $v_h^2 \sim GM_h/r_h$. This relation can be written as

$$v_c \sim v_h \Rightarrow \frac{M_c}{R_c} \sim \frac{M_h}{r_h}. \quad (105)$$

The core mass-radius relation $M_c(R_c)$ can be obtained from the Gaussian ansatz yielding [107]

$$M_c = \frac{3.76 \frac{\hbar^2}{Gm^2 R_c}}{1 - 3 \frac{a_s \hbar^2}{Gm^3 R_c^2}} \quad (106)$$

or, equivalently,

$$R_c = 1.87 \frac{\hbar^2}{Gm^2 M_c} \left(1 \pm \sqrt{1 + 0.849 \frac{Gma_s M_c^2}{\hbar^2}} \right). \quad (107)$$

On the other hand, assuming that the atmosphere is isothermal, the halo mass-radius relation $M_h(r_h)$ is given by [169]

$$M_h = 1.76 \Sigma_0 r_h^2, \quad (108)$$

where $\Sigma_0 = 141 M_\odot/\text{pc}^2$ is the universal surface density of DM halos inferred from the observations [282–284]. Combining Eqs. (105)–(108), we obtain the core mass–halo mass relation $M_c(M_h)$ under the form

$$M_c = 2.23 \frac{\hbar \Sigma_0^{1/4} M_h^{1/4}}{G^{1/2} m} \left(1 + 1.06 \frac{a_s}{m} \Sigma_0^{1/2} M_h^{1/2} \right)^{1/2}. \quad (109)$$

Writing $M_c = M_h$ for the minimum halo, we obtain

$$(M_h)_{\min}^{3/2} = 4.99 \frac{\hbar^2 \Sigma_0^{1/2}}{G m^2} \left(1 + 1.06 \frac{a_s}{m} \Sigma_0^{1/2} (M_h)_{\min}^{1/2} \right). \quad (110)$$

This equation determines the mass $(M_h)_{\min}$ of the minimum halo as a function of m and a_s . Inversely, for given $(M_h)_{\min}$, it determines the relation between m and a_s . A universal relation can be obtained as follows [179,181]. For a given value of the minimum halo mass $(M_h)_{\min}$ we introduce the scales [see Eqs. (204) and (207) of [179]]

$$m_0 = 2.23 \frac{\hbar \Sigma_0^{1/4}}{G^{1/2} (M_h)_{\min}^{3/4}} \quad (111)$$

and

$$a'_* = 2.11 \frac{\hbar}{G^{1/2} \Sigma_0^{1/4} (M_h)_{\min}^{5/4}}. \quad (112)$$

For example, taking $(M_h)_{\min} = 10^8 M_\odot$, we get $m_0 = 2.25 \times 10^{-22}$ eV/ c^2 and $a'_* = 4.95 \times 10^{-62}$ fm. With these scales, the normalized DM particle mass–scattering length relation (110) needed to reproduce the minimum halo (ground state) can be written as [see Eq. (208) of [179]]

$$\frac{a_s}{a'_*} = \left(\frac{m}{m_0} \right)^3 - \frac{m}{m_0} \quad (113)$$

and the normalized core mass–halo mass relation (109) can be written as¹⁷

$$\frac{M_c}{(M_h)_{\min}} = \frac{m_0}{m} \left(\frac{M_h}{(M_h)_{\min}} \right)^{1/4} \times \sqrt{1 + \frac{m_0 a_s}{m a'_*} \left(\frac{M_h}{(M_h)_{\min}} \right)^{1/2}}. \quad (114)$$

This leads to the universal curve plotted in Fig. 19 of [179]. The only input is the DM particle mass m or, equivalently, its scattering length a_s [they are related to each other by Eq. (113)]. The minimum halo mass $(M_h)_{\min}$ obtained from the observations determines the scales m_0 and a'_* . We have also established the following relation [see Eq. (146) of [179]]:

$$\frac{M_h}{M_\odot} = 6.01 \times 10^{-6} \left(\frac{M_v}{M_\odot} \right)^{4/3} \quad (115)$$

¹⁷This expression can be obtained from Eqs. (205), (206), and (223) of [179].

between the halo mass M_h used in our papers [169,179,181] and the virial halo mass M_v used in [126].

A. Noninteracting bosons

For noninteracting bosons, the core mass–halo mass relation is [see Eq. (226) of [179]]

$$M_c = 2.23 \left(\frac{\hbar^4 \Sigma_0 M_h}{G^2 m^4} \right)^{1/4}. \quad (116)$$

For $a_s = 0$ the mass of the boson is given by $m = m_0 = 2.25 \times 10^{-22}$ eV/ c^2 .¹⁸ For a DM halo of mass $M_h = 10^{12} M_\odot$ similar to the one that surrounds our Galaxy, we obtain a core mass $M_c = 10^9 M_\odot$ and a core radius $R_c = 63.5$ pc. The quantum core represents a bulge or a nucleus. It cannot mimic a SMBH because it is too much extended ($Rc^2/GM \sim 10^6 \gg 1$).¹⁹

The maximum mass and the minimum radius of a noninteracting boson star at $T = 0$ set by general relativity are [233,234]

$$M_{\max}^{\text{GR}} = 0.633 \frac{\hbar c}{Gm}, \quad R_{\min}^{\text{GR}} = 9.53 \frac{GM_{\max}}{c^2}. \quad (117)$$

These scalings can be obtained as explained in Appendix B.2 of [107]. For a boson of mass $m = 2.25 \times 10^{-22}$ eV/ c^2 , we obtain $M_{\max}^{\text{GR}} = 3.76 \times 10^{11} M_\odot$ and $R_{\min}^{\text{GR}} = 0.171$ pc. The maximum mass is much larger than the typical quantum core mass of a DM halo. According to Eq. (116) the mass of the soliton would be equal to the maximum mass ($M_c = M_{\max}^{\text{GR}}$) in a DM halo of mass $M_h = 6.49 \times 10^{-3} c^4 / (G^2 \Sigma_0) = 2.01 \times 10^{22} M_\odot$ (this expression is independent of the boson mass) [181]. Such a large halo mass is clearly unrealistic (the biggest DM halos observed in the Universe have a mass $M_h \sim 10^{14} M_\odot$). Therefore, the soliton present at the center of a noninteracting BECDM halo can never collapse toward a SMBH. This conclusion was first reached in Appendix C of [181]. Since $M_c \ll M_{\max}^{\text{GR}}$ in all realistic DM halos, a nonrelativistic approach is justified.

Remark:—A very massive object (Sagittarius A*) resides at the center of our Galaxy. This object has a mass $M = 4.2 \times 10^6 M_\odot$ associated with a Schwarzschild radius $R_S = 4.02 \times 10^{-7}$ pc. Its radius is not known exactly but it must be less than $R_P = 6 \times 10^{-4}$ pc, the S2 star pericenter ($R_P = 1492 R_S$) [285]. This object is believed to be a SMBH but it could also be a compact object such as a boson star or a fermion ball. Let us assume that this object

¹⁸In the numerical applications we assume that $(M_h)_{\min} = 10^8 M_\odot$.

¹⁹It can be shown that the mass of the soliton is of the order of the de Broglie length. Indeed, from Eqs. (105) and (43) we get $R_c \sim \lambda_{\text{dB}}$ with $\lambda_{\text{dB}} \sim \hbar / (mv)$ where $v \sim v_c \sim v_h \sim (GM_h/r_h)^{1/2}$.

is a noninteracting boson star (soliton). Using the non-relativistic mass-radius relation from Eq. (43) with $M = 4.2 \times 10^6 M_\odot$ and $R = 6 \times 10^{-4}$ pc, we find that the mass of the boson is $m = 1.84 \times 10^{-18}$ eV/ c^2 [using the expression of the maximum mass from Eq. (117) with $M = 4.2 \times 10^6 M_\odot$ we get $m = 2.01 \times 10^{-17}$ eV/ c^2 but this situation is too extreme]. These values are forbidden by our model which assumes that the ground state of the self-gravitating Bose gas corresponds to a minimum halo of mass $M = 10^8 M_\odot$ and radius $R = 1$ kpc. However, if we relax this assumption, it may be possible to construct a realistic model of the Milky Way (MW) in which a noninteracting boson star mimics a SMBH.

B. Repulsive self-interaction in the TF limit

For bosons with a repulsive self-interaction in the TF limit, the core mass–halo mass relation is [see Eq. (229) of [179]]

$$M_c = 2.30 \left(\frac{\hbar^2 \Sigma_0 a_s M_h}{G m^3} \right)^{1/2}. \quad (118)$$

In the TF limit, the ratio a_s/m^3 is given by $a_s/m^3 = a'_*/m_0^3 = 4.35 \times 10^3$ fm/(eV/ c^2)³. For a DM halo of mass $M_h = 10^{12} M_\odot$ similar to the one that surrounds our Galaxy, we obtain a core mass $M_c = 10^{10} M_\odot$ and a core radius $R_c = 635$ pc. The quantum core represents a bulge or a nucleus. It cannot mimic a SMBH because it is too much extended ($Rc^2/GM \sim 10^6 \gg 1$).

The maximum mass and the minimum radius of a self-interacting boson star at $T = 0$ in the TF limit set by general relativity are [228,235,236]

$$M_{\max}^{\text{GR}} = 0.307 \frac{\hbar c^2 \sqrt{a_s}}{(Gm)^{3/2}}, \quad R_{\min}^{\text{GR}} = 6.25 \frac{GM_{\max}}{c^2}. \quad (119)$$

These scalings can be obtained as explained in Appendix B. 3. of [107]. For a ratio $a_s/m^3 = 4.35 \times 10^3$ fm/(eV/ c^2)³, we obtain $M_{\max} = 2.35 \times 10^{15} M_\odot$ and $R_{\min} = 703$ pc. The maximum mass is much larger than the typical quantum core mass of a DM halo. According to Eq. (118) the mass of the soliton would be equal to the maximum mass ($M_c = M_{\max}^{\text{GR}}$) in a DM halo of mass $M_h = 0.0178c^4/(G^2\Sigma_0) = 5.51 \times 10^{22} M_\odot$ (this expression is independent of the ratio a_s/m^3) [181]. Such a large halo mass is clearly unrealistic (the biggest DM halos observed in the Universe have a mass $M_h \sim 10^{14} M_\odot$). Therefore, the quantum core present at the center of a BECDM halo with repulsive self-interactions can never collapse toward a SMBH. This conclusion was first reached in Appendix C of [181]. Since $M_c \ll M_{\max}^{\text{GR}}$ in all realistic DM halos, a nonrelativistic approach is justified.

Remark:—Let us assume that the object at the center of the MW is a self-interacting boson star. Using the

nonrelativistic mass-radius relation (48) with $R = 6 \times 10^{-4}$ pc we find that $a_s/m^3 = 1.18 \times 10^{-9}$ fm(eV/ c^2)³ [using the expression of the maximum mass from Eq. (119) with $M = 4.2 \times 10^6 M_\odot$ we get $a_s/m^3 = 1.39 \times 10^{-14}$ fm(eV/ c^2)³ but this situation is too extreme]. These values are forbidden by our model which assumes that the ground state of the self-gravitating Bose gas corresponds to a minimum halo of mass $M = 10^8 M_\odot$ and radius $R = 1$ kpc. However, if we relax this assumption, it may be possible to construct a realistic model of the MW in which a self-interacting boson star mimics a SMBH.

C. Attractive self-interaction

For bosons with an attractive self-interaction, the core mass–halo mass relation (see Fig 19 in [179]) presents a maximum when the core mass reaches the critical value [see Eqs. (181) and (235) of [179]]

$$(M_c)_{\max} = 1.085 \frac{\hbar}{\sqrt{Gm|a_s|}} = 10.9 \left(\frac{f^2 \hbar}{c^3 m^2 G} \right)^{1/2} \quad (120)$$

at which it becomes unstable and collapses [107,145]. The collapse of the core, leading to a dense axion star (soliton), a black hole, or a bosenova [145,156,201,204,207,210,211,214,215], occurs in a DM halo of mass [see Eqs. (233) and (234) of [179]]

$$(M_h)_{\max} = 0.223 \frac{m^2}{a_s^2 \Sigma_0} = 2255 \frac{f^4}{\hbar^2 c^6 \Sigma_0}. \quad (121)$$

We note that the maximum halo mass $(M_h)_{\max}$ depends only on f while the maximum core mass $(M_c)_{\max}$ depends on f and m .

The maximum mass of a self-gravitating BEC made of bosons with mass $m_{\text{th}} = 2.92 \times 10^{-22}$ eV/ c^2 and scattering length $(a_s)_{\text{th}} = -3.18 \times 10^{-68}$ fm (corresponding to $f_{\text{th}} = 1.34 \times 10^{17}$ GeV) is $M_{\max} = 5.10 \times 10^{10} M_\odot$ and the corresponding radius is $R_{99}^* = 1.09$ pc. The minimum halo ($M = 10^8 M_\odot$, $R = 1$ kpc) has a mass much smaller than the maximum mass ($M < M_{\max}$), so it is stable. The halo mass at which the core mass would become unstable ($M_c = M_{\max}$) and collapse is $(M_h)_{\max} = 1.01 \times 10^{20} M_\odot$. Since the largest DM halos observed in the Universe have a much smaller mass, of the order of $M_h \sim 10^{14} M_\odot \ll (M_h)_{\max}$, we conclude that the quantum cores of BECDM halos with an attractive self-interaction are always stable [$M_c < (M_c)_{\max}$]. Furthermore, since $M_h \ll (M_h)_{\max}$, the attractive self-interaction is negligible. This corroborates our previous claims [179,181] that the attractive self-interaction of the bosons can be neglected for what concerns the structure of DM halos in the nonlinear regime: Everything happens as if the bosons were not self-interacting.

Remark:—We recall that the theoretical value $f_{\text{th}} = 1.34 \times 10^{17}$ GeV comes from the constraints from particle physics and cosmology [147] (see Sec. IV D). It may be interesting to relax these constraints and consider arbitrary values of f . In that case, we find that an attractive self-interaction would be important in realistic DM halos of mass $M_h < 10^{14} M_\odot$, and lead to the collapse of their quantum core when $M_h = (M_h)_{\text{max}}$ [corresponding to $M_c = (M_c)_{\text{max}}$], if $f < 4.22 \times 10^{15}$ GeV [the bound corresponds to $(M_h)_{\text{max}} = 10^{14} M_\odot$ in Eq. (121)]. If values of f smaller than 4.22×10^{15} GeV are allowed, then the quantum core of a DM halo of mass $(M_h)_{\text{max}}$ [satisfying $(M_h)_{\text{max}} < 10^{14} M_\odot$] reaches the critical mass and collapses. This is the case of the BECcrit model, corresponding to $m_c = 2.19 \times 10^{-22}$ eV/ c^2 and $f_c = 1.97 \times 10^{14}$ GeV, for which $(M_h)_{\text{max}} = (M_c)_{\text{max}} = 10^8 M_\odot$ and $R_*^{99} = 1$ kpc. On the other hand, for $f = 1.34 \times 10^{15}$ GeV and $m = 10^{-22}$ eV/ c^2 we find that $(M_h)_{\text{max}} \sim 10^{12} M_\odot$, $(M_c)_{\text{max}} \sim 10^9 M_\odot$, and $R_*^{99} \sim 300$ pc. The collapse of the quantum core leads to a dense axion star (soliton) [156,201,204] or a bosonova [210].²⁰ However, we recall that values of f smaller than 4.22×10^{15} GeV are outside of the range 10^{16} GeV $\leq f \leq 10^{18}$ GeV predicted by particle physics and cosmology [147], so that, according to these constraints, we do not expect the collapse of the core to occur in realistic DM halos of mass $M_h < 10^{14} M_\odot$ (as discussed above).

D. Fermions

For fermions, the core mass–halo mass relation is (see Sec. VI.C of [179])

$$M_c = 3.83 \frac{\hbar^{3/2}}{m^2} \left(\frac{M_h \Sigma_0}{G^2} \right)^{3/8}. \quad (122)$$

The mass of the fermion required to account for the characteristics of the minimum halo is given by $m = 170$ eV/ c^2 (see Sec. II.A of [179]). For a DM halo of mass $M_h = 10^{12} M_\odot$ similar to the one that surrounds our Galaxy, we obtain a core mass $M_c = 4.47 \times 10^9 M_\odot$ and a core radius $R_c = 284$ pc. The quantum core represents a bulge or a nucleus. It cannot mimic a SMBH because it is too much extended ($Rc^2/GM \sim 10^6 \gg 1$).

The maximum mass and the minimum radius of a fermion star at $T = 0$ set by general relativity are [232]

$$M_{\text{max}}^{\text{GR}} = 0.384 \left(\frac{\hbar c}{G} \right)^{3/2} \frac{1}{m^2}, \quad R_{\text{min}}^{\text{GR}} = 8.73 \frac{GM_{\text{max}}^{\text{GR}}}{c^2}. \quad (123)$$

²⁰It does not lead to a SMBH which would be obtained for much larger values of f ($> 10^{18}$ GeV) [211,215] for which our previous assumptions do not apply.

These scalings can be obtained as explained in Appendix B.1 of [107]. For a fermion of mass $m = 170$ eV/ c^2 , we obtain $M_{\text{max}} = 2.17 \times 10^{13} M_\odot$ and $R_{\text{min}}^{\text{GR}} = 8.85$ pc. The maximum mass is much larger than the typical quantum core mass of a DM halo. According to Eq. (122) the mass of the fermion ball would be equal to the maximum mass ($M_c = M_{\text{max}}^{\text{GR}}$) in a DM halo of mass $M_h = 2.17 \times 10^{-3} c^4 / (G^2 \Sigma_0) = 6.71 \times 10^{21} M_\odot$ (this expression is independent of the fermion mass m) [181]. Such a large halo mass is clearly unrealistic (the biggest DM halos observed in the Universe have a mass $M_h \sim 10^{14} M_\odot$). Therefore, the fermion ball present at the center of a fermionic DM halo can never collapse toward a SMBH. This conclusion was first reached in Appendix C of [181]. Since $M_c \ll M_{\text{max}}^{\text{GR}}$ in all realistic DM halos, a nonrelativistic approach is justified.

Remark:—Let us assume that the object at the center of the MW is a fermion ball. Using the nonrelativistic mass–radius relation [see Eq. (6) in [179]]

$$M = 91.9 \frac{\hbar^6}{G^3 m^8 R^3} \quad (124)$$

with $M = 4.2 \times 10^6 M_\odot$ and $R = 6 \times 10^{-4}$ pc we get $m = 54.6$ keV/ c^2 [using the expression of the maximum mass from Eq. (123) with $M = 4.2 \times 10^6 M_\odot$ we get $m = 386$ keV/ c^2 but this situation is too extreme]. These values are forbidden by our model which assumes that the ground state of the self-gravitating Fermi gas corresponds to a minimum halo of mass $M = 10^8 M_\odot$ and radius $R = 1$ kpc. However, if we relax this assumption, it is possible to construct a realistic model of the MW in which a fermion ball mimics a SMBH. Such a model has been developed in [66,74] (see also [47,51,69]).

E. Conclusion

Following our previous works (see in particular Appendix C of [181]), we have shown that the quantum cores of bosonic and fermionic DM halos have a mass M_c much smaller than the general relativistic maximum mass $M_{\text{max}}^{\text{GR}}$ so they cannot collapse toward a SMBH. They are essentially Newtonian objects ($M_c \ll M_{\text{max}}^{\text{GR}}$). In the case of bosons with attractive self-interactions, provided that f lies in the range 10^{16} GeV $\leq f \leq 10^{18}$ GeV predicted by particle physics and cosmology, the core mass M_c of realistic DM halos ($M_h < 10^{14} M_\odot$) is always smaller than the maximum mass M_{max} found in [107] so they do not collapse. Therefore, the quantum cores of bosonic and fermionic DM halos are expected to be stable in all cases of astrophysical interest. They represent large quantum bulges. They may, however, evolve collisionally on a secular timescale and ultimately collapse toward a SMBH via the process of gravothermal catastrophe [286] followed by a dynamical instability of general relativistic

origin [287] if the halo mass M_h is sufficiently large (above the microcanonical critical point), as advocated in [169]. We have also shown that bosons with an attractive self-interaction behave essentially as noninteracting bosons in situations of astrophysical interest while bosons with a repulsive self-interaction can be very different from noninteracting bosons (their mass m may be 18 orders of magnitude larger). These conclusions were first reached in [179,181].

VI. JEANS MASS-RADIUS RELATION

In this section, we study how the Jeans length λ_J and the Jeans mass M_J of self-gravitating BECs depend on the density ρ . We apply these results in a cosmological context, during the matter era, where the density of BECDM evolves with time as (see, e.g., [153] for more details)

$$\frac{\rho}{\text{g/m}^3} = 2.25 \times 10^{-24} a^{-3}, \quad (125)$$

where a is the scale factor. The beginning of the matter era, which can be identified with the epoch of radiation-matter equality (i.e., the transition between the radiation era and the matter era), occurs at $a_{\text{eq}} = 2.95 \times 10^{-4}$. At that moment, the DM density is $\rho_{\text{eq}} = 8.77 \times 10^{-14} \text{ g/m}^3$. In comparison, the present density of DM is $\rho_0 = 2.25 \times 10^{-24} \text{ g/m}^3$ (corresponding to $a_0 = 1$). In the following, we compute the Jeans scales λ_J and M_J for any value of the density between the epoch of radiation-matter equality ρ_{eq} and the present epoch ρ_0 .

The Jeans instability analysis is valid during the linear regime of structure formation (it describes their initiation) which is expected to be close to the epoch of radiation-matter equality which marks the beginning of the matter era. By contrast, at the present epoch, nonlinear effects have become important (the DM halos are already formed) and the Jeans instability analysis is not valid anymore except at very large scales. We stress that the Jeans scales can only give an order of magnitude of the size and mass of the DM halos since these objects result from a very nonlinear process of free fall and violent relaxation which extends far beyond the linear regime. It is therefore not straightforward to relate quantitatively the characteristic sizes, masses, and densities of DM halos to the Jeans scales. Nevertheless, the Jeans approach provides a simple first step toward the problem of structure formation.

Let us consider a standard BEC at $T = 0$ with an equation of state given by Eq. (20). Using the corresponding expression of the speed of sound, the Jeans wave number (60) can be written as [107]

$$k_J^2 = \frac{8\pi|a_s|\rho}{m} \left[\sqrt{1 + \frac{Gm^4}{4\pi a_s^2 \hbar^2 \rho}} - \text{sgn}(a_s) \right]. \quad (126)$$

The Jeans radius and the Jeans mass defined by Eq. (63) are then given by

$$R_J = \frac{\left(\frac{\pi m}{8|a_s|\rho}\right)^{1/2}}{\left[\sqrt{1 + \frac{Gm^4}{4\pi a_s^2 \hbar^2 \rho}} - \text{sgn}(a_s)\right]^{1/2}}, \quad (127)$$

$$M_J = \frac{\frac{4}{3}\pi\left(\frac{\pi m}{8|a_s|\rho}\right)^{3/2}}{\rho^{1/2} \left[\sqrt{1 + \frac{Gm^4}{4\pi a_s^2 \hbar^2 \rho}} - \text{sgn}(a_s)\right]^{3/2}}. \quad (128)$$

Eliminating the density between Eqs. (127) and (128), we obtain the Jeans mass-radius relation

$$M_J = \frac{\frac{\pi^4}{12} \frac{\hbar^2}{Gm^2 R_J}}{1 - \pi^2 \frac{a_s \hbar^2}{Gm^3 R_J^2}}. \quad (129)$$

As noted in [107], this expression is similar to the approximate mass-radius relation of BECDM halos given by Eq. (69).²¹ Comparing Eqs. (69) and (129), we get $a_J = \pi^4/12 \simeq 8.12$ and $b_J = \pi$ which are close to the values of a and b obtained in Sec. III. This agreement is striking because the Jeans mass-radius relation [Eq. (129)] is valid in the linear regime of structure formation close to spatial homogeneity while the mass-radius relation of BECDM halos [Eq. (69)] is valid in the strongly nonlinear regime of structure formation (after free fall and violent relaxation) for very inhomogeneous objects. Before studying the relations (127)–(129) in the general case, we consider particular limits of these relations.

A. NI limit

In the NI limit ($a_s = 0$), the Jeans length and the Jeans mass are given by [76,79,87,102,107]

$$\lambda_J = 2\pi \left(\frac{\hbar^2}{16\pi G\rho m^2}\right)^{1/4}, \quad M_J = \frac{1}{6}\pi \left(\frac{\pi^3 \hbar^2 \rho^{1/3}}{Gm^2}\right)^{3/4}. \quad (130)$$

They can be written as

$$\frac{\lambda_J}{\text{pc}} = 1.16 \times 10^{-12} \left(\frac{\text{eV}/c^2}{m}\right)^{1/2} \left(\frac{\text{g/m}^3}{\rho}\right)^{1/4}, \quad (131)$$

$$\frac{M_J}{M_\odot} = 1.20 \times 10^{-20} \left(\frac{\text{eV}/c^2}{m}\right)^{3/2} \left(\frac{\rho}{\text{g/m}^3}\right)^{1/4}. \quad (132)$$

²¹The similarity between the mass-radius relation obtained from the f -ansatz and from the Jeans instability study is discussed at a general level in Appendix G.

Using Eq. (125), we find that the Jeans length increases as $a^{3/4}$ while the Jeans mass decreases as $a^{-3/4}$ (the comoving Jeans length decreases as $a^{-1/4}$). Eliminating the density between the relations of Eq. (130), we obtain

$$M_J \lambda_J = \frac{\pi^4 \hbar^2}{6 G m^2}. \quad (133)$$

This relation is similar to the mass-radius relation (43) of Newtonian BECDM halos made of noninteracting bosons [77,107,108].

B. TF limit

Let us consider bosons with a repulsive self-interaction ($a_s > 0$). In the TF limit ($\hbar = 0$), the Jeans length and the Jeans mass are given by [107]

$$\lambda_J = 2\pi \left(\frac{a_s \hbar^2}{G m^3} \right)^{1/2}, \quad M_J = \frac{1}{6} \pi \rho \left(\frac{4\pi^2 a_s \hbar^2}{G m^3} \right)^{3/2}. \quad (134)$$

They can be written as

$$\frac{\lambda_J}{\text{pc}} = 34.9 \left(\frac{a_s}{\text{fm}} \right)^{1/2} \left(\frac{eV/c^2}{m} \right)^{3/2}, \quad (135)$$

$$\frac{M_J}{M_\odot} = 3.30 \times 10^{20} \left(\frac{a_s}{\text{fm}} \right)^{3/2} \left(\frac{eV/c^2}{m} \right)^{9/2} \frac{\rho}{\text{g/m}^3}. \quad (136)$$

We note that the Jeans length is independent of the density (the comoving Jeans length decreases as a^{-1}) [107]. Using Eq. (125), we find that the Jeans mass decreases as a^{-3} . The relation from Eq. (134) is similar to the relation (48) determining the radius of a self-interacting BECDM halo in the TF approximation [78,82,89,96,98,107,228].

C. NG limit

Let us consider bosons with an attractive self-interaction ($a_s < 0$). In the nongravitational limit ($G = 0$), the Jeans length and the Jeans mass²² are given by [107]

$$\lambda_J = 2\pi \left(\frac{m}{16\pi |a_s| \rho} \right)^{1/2}, \quad M_J = \frac{\pi}{6} \frac{1}{\rho^{1/2}} \left(\frac{\pi m}{4|a_s|} \right)^{3/2}. \quad (137)$$

They can be written as

²²We call them ‘‘Jeans length’’ and ‘‘Jeans mass’’ by an abuse of language since there is no gravity in the present situation. The instability is a purely ‘‘hydrodynamic instability’’ (also called ‘‘tachyonic instability’’) due to the attractive self-interaction ($a_s < 0$) which yields a negative squared speed of sound ($c_s^2 < 0$). The ‘‘Jeans’’ terminology will make sense, however, in the general case (see Sec. VIE) where the instability is due to the combined effect of self-gravity and self-interaction.

$$\frac{\lambda_J}{\text{pc}} = 3.83 \times 10^{-26} \left(\frac{\text{fm}}{|a_s|} \right)^{1/2} \left(\frac{m}{eV/c^2} \right)^{1/2} \left(\frac{\text{g/m}^3}{\rho} \right)^{1/2}, \quad (138)$$

$$\frac{M_J}{M_\odot} = 4.36 \times 10^{-61} \left(\frac{\text{fm}}{|a_s|} \right)^{3/2} \left(\frac{m}{eV/c^2} \right)^{3/2} \left(\frac{\text{g/m}^3}{\rho} \right)^{1/2}. \quad (139)$$

Using Eq. (125), we find that the Jeans length and the Jeans mass both increase as $a^{3/2}$ (the comoving Jeans length increases as $a^{1/2}$). Eliminating the density between the relations of Eq. (137), we obtain

$$M_J = \frac{\pi^2}{24} \frac{m}{|a_s|} \lambda_J. \quad (140)$$

This relation is similar to the mass-radius relation of nongravitational BECDM halos with an attractive self-interaction given by Eq. (52) [108]. We recall, however, that these equilibrium states (valid in the nonlinear regime of structure formation) are unstable so they cannot arise in practice (see [107] for detail). Therefore, only the relations (137)–(140) obtained from the Jeans analysis in the linear regime of structure formation are physically meaningful. They determine the initiation of structures (clumps) in a homogeneous BEC due to the attractive self-interaction of the bosons. Their evolution in the nonlinear regime requires a specific analysis. Since these clumps cannot evolve toward stable DM halos with mass $M \sim M_J$ and radius $R \sim R_J$, they are expected to collapse toward smaller structures until repulsive terms in the self-interaction potential (such as φ^6 terms not considered here) come into play [156].

Remark: In the NG limit, the maximum growth rate of the instability is given by [see Eq. (66)]

$$\gamma_{\text{max}} = \frac{4\pi |a_s| \hbar \rho}{m^2}. \quad (141)$$

It corresponds to a wavelength [see Eq. (67)]

$$\lambda_m = 2\pi \left(\frac{m}{8\pi |a_s| \rho} \right)^{1/2} = \sqrt{2} \lambda_J. \quad (142)$$

D. Repulsive self-interaction

In order to determine the evolution of the Jeans scales with the density, we need to specify the parameters of the DM particle. For illustration, we use the parameters obtained in Sec. IV (see also Appendix D of [148] and Sec. II of [179]). They have been obtained in order to match the characteristics of a minimum halo of radius $R \sim 1$ kpc and mass $M \sim 10^8 M_\odot$, similar to Fornax, interpreted as the ground state of a self-gravitating BEC. We shall use this

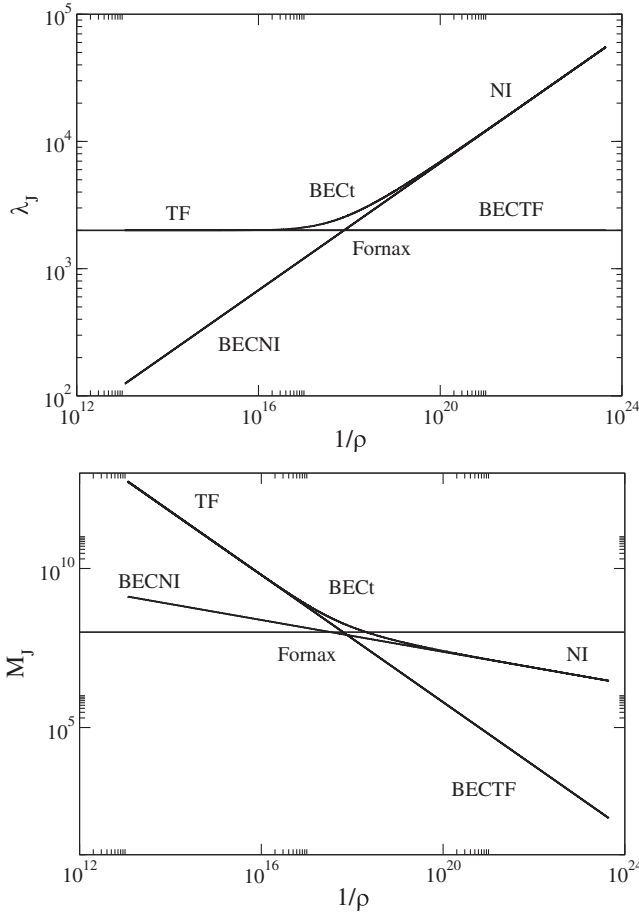


FIG. 6. Evolution of the Jeans length and Jeans mass with the inverse density of the universe for bosons with a repulsive self-interaction (λ_J is in pc, M_J is in solar masses M_\odot , and ρ is in g/m^3) for the three models BECNI, BECTF, and BECt considered in the text. Here and in the following figures we have indicated the values $\lambda_J/2 = 1$ kpc, $M_J = 10^8 M_\odot$, and $\rho = 1.62 \times 10^{-18} \text{ g}/\text{m}^3$ corresponding to the minimum halo (Fornax) for reference (see Sec. VIF).

procedure to determine the parameters of the DM particle, and then compute the Jeans scales at the epoch of radiation-matter equality and at the present epoch, instead of trying to determine the parameters of the DM particle directly from the Jeans scales.²³ In the present section, we consider the case of bosons with a repulsive self-interaction (or no self-interaction). We consider different types of DM particles denoted BECNI, BECTF, and BECt in Sec. IV. For each of these particles, the evolution of the Jeans length λ_J and Jeans mass M_J as a function of the inverse density $1/\rho$ (which increases with time as the Universe expands) is plotted in Fig. 6. The Jeans mass-radius relation (parametrized by the density) is plotted in Fig. 7. The curves start

²³We believe that this alternative procedure, often used in the literature, is less accurate.

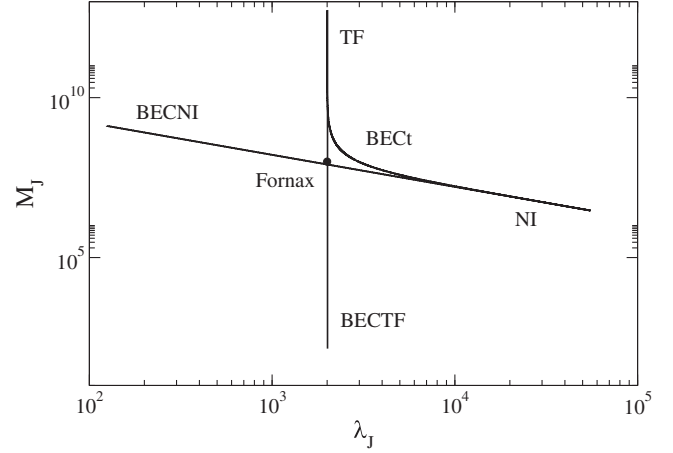


FIG. 7. Jeans-mass radius relation for bosons with a repulsive self-interaction for the three models BECNI, BECTF, and BECt described in the text. We see that the Jeans mass-radius relation (linear regime) is similar to the mass-radius relation of DM halos (nonlinear regime) represented in Fig. 2. The bullet corresponds to the typical mass and radius of dSphs like Fornax.

from the epoch of matter-radiation equality and end at the present epoch.

Generically, as the density of the universe decreases, the BEC is first in the TF regime and then in the NI regime. In the TF regime, the Jeans length is constant while the Jeans mass decreases as ρ (see Sec. VIB). In the NI regime, the Jeans length increases as $\rho^{-1/4}$ while the Jeans mass decreases as $\rho^{1/4}$ (see Sec. VIA). The transition between the TF regime and the NI regime occurs at a typical density

$$\rho_s = \frac{Gm^4}{16\pi\hbar^2 a_s^2} \quad (143)$$

obtained by equating Eqs. (130) and (134). At that point

$$(M_J)_s = \frac{\pi^3}{12} \frac{\hbar}{\sqrt{Gma_s}} \quad (144)$$

and

$$(\lambda_J)_s = 2\pi \left(\frac{a_s \hbar^2}{Gm^3} \right)^{1/2}. \quad (145)$$

The BEC is always in the NI regime (during the period going from the epoch of matter-radiation equality to the present epoch) if $1/\rho_s < 1/\rho_{\text{eq}}$, i.e., if

$$\frac{a_s}{m^2} < \left(\frac{G}{16\pi\hbar^2 \rho_{\text{eq}}} \right)^{1/2} = 3.71 \times 10^{-21} \frac{\text{fm}}{(\text{eV}/c^2)^2}. \quad (146)$$

Combining this inequality with the $m(a_s)$ relation of Sec. IV, we find that the BEC is always in the NI regime if $0 \leq a_s \leq 3.16 \times 10^{-64} \text{ fm}$ (and $m \sim 2.92 \times 10^{-22} \text{ eV}/c^2$).

This corresponds to $0 \leq \lambda \leq 1.17 \times 10^{-92}$. On the other hand, the BEC is always in the TF regime (during the same period) if $1/\rho_s > 1/\rho_0$, i.e., if

$$\frac{a_s}{m^2} > \left(\frac{G}{16\pi\hbar^2\rho_0} \right)^{1/2} = 7.32 \times 10^{-16} \frac{\text{fm}}{(\text{eV}/c^2)^2}. \quad (147)$$

Combining this inequality with the $m(a_s)$ relation of Sec. IV, we find that the BEC is always in the TF regime if $3.65 \times 10^{-53} \text{ fm} \leq a_s \leq (a_s)_{\text{max}} = 4.41 \times 10^{-6} \text{ fm}$ (and $2.23 \times 10^{-19} \text{ eV}/c^2 \leq m \leq m_{\text{max}} = 1.10 \times 10^{-3} \text{ eV}/c^2$). This corresponds to $1.04 \times 10^{-78} \leq \lambda \leq \lambda_{\text{max}} = 6.18 \times 10^{-16}$.

BECNI: Let us consider noninteracting ULAs with a mass $m = 2.92 \times 10^{-22} \text{ eV}/c^2$ determined by the characteristics of the minimum halo (see Sec. IV). At the epoch of radiation-matter equality, we find $\lambda_J = 124 \text{ pc}$ and $M_J = 1.31 \times 10^9 M_\odot$ (the comoving Jeans length is $\lambda_J^c = \lambda_J/a = 0.420 \text{ Mpc}$). At the present epoch, we find $\lambda_J = 55.3 \text{ kpc}$ and $M_J = 2.94 \times 10^6 M_\odot$.

BECTF: Let us consider self-interacting bosons with a mass $m = 1.10 \times 10^{-3} \text{ eV}/c^2$ and a scattering length $a_s = 4.41 \times 10^{-6} \text{ fm}$ (this yields $\lambda = 6.18 \times 10^{-16}$). This corresponds to a ratio $a_s/m^3 = 3.28 \times 10^3 \text{ fm}/(\text{eV}/c^2)^3$ determined by the radius of the minimum halo and to a ratio $4\pi a_s^2/m = 1.25 \text{ cm}^2/\text{g}$ determined by the constraint set by the Bullet Cluster assuming that the bound is reached (see Sec. IV). For the period considered, the BEC is always in the TF regime. At the epoch of radiation-matter equality, we find $\lambda_J = 2.01 \text{ kpc}$ and $M_J = 5.51 \times 10^{12} M_\odot$ (the comoving Jeans length is $\lambda_J^c = \lambda_J/a = 6.81 \text{ Mpc}$). At the present epoch we find $\lambda_J = 2.01 \text{ kpc}$ and $M_J = 141 M_\odot$.

BECT: Let us consider self-interacting bosons with a mass $m = 2.92 \times 10^{-22} \text{ eV}/c^2$ and a scattering length $a_s = 8.13 \times 10^{-62} \text{ fm}$ (this yields $\lambda = 3.02 \times 10^{-90}$). This corresponds to a ratio $a_s/m^3 = 3.28 \times 10^3 \text{ fm}/(\text{eV}/c^2)^3$ determined by the radius of the minimum halo and to a scattering length chosen such that the minimum halo is just at the transition between the TF regime and the NI regime (see Sec. IV). For the period considered, the BEC is first in the TF regime and then in the NI regime (the transition occurs at a typical density $\rho_s = 1.33 \times 10^{-18} \text{ g}/\text{m}^3$). At the epoch of radiation-matter equality, we find $\lambda_J = 2.00 \text{ kpc}$ and $M_J = 5.39 \times 10^{12} M_\odot$ (the comoving Jeans length is $\lambda_J^c = \lambda_J/a = 6.78 \text{ Mpc}$). At the present epoch we find $\lambda_J = 55.3 \text{ kpc}$ and $M_J = 2.94 \times 10^6 M_\odot$. In the TF regime, the BECt model behaves as the BECTF model (because they have the same ratio a_s/m^3) and in the NI regime, the BECt model behaves as the BECNI model corresponding to noninteracting ULAs (because they have the same mass m). This is apparent in Figs. 6 and 7.

BECf: Let us consider self-interacting bosons with a mass $m = 3 \times 10^{-21} \text{ eV}/c^2$ and a scattering length $a_s = 1.11 \times 10^{-58} \text{ fm}$ (this yields $\lambda = 4.24 \times 10^{-86}$). This fiducial model is motivated by cosmological considerations

[127]. It is similar to the BECt model. For the period considered, the BEC is first in the TF regime and then in the NI regime (the transition occurs at a typical density $\rho_s = 7.93 \times 10^{-21} \text{ g}/\text{m}^3$). At the epoch of radiation-matter equality, we find $\lambda_J = 2.24 \text{ kpc}$ and $M_J = 7.61 \times 10^{12} M_\odot$ (the comoving Jeans length is $\lambda_J^c = \lambda_J/a = 7.59 \text{ Mpc}$). At the present epoch we find $\lambda_J = 17.3 \text{ kpc}$ and $M_J = 9.05 \times 10^4 M_\odot$.

Remark:—ULA clumps formed in the linear regime by Jeans instability may evolve, in the nonlinear regime, into stable DM halos with mass $M \sim M_J$ and radius $R \sim R_J$ since self-gravitating BECs with a repulsive self-interaction are stable. They can then increase their mass by mergings and accretion (or possibly lose mass) leading to the DM halos observed in the universe. Large DM halos have a core-halo structure resulting from violent relaxation and gravitational cooling. The core mass-halo mass of self-interacting BECs has been determined in [169,179,181]. We have seen in Sec. V that the quantum core is always stable (it does not collapse toward a SMBH).

E. Attractive self-interaction

In this section, we consider the case of bosons with an attractive self-interaction. We consider different types of DM particles denoted BECcrit, BECth, and QCD axions in Sec. IV. For each of these particles, the evolution of the Jeans length λ_J and Jeans mass M_J as a function of the inverse density $1/\rho$ (which increases with time as the universe expands) is plotted in Fig. 8. The Jeans mass-radius relation (parametrized by the density) is plotted in Fig. 9. The curves start from the epoch of matter-radiation equality and end at the present epoch.

Generically, as the density of the universe decreases, the BEC is first in the NG regime and then in the NI regime. In the NG regime the Jeans length and the Jeans mass both increase as $\rho^{-1/2}$ (see Sec. VIC). In the NI regime the Jeans length increases as $\rho^{-1/4}$ while the Jeans mass decreases as $\rho^{1/4}$ (see Sec. VIA). There is a maximum Jeans mass

$$(M_J)_{\text{max}} = \frac{\pi^3}{24} \frac{\hbar}{\sqrt{Gm|a_s|}}, \quad (148)$$

corresponding to a Jeans length

$$(\lambda_J)_* = 2\pi \left(\frac{|a_s|\hbar^2}{Gm^3} \right)^{1/2}, \quad (149)$$

at the density

$$\rho_* = \frac{Gm^4}{32\pi\hbar^2 a_s^2}. \quad (150)$$

The transition between the NG regime and the NI regime occurs at a typical density

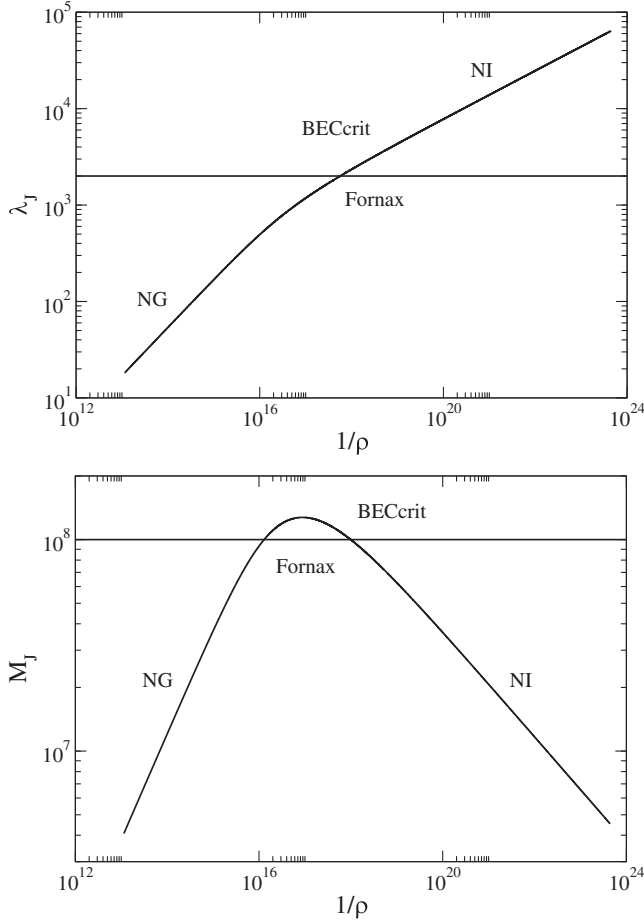


FIG. 8. Evolution of the Jeans length and Jeans mass with the inverse density of the universe for bosons with an attractive self-interaction (λ_J is in pc, M_J is in solar masses M_\odot , and ρ is in g/m^3) for the BECcrit model described in the text.

$$\rho_s = \frac{Gm^4}{16\pi\hbar^2 a_s^2}, \quad (151)$$

obtained by equating Eqs. (130) and (137). At that point

$$(M_J)_s = \frac{\pi^3}{12} \frac{\hbar}{\sqrt{Gm|a_s|}} \quad (152)$$

and

$$(\lambda_J)_s = 2\pi \left(\frac{|a_s|\hbar^2}{Gm^3} \right)^{1/2}. \quad (153)$$

These scales are similar to those corresponding to the maximum mass [we have $\rho_s = 2\rho_*$, $(M_J)_s = 2(M_J)_{\max}$ and $(\lambda_J)_s = (\lambda_J)_*$]. The BEC is always in the NI regime (during the period going from the epoch of matter-radiation equality to the present epoch) if $1/\rho_s < 1/\rho_{\text{eq}}$, i.e., if

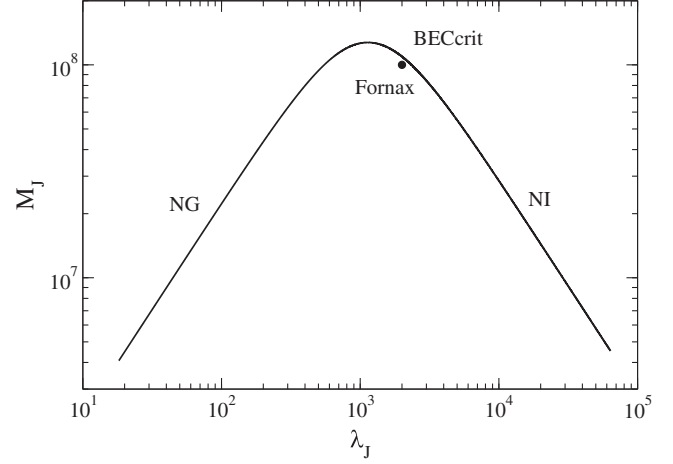


FIG. 9. Jeans-mass radius relation for bosons with an attractive self-interaction for the BECcrit model described in the text. We note that the Jeans mass-radius relation (linear regime) is similar to the mass-radius relation of DM halos (nonlinear regime) represented in Fig. 3.

$$\frac{|a_s|}{m^2} < \left(\frac{G}{16\pi\hbar^2\rho_{\text{eq}}} \right)^{1/2} = 3.71 \times 10^{-21} \frac{\text{fm}}{(\text{eV}/c^2)^2}. \quad (154)$$

Combining this inequality with the $m(a_s)$ relation of Sec. IV, we find that the BEC is always in the NI regime if $-3.16 \times 10^{-64} \text{ fm} \leq a_s \leq 0$ and $m \sim 2.92 \times 10^{-22} \text{ eV}/c^2$. This corresponds to $-1.18 \times 10^{-92} \leq \lambda \leq 0$ and $f \geq 1.35 \times 10^{15} \text{ GeV}$. On the other hand, the BEC is always in the NG regime (during the same period) if $1/\rho_s > 1/\rho_0$, i.e., if

$$\frac{|a_s|}{m^2} > \left(\frac{G}{16\pi\hbar^2\rho_0} \right)^{1/2} = 7.32 \times 10^{-16} \frac{\text{fm}}{(\text{eV}/c^2)^2}. \quad (155)$$

Combining this inequality with the $m(a_s)$ relation of Sec. IV, we find that the BEC is always in the NG regime if $-1.39 \times 10^{-65} \text{ fm} \leq a_s \leq 0$ and $m \leq 1.38 \times 10^{-25} \text{ eV}/c^2$. This corresponds to $-2.44 \times 10^{-97} \leq \lambda \leq 0$ and $f \sim f_{\min} = 1.39 \times 10^{14} \text{ GeV}$ (see Appendix E 4).

BECcrit: Let us consider self-interacting bosons with a mass $m = 2.19 \times 10^{-22} \text{ eV}/c^2$ and a scattering length $a_s = -1.11 \times 10^{-62} \text{ fm}$ (this yields $\lambda = -3.10 \times 10^{-91}$ and $f = 1.97 \times 10^{14} \text{ GeV}$). These values are obtained by requiring that the minimum halo is critical (see Sec. IV). For the period considered, the BEC is first in the NG regime and then in the NI regime (the transition occurs at a typical density $\rho_s = 2.25 \times 10^{-17} \text{ g}/\text{m}^3$). The Jeans mass is maximal at the density $\rho_* = 1.13 \times 10^{-17} \text{ g}/\text{m}^3$. At that density $(M_J)_{\max} = 1.27 \times 10^8 M_\odot$ and $(\lambda_J)_* = 1.13 \text{ kpc}$. At the epoch of radiation-matter equality, we find $\lambda_J = 18.2 \text{ pc}$ and $M_J = 4.08 \times 10^6 M_\odot$ (the comoving Jeans length is $\lambda_J^c = \lambda_J/a = 0.0617 \text{ Mpc}$). At the present epoch, we find $\lambda_J = 63.8 \text{ kpc}$ and $M_J = 4.53 \times 10^6 M_\odot$. When $\rho > \rho_s =$

$2.25 \times 10^{-17} \text{ g/m}^3$ the system is in the NG regime. It undergoes a hydrodynamic or tachyonic instability whose maximum growth rate is given by Eq. (141). At radiation-matter equality, we find $\gamma_{\text{max}} = 8.46 \times 10^{-12} \text{ s}^{-1}$. The growth rate of the instability is about 100 times larger than the Hubble rate $H = \dot{a}/a = (8\pi G\rho/3)^{1/2} = 2.21 \times 10^{-13} \text{ s}^{-1}$. Therefore, it is justified to assume in the stability analysis that the background is static (see Sec. II D). We thus find that the perturbation grows exponentially rapidly²⁴ on a timescale $\tau = 1/\gamma = 3.75 \times 10^3 \text{ yrs}$ and forms clumps of size $\lambda_m = \sqrt{2}\lambda_J = 25.7 \text{ pc}$ [see Eq. (142)] and mass $M_m = 2^{3/2}M_J = 1.15 \times 10^7 M_\odot$ [153]. Writing the evolution of the density contrast as $\delta(t) = \delta_i e^{\gamma t}$ and taking $\delta_i \sim 10^{-5}$ at the initial time of radiation-matter equality, we find that $\delta \sim 1$ in a time $t \sim 11.5\tau \sim 4.32 \times 10^4 \text{ yrs}$.

BECth: Let us consider self-interacting bosons with a mass $m = 2.92 \times 10^{-22} \text{ eV}/c^2$ and a scattering length $a_s = -3.18 \times 10^{-68} \text{ fm}$ (this yields $\lambda = -1.18 \times 10^{-96}$ and $f = 1.34 \times 10^{17} \text{ GeV}$). These values are obtained by using constraints from particle physics and cosmology (see Sec. IV D). For the period considered, the BEC is always in the NI regime (see the BECNI case studied above). At the epoch of radiation-matter equality, we find $\lambda_J = 124 \text{ pc}$ and $M_J = 1.31 \times 10^9 M_\odot$ (the comoving Jeans length is $\lambda_J^c = \lambda_J/a = 0.420 \text{ Mpc}$). At the present epoch, we find $\lambda_J = 55.3 \text{ kpc}$ and $M_J = 2.94 \times 10^6 M_\odot$. The Jeans mass is always much below the maximum Jeans mass $(M_J)_{\text{max}} = 6.52 \times 10^{10} M_\odot$ reached at a density $\rho_* = 4.33 \times 10^{-6} \text{ g/m}^3$. These results show that the effect of an attractive self-interaction is negligible for what concerns the formation of structures (clumps) in the linear regime: Everything happens *as if* the bosons were not self-interacting.

QCD axions: Let us consider QCD axions with a mass $m = 10^{-4} \text{ eV}/c^2$ and a scattering length $a_s = -5.8 \times 10^{-53} \text{ m}$ (this yields $\lambda = -7.39 \times 10^{-49}$ and $f = 5.82 \times 10^{10} \text{ GeV}$). For the period considered (matter era), the axions are always in the NI regime. At the epoch of radiation-matter equality, we find $\lambda_J = 2.13 \times 10^{-7} \text{ pc}$ and $M_J = 6.52 \times 10^{-18} M_\odot$ (the comoving Jeans length is $\lambda_J^c = \lambda_J/a = 7.22 \times 10^{-10} \text{ Mpc}$). At the present epoch we find $\lambda_J = 9.45 \times 10^{-5} \text{ pc}$ and $M_J = 1.47 \times 10^{-20} M_\odot$. The Jeans mass is always much below the maximum Jeans mass $(M_J)_{\text{max}} = 8.25 \times 10^{-14} M_\odot$ reached at a density $\rho_* = 1.79 \times 10^4 \text{ g/m}^3$. These results show that the effect of an attractive self-interaction is negligible for what

concerns the formation of structures (clumps) in the linear regime: Everything happens *as if* the QCD axions were not self-interacting.²⁵ Furthermore, the Jeans scales computed above are much smaller than the galactic scales, indicating that QCD axions essentially behave as CDM.

Remark: Noninteracting QCD axion clumps formed in the linear regime by Jeans instability may evolve, in the nonlinear regime, into stable dilute axion stars since non-interacting self-gravitating BECs are stable. They can then increase their mass by mergings and accretion (or possibly lose mass). If their mass passes above the maximum mass $M_{\text{max}} = 6.46 \times 10^{-14} M_\odot$ [107] they undergo gravitational collapse, leading to a bosonova or a dense axion star (see Sec. IV E). Nongravitational clumps of DM particles corresponding to the BECcrit parameters formed in the linear regime by Jeans instability cannot evolve, in the nonlinear regime, into stable configurations since non-gravitational BECs are unstable (see Sec. VI C). Therefore, they are expected to directly collapse, leading to bosonovae or dense solitons.²⁶ Noninteracting clumps of DM particles corresponding to the BECth parameters formed in the linear regime by Jeans instability may evolve, in the nonlinear regime, into stable DM halos with a core-halo profile since noninteracting self-gravitating BECs are stable. They can then increase their mass by mergings and accretion. We have seen in Sec. V C that, for realistic DM halos, the core mass M_c is always smaller than the critical mass M_{max} [107] so the quantum core (soliton) is always stable.

F. An optimal cosmological density

Except for QCD axions, all the models that we have considered above are based on values of m and a_s that are consistent with the properties of the minimum halo (see Sec. IV). Therefore, by construction, we have $M_J \sim 10^8 M_\odot$ and $R_J \sim 1 \text{ kpc}$ at a particular density $\rho = 3M/4\pi R^3 = 1.62 \times 10^{-18} \text{ g/m}^3$ during the evolution of the universe. This “optimal” density corresponds to a scale factor $a = 0.0111$ and a redshift $z = 1/a - 1 = 88.6$. If the structures formed at this epoch, they would have a Jeans mass and a Jeans radius comparable to the mass and size of the minimum halo ($M \sim 10^8 M_\odot$ and $R \sim 1 \text{ kpc}$). Actually, structures may form at a different epoch and evolve by accreting or losing mass during the nonlinear regime. The relation between the Jeans scales (in the linear regime) and the actual scales of DM halos (in the nonlinear regime) is not straightforward and usually requires one to study the nonlinear process of structure formation numerically.

²⁴This is at variance with the situation where the instability is of gravitational origin. In that case, γ is of the order of the Hubble rate H and it is compulsory to take into account the expansion of the universe in the stability analysis [278]. It is then found that $\delta(t)$ increases algebraically rapidly with time instead of exponentially rapidly.

²⁵This result is valid in the matter era. In the very early universe, QCD axions can form clumps of mass $M \sim 10^{-12} M_\odot$ and radius $R \sim 10^9 \text{ m}$ called axitons [230,288,289]. This is due to their attractive self-interaction (self-gravity is negligible in that regime).

²⁶Another possibility is that they become effectively non-interacting in the nonlinear regime and form stable dilute solitons.

VII. CONCLUSION

In this paper, following previous works on the subject, we have considered the possibility that DM is made of bosons in the form of self-gravitating BECs. This model is interesting because it may solve the small-scale problems of the standard CDM model such as the core-cusp problem and the missing satellite problem. Indeed, in the linear regime of structure formation due to the Jeans instability, quantum mechanics (Heisenberg uncertainty principle) or a repulsive self-interaction ($a_s > 0$) leads to a finite Jeans length λ_J even at $T = 0$. Therefore, gravitational collapse can take place only above a sufficiently large size and a sufficiently large mass (i.e., above λ_J and M_J). The existence of a minimum size and a minimum mass is in agreement with the observations. By contrast, in the classical pressureless CDM model ($\hbar = P = 0$), the Jeans length and the Jeans mass vanish ($\lambda_J = M_J = 0$), or are very small, implying the possibility of formation of structures at all scales in contradiction with the observations. On the other hand, in the nonlinear regime of structure formation (after the system has experienced free fall, violent relaxation, gravitational cooling, and virialization), the BECDM model leads to DM halos with a core, i.e., the central density is finite instead of diverging as r^{-1} for $r \rightarrow 0$ as in the CDM model. The prediction of DM halos with a core rather than a cusp is again in agreement with the observations.

According to the above results, the BECDM model predicts the existence of a “minimum DM halo” which corresponds to the ground state of the self-gravitating BEC at $T = 0$. We have identified this minimum (ultracompact) halo with dSphs like Fornax with a typical radius $R_{\min} = 1$ kpc and a typical mass $M_{\min} = 10^8 M_{\odot}$.²⁷ The ground state of the self-gravitating BEC also describes the quantum core of larger halos with $M_h > M_{\min}$. This quantum core is surrounded by an approximately isothermal atmosphere (mimicking the NFW profile) yielding flat rotation curves at large distances as discussed in, e.g., [169].

We have first determined an accurate expression of the core mass-radius relation $M(R)$ of self-gravitating BECs by combining approximate analytical results obtained from the Gaussian ansatz [107] with exact asymptotic results obtained by solving the GPP equations numerically [108]. Assuming that this mass-radius relation describes the minimum DM halo with $R_{\min} = 1$ kpc and $M_{\min} = 10^8 M_{\odot}$ (as well as the cores of larger DM halos) we have obtained an accurate expression of the DM mass-scattering length relation $m(a_s)$. This relation determines the mass m that the DM particle with a scattering length a_s should have in order to yield results that are consistent with the mass

²⁷We have taken these values for convenience. The numerical applications of our model could be refined by considering more accurate values of M_{\min} and R_{\min} but the order of magnitude of our results should be correct.

and size of the minimum halo typically representing a dSph.

For noninteracting bosons, we found

$$m = 2.92 \times 10^{-22} \text{ eV}/c^2, \quad (156)$$

which is the typical mass of the DM particle considered in FDM scenarios.

For bosons with an attractive self-interaction, we found that the mass of the DM particle is restricted by the inequality

$$2.19 \times 10^{-22} \text{ eV}/c^2 < m < 2.92 \times 10^{-22} \text{ eV}/c^2; \quad (157)$$

otherwise, dSphs like Fornax would be unstable (their mass would be above the maximum mass M_{\max} found in [107]). Therefore, an attractive self-interaction almost does not change the typical mass of the DM particle required to match the characteristics of the minimum halo (the boson mass is just a little smaller than the value from Eq. (156) in the noninteracting model). In addition, in line with our previous works [153,179,181], we have shown that, in situations of astrophysical interest, the effect of an attractive self-interaction is negligible both in the linear (see Sec. VI E) and nonlinear (see Sec. V C) regimes of structure formation. Therefore, in practice, bosons with an attractive self-interaction can be considered as noninteracting.²⁸

For bosons with a repulsive self-interaction, we found that the mass of the DM particle is restricted by the inequality

$$2.92 \times 10^{-22} \text{ eV}/c^2 < m < 1.10 \times 10^{-3} \text{ eV}/c^2, \quad (158)$$

where the maximum bound arises from the Bullet Cluster constraint. Therefore, a repulsive self-interaction can increase the typical mass of the DM particle by 18 orders of magnitude with respect to its value in the noninteracting case. As noted in Appendix D.4 of [148], a mass larger than $2.92 \times 10^{-22} \text{ eV}/c^2$ could alleviate some tensions with the observations of the Lyman- α forest encountered in the noninteracting model. Therefore, the self-interacting BEC model (with a repulsive self-interaction) may provide a solution to this problem. We have considered two typical self-interacting BEC models corresponding to $m = 1.10 \times 10^{-3} \text{ eV}/c^2$ and $a_s = 4.41 \times 10^{-6} \text{ fm}$ (BECTF) and $m = 2.92 \times 10^{-22} \text{ eV}/c^2$ and $a_s = 8.13 \times 10^{-62} \text{ fm}$ (BEct).

²⁸These conclusions are valid for ULAs with $m_{\text{th}} = 2.92 \times 10^{-22} \text{ eV}/c^2$ and $(a_s)_{\text{th}} = -3.18 \times 10^{-68} \text{ fm}$ (BEct_{th}) that may form DM halos while fulfilling the constraints from particle physics and cosmology (see Secs. IV D). By contrast, the attractive self-interaction of QCD axions is crucial in the context of QCD axion stars (see Sec. IV E) while being negligible in the linear regime of structure formation (see Sec. VI E). This suggests that the attractive self-interaction of QCD axions becomes important in the nonlinear regime of structure formation.

We have then shown that the Jeans mass-radius relation $M_J(R_J)$, which is valid in the linear regime of structure formation, is similar to the mass-radius relation $M(R)$ of the minimum BECDM halo (or to the core mass-radius relation of larger halos), corresponding to the ground state of the GPP equations, which is valid in the nonlinear regime of structure formation. This analogy allows us to directly apply some results obtained in the context of (nonlinear) self-gravitating BECs to the Jeans (linear) instability problem and vice versa.

The two curves $M_J(R_J)$ and $M(R)$ are parametrized by a typical density [the density of the universe for the $M_J(R_J)$ relation and the average—or central—density of the BEC for the $M(R)$ relation] going from high values to low values.²⁹ For noninteracting bosons, the mass decreases as the radius increases. For bosons with a repulsive self-interaction, there is a minimum radius at which $M \rightarrow +\infty$ corresponding to the TF limit. The mass decreases as the radius increases, going from the TF limit (high densities) to the NI limit (low densities). For bosons with an attractive self-interaction, the mass first increases as the radius increases, reaches a maximum value M_{\max} , and then decreases, going from the NG limit (high densities) to the NI limit (low densities).

Despite these analogies, the curves $M_J(R_J)$ and $M(R)$ have a very different physical interpretation. The curve $M_J(R_J)$ determines the Jeans mass and the Jeans radius at different epochs in the history of the universe characterized by its density ρ [in that case it is more relevant to plot $M_J(\rho)$ and $R_J(\rho)$ individually]. The Jeans scales determine the minimum mass and the minimum size of a condensation that can become unstable and form a clump. We must be careful, however, that the Jeans instability study is valid only in the linear regime of structure formation. As a result, the interpretation of the curve $M_J(R_J)$ and its domain of validity is not straightforward. In principle, the results of the linear Jeans instability study are valid only in a sufficiently young universe (typically the beginning of the matter era) where $\rho_{\text{eq}} = 8.77 \times 10^{-14} \text{ g/m}^3$. It is not clear if we can apply the results of the Jeans instability study at later epochs. On the other hand, the curve $M(R)$ determines the mass-radius relation of DM halos that are formed in the nonlinear regime of structure formation after having experienced free fall, violent relaxation, gravitational cooling, and virialization. It applies to the minimum halo

or to the quantum core of larger halos.³⁰ We expect that the mass and the size of the minimum halo is of the order of the Jeans mass and Jeans radius ($M \sim M_J$ and $R \sim R_J$) calculated at the “relevant” epoch of structure formation. There is, however, an uncertainty about what this epoch is (see Sec. VIF). Furthermore, the relation between the Jeans scales and the characteristics of DM halos is not straightforward. In practice, the linear Jeans instability occurs at a certain epoch, leading to weakly inhomogeneous clumps of mass M_J and radius R_J . Then, these clumps evolve in the nonlinear regime ultimately leading to DM halos of minimum mass $M \sim M_J$ and minimum radius $R \sim R_J$. The DM halos may also merge (or inversely lose mass) so that their actual mass M and radius R may be different from M_J and R_J . On the other hand, the $M(R)$ relation may present regions of instability such as the NG branch of Fig. 3. The solutions on these branches cannot correspond to observable DM halos since they are unstable. These branches are therefore forbidden in the nonlinear problem of structure formation. However, the corresponding branches in the Jeans mass-radius relation $M_J(R_J)$ have their usual interpretation. They determine the mass and size triggering the gravitational instability in the linear regime. The existence of stable and unstable branches in the mass-radius relation $M(R)$ of DM halos leads to the different evolutions described at the end of Secs. VID and VIE. Typically, we have two possibilities:

- (i) Consider first a branch of the $M_J(R_J)$ relation such that the corresponding branch of the $M(R)$ relation is stable (for example, the NI branch or the TF branch). In that case, clumps of mass M_J and R_J formed in the linear regime by Jeans instability evolve, in the nonlinear regime, into stable DM halos of mass $M \sim M_J$ and radius $R \sim R_J$. They can then increase their mass by mergings and accretion (or possibly lose mass) leading to the DM halos observed in the universe.
- (ii) Consider now a branch of the $M_J(R_J)$ relation such that the corresponding branch of the $M(R)$ relation is unstable (for example, the NG branch). In that case, clumps of mass M_J and R_J formed in the linear regime by Jeans instability cannot evolve, in the nonlinear regime, into DM halos of mass $M \sim M_J$

²⁹In cosmology, it is natural to follow the series of equilibria $M_J(R_J)$ from high to low values of the density because this corresponds to the temporal evolution of the universe (from early to late epochs). In the context of DM halos, as in the case of compact stars [273], it may be more relevant to follow the series of equilibria $M(R)$ from low to high values of the density because this corresponds to their natural evolution.

³⁰In principle, even if we know the parameters of the DM particle (its mass m and scattering length a_s), we cannot determine the mass M and the radius R of the minimum halo individually. We just know its mass-radius relation $M(R)$. However, if we assume a universal value $\Sigma_0 = 141 M_\odot/\text{pc}^2$ of the surface density of DM halos compatible with the observations, then we can determine the mass $(M_h)_{\min}$ and the radius $(R_h)_{\min}$ of the minimum halo individually. This is done in [169] and in Sec. II of [179] where the mass $(M_h)_{\min}$ and the radius $(R_h)_{\min}$ of the minimum halo are expressed in terms of m , a_s , and Σ_0 . We can then see if they coincide with the Jeans scales (see Appendix I of [179]).

and radius $R \sim R_J$ since such halos are unstable. They rather undergo an explosion [210] or a violent (nonlinear) gravitational collapse leading presumably to smaller and denser objects stabilized by higher order repulsive terms (e.g., φ^6 terms) in the self-interaction potential [156,201,204]. Another possibility is that the clumps migrate from the nongravitational branch to the noninteracting branch during the nonlinear regime of structure formation so that they can ultimately form stable structures.

In the present paper, we have illustrated our results for bosons interacting via a φ^4 potential. We have considered the case of a vanishing ($a_s = 0$), repulsive ($a_s > 0$), or attractive ($a_s < 0$) self-interaction. The model of noninteracting bosons (FDM) leads to a boson mass $m \sim 10^{-22}$ eV/ c^2 that creates some tensions with the observations of the Lyman- α forest [147]. These observations require a larger mass of at least 1 order of magnitude. We have shown that the model of bosons with an attractive self-interaction necessitates a mass even smaller than $m \sim 10^{-22}$ eV/ c^2 (according to Fig. 4 the mass m decreases as $|a_s|$ increases when $a_s < 0$). This model is therefore also in tension with the observations. By contrast, the model of bosons with a repulsive self-interaction allows a boson mass which can be up to 18 orders of magnitude larger than $m \sim 10^{-22}$ eV/ c^2 (according to Fig. 4 the mass m increases as a_s increases when $a_s > 0$). As noted in [148] this model could alleviate some tensions with the observations of the Lyman- α forest encountered in the noninteracting model. As a result, a repulsive self-interaction ($a_s > 0$) is privileged over an attractive self-interaction ($a_s < 0$) [169]. A repulsive self-interaction is also favored by cosmological constraints [127,148] which yield a fiducial model with a mass $m = 3 \times 10^{-21}$ eV/ c^2 and a scattering length $a_s = 1.11 \times 10^{-58}$ fm (BEcf). We recall that theoretical models of particle physics usually lead to particles with an attractive self-interaction (e.g., the QCD axion). However, some authors [143,182] have pointed out the possible existence of particles with a repulsive self-interaction (e.g., the light majoron).

APPENDIX A: DERIVATION OF THE SCHRÖDINGER EQUATION

In this appendix, we briefly recall the derivation of the Schrödinger equation from the formalism of scale relativity [290]. We follow the presentation given in Ref. [291].

Nottale [290] has shown that the equation that governs the motion of a particle in a nondifferentiable (fractal) spacetime can be written in the form of the fundamental equation of dynamics,

$$\frac{DU}{Dt} = -\nabla\Phi, \quad (\text{A1})$$

where $\mathbf{F} = -\nabla\Phi$ is the force by unit of mass exerted on a particle, provided that $\mathbf{U}(\mathbf{r}, t)$ is interpreted as a complex velocity field and D/Dt is a complex time derivative operator (or covariant derivative) defined by

$$\frac{D}{Dt} = \frac{\partial}{\partial t} + \mathbf{U} \cdot \nabla - i\mathcal{D}\Delta, \quad (\text{A2})$$

where \mathcal{D} is the fractal fluctuation parameter in the theory of scale relativity. Using the expression (A2) of the covariant derivative, Eq. (A1) can be rewritten as a complex viscous Burgers equation

$$\frac{\partial\mathbf{U}}{\partial t} + (\mathbf{U} \cdot \nabla)\mathbf{U} = i\mathcal{D}\Delta\mathbf{U} - \nabla\Phi \quad (\text{A3})$$

with an imaginary viscosity $\nu = i\mathcal{D}$. It can be shown [290] that the complex velocity field can be written as the gradient of a complex action:

$$\mathbf{U} = \frac{\nabla S}{m}. \quad (\text{A4})$$

This defines a potential flow. As a consequence, the flow is irrotational: $\nabla \times \mathbf{U} = \mathbf{0}$. Using the well-known identities of fluid mechanics $(\mathbf{U} \cdot \nabla)\mathbf{U} = \nabla(\mathbf{U}^2/2) - \mathbf{U} \times (\nabla \times \mathbf{U})$ and $\Delta\mathbf{U} = \nabla(\nabla \cdot \mathbf{U}) - \nabla \times (\nabla \times \mathbf{U})$ which reduce to $(\mathbf{U} \cdot \nabla)\mathbf{U} = \nabla(\mathbf{U}^2/2)$ and $\Delta\mathbf{U} = \nabla(\nabla \cdot \mathbf{U})$ for an irrotational flow, and using the identity $\nabla \cdot \mathbf{U} = \Delta S/m$ resulting from Eq. (A4), we find that Eq. (A3) is equivalent to the complex quantum Hamilton-Jacobi (or Bernoulli) equation

$$\frac{\partial S}{\partial t} + \frac{1}{2m}(\nabla S)^2 - i\mathcal{D}\Delta S + m\Phi = 0. \quad (\text{A5})$$

We now define the wave function $\psi(\mathbf{r}, t)$ through the complex Cole-Hopf transformation

$$S = -2im\mathcal{D} \ln \psi. \quad (\text{A6})$$

Substituting Eq. (A6) into Eq. (A5), and using the identity

$$\Delta(\ln \psi) = \frac{\Delta\psi}{\psi} - \frac{1}{\psi^2}(\nabla\psi)^2, \quad (\text{A7})$$

we obtain the equation

$$i\mathcal{D} \frac{\partial\psi}{\partial t} = -\mathcal{D}^2 \Delta\psi + \frac{1}{2}\Phi\psi. \quad (\text{A8})$$

This equation coincides with the Schrödinger equation

$$i\hbar \frac{\partial\psi}{\partial t} = -\frac{\hbar^2}{2m} \Delta\psi + m\Phi\psi \quad (\text{A9})$$

provided that we set

$$\mathcal{D} = \frac{\hbar}{2m}, \quad (\text{A10})$$

which is the expression of the Nelson [292] diffusion coefficient of quantum mechanics. With this identification, the Cole-Hopf transformation of fluid mechanics [Eq. (A6)] is equivalent to the WKB formula

$$\psi = e^{iS/\hbar}, \quad (\text{A11})$$

and the Schrödinger equation (A9) is equivalent to the fundamental equation of dynamics (A1).

APPENDIX B: EQUIVALENCE BETWEEN THE STABILITY CRITERIA BASED ON THE ENERGY PRINCIPLE AND ON THE EQUATION OF PULSATIONS

In this appendix, we discuss the equivalence between the stability criterion based on the energy principle (see Appendix B 1) and the stability criterion based on the equation of pulsations (see Appendix B 2).

1. Energy principle

The GPP equations (1) and (2), or equivalently the quantum Euler equations (10)–(13), conserve the mass M and the energy E_{tot} defined by Eqs. (21) and (22) (see, e.g., Appendix E of [107]). Using very general arguments [293], this implies the following:

- (i) *An equilibrium state of the GPP equations is an extremum of energy at fixed mass.* This result can be proven as follows. Let us write the variational problem for the first variations as

$$\delta E_{\text{tot}} - \frac{\mu}{m} \delta M = 0, \quad (\text{B1})$$

where μ (global chemical potential) is a Lagrange multiplier taking into account the mass constraint. Using Eqs. (B31)–(B34), and treating the perturbations $\delta \mathbf{u}$ and $\delta \rho$ independently, we obtain $\mathbf{u} = \mathbf{0}$ (the equilibrium state is static) and the quantum Gibbs condition (see footnote 8)

$$Q + mh + m\Phi = \mu, \quad (\text{B2})$$

which is equivalent to the condition of quantum hydrostatic equilibrium (see Sec. II C and Appendix B 2).

- (ii) *An equilibrium state of the GPP equations is stable if, and only if, it is a minimum of energy at fixed mass.* We will establish this result in Appendix B 3 directly from the equation of pulsations. Since $\delta^2 \Theta_c$ depends only on $\delta \mathbf{u}$ and is positive [see Eq. (B35) with $\mathbf{u} = \mathbf{0}$], and since the perturbations $\delta \mathbf{u}$ and $\delta \rho$ are treated independently, we can equivalently claim

that an equilibrium state of the GPP equations is stable if, and only if, it is a minimum of the reduced energy $E_{\text{tot}}^* = \Theta_Q + U + W$ (excluding the classical kinetic energy) at fixed mass. The condition of dynamical stability based on the energy principle is therefore

$$\delta^2 E_{\text{tot}}^* > 0 \quad (\text{B3})$$

for all perturbations $\delta \rho$ that conserve mass ($\delta M = 0$). Using the identities of Appendix B 4, we find that the second order variations of the energy are given by

$$\delta^2 E_{\text{tot}}^* = \frac{1}{2} \int \left(\frac{\delta Q}{m} + \delta h + \delta \Phi \right) \delta \rho d\mathbf{r} \quad (\text{B4})$$

or, equivalently, by

$$\begin{aligned} \delta^2 E_{\text{tot}}^* = & \frac{1}{2} \int h'(\rho) (\delta \rho)^2 d\mathbf{r} + \frac{1}{2} \int \delta \Phi \delta \rho d\mathbf{r} \\ & + \frac{\hbar^2}{8m^2} \int \frac{1}{\rho} \left[(\nabla \delta \rho)^2 + \left(\frac{\Delta \rho}{\rho} - \frac{(\nabla \rho)^2}{\rho^2} \right) (\delta \rho)^2 \right] d\mathbf{r}, \end{aligned} \quad (\text{B5})$$

where we recall that $h'(\rho) = P'(\rho)/\rho$ (see Appendix H).

Remark:—The minimization problem (39) expressing the energy principle is a criterion of nonlinear dynamical stability resulting from the fact that E_{tot} and M are conserved by the GPP equations [293]. It provides a necessary and sufficient condition of dynamical stability since it takes into account all the invariants of the GPP equations.

2. Equation of pulsations

The quantum Euler-Poisson equations (10)–(13) may be written as

$$\frac{\partial \rho}{\partial t} + \nabla \cdot (\rho \mathbf{u}) = 0, \quad (\text{B6})$$

$$\frac{\partial \mathbf{u}}{\partial t} + (\mathbf{u} \cdot \nabla) \mathbf{u} = -\frac{1}{m} \nabla Q - \nabla h - \nabla \Phi, \quad (\text{B7})$$

$$\Delta \Phi = 4\pi G \rho, \quad (\text{B8})$$

where we have introduced the enthalpy $h(\rho) = V'(\rho)$ through the relation (see Appendix H)

$$\nabla h = \frac{\nabla P}{\rho}. \quad (\text{B9})$$

A steady state of the quantum Euler equation (B7) satisfies the condition of quantum hydrostatic equilibrium (see Sec. IIC)

$$\frac{\nabla Q}{m} + \nabla h + \nabla \Phi = \mathbf{0}, \quad (\text{B10})$$

which is equivalent to Eq. (B2). Combined with the Poisson equation (B8) we obtain the fundamental differential equation determining the equilibrium structure of a self-gravitating BEC under the form

$$\frac{\Delta Q}{m} + \Delta h = -4\pi G\rho, \quad (\text{B11})$$

where the density can be viewed as a function $\rho(h)$ of the enthalpy. This equation is equivalent to Eq. (37).

Let us consider a stationary solution of the quantum Euler-Poisson equations (B6)–(B8) satisfying $\mathbf{u} = \mathbf{0}$ and the condition of quantum hydrostatic equilibrium (B10). The linearized quantum Euler-Poisson equations around this equilibrium state are

$$\frac{\partial \delta \rho}{\partial t} + \nabla \cdot (\rho \delta \mathbf{u}) = 0, \quad (\text{B12})$$

$$\frac{\partial \delta \mathbf{u}}{\partial t} = -\frac{1}{m} \nabla \delta Q - \nabla \delta h - \nabla \delta \Phi, \quad (\text{B13})$$

$$\Delta \delta \Phi = 4\pi G \delta \rho. \quad (\text{B14})$$

It is convenient to introduce the Lagrangian displacement $\vec{\zeta} = \delta \mathbf{r}$ such that

$$\delta \mathbf{u} = \frac{\partial \vec{\zeta}}{\partial t}. \quad (\text{B15})$$

The linearized continuity equation (B12) leads to the relation

$$\delta \rho = -\nabla \cdot (\rho \vec{\zeta}). \quad (\text{B16})$$

Writing the evolution of the perturbation as $e^{-i\omega t}$, Eq. (B15) implies that $\delta \mathbf{u} = -i\omega \vec{\zeta}$. On the other hand, the linearized quantum Euler equation (B13) becomes

$$\omega^2 \vec{\zeta} = \frac{1}{m} \nabla \delta Q + \nabla \delta h + \nabla \delta \Phi. \quad (\text{B17})$$

Using Eq. (B16) and Eqs. (B39)–(B42), the first order variations δQ , δh , and $\delta \Phi$ can be expressed in terms of $\vec{\zeta}$. In this manner, Eq. (B17) represents the quantum generalization of the equation of pulsations in the form given by Chandrasekhar [294]. This is an eigenvalue equation determining the possible pulsations of the system. The equilibrium state is stable if $\omega^2 > 0$ for all modes (in that

case the perturbation oscillates) and unstable if $\omega^2 < 0$ for some modes (in that case the perturbation grows exponentially rapidly). Using Eqs. (B16), (B39), and (B48), we can rewrite Eq. (B17) more explicitly as

$$\omega^2 \vec{\zeta} = \frac{1}{m} \nabla \delta Q - \nabla \left[\frac{P'(\rho)}{\rho} \nabla \cdot (\rho \vec{\zeta}) \right] - 4\pi G \rho \vec{\zeta}. \quad (\text{B18})$$

Alternatively, combining Eqs. (B16) and (B17), we can write the quantum equation of pulsations under the form

$$-\omega^2 \delta \rho = \nabla \cdot \left[\rho \left(\frac{\nabla \delta Q}{m} + \nabla \delta h + \nabla \delta \Phi \right) \right], \quad (\text{B19})$$

where δQ , δh , and $\delta \Phi$ are expressed in terms of $\delta \rho$ through Eqs. (B39)–(B42).

If we consider a spherically symmetric distribution of matter, and consider radial perturbations, it is convenient to introduce the quantity q from the relation [295]

$$\delta \rho = \frac{1}{4\pi r^2} \frac{dq}{dr}. \quad (\text{B20})$$

Physically, $q(r, t) = \delta M(r, t) = \int_0^r \delta \rho(r', t) 4\pi r'^2 dr'$ represents the perturbed mass within the sphere of radius r . The perturbed Newton equation takes the form

$$\frac{d\delta \Phi}{dr} = \frac{Gq}{r^2}. \quad (\text{B21})$$

Since

$$\delta \rho = -\frac{1}{r^2} \frac{d}{dr} (r^2 \rho \zeta), \quad (\text{B22})$$

we obtain the relation

$$\zeta = -\frac{q}{4\pi \rho r^2}. \quad (\text{B23})$$

Starting from Eq. (B18) or from Eq. (B19), and using Eq. (B23) or Eq. (B20), we obtain

$$\frac{d}{dr} \left(\frac{P'(\rho)}{4\pi \rho r^2} \frac{dq}{dr} \right) + \frac{Gq}{r^2} + \frac{1}{m} \frac{d\delta Q}{dr} = -\frac{\omega^2}{4\pi \rho r^2} q. \quad (\text{B24})$$

This is the quantum generalization of the equation of pulsations in the form given by Chavanis (see Appendix A of [295]). Starting from Eq. (B18) or from Eq. (B24), we obtain after some calculations

$$\frac{d}{dr} \left[\gamma P \frac{1}{r^2} \frac{d}{dr} (r^2 \zeta) \right] - \frac{4}{r} \frac{dP}{dr} \zeta - \frac{\rho}{m} \Delta Q \zeta - \frac{\rho}{m} \frac{d\delta Q}{dr} = -\omega^2 \rho \zeta, \quad (\text{B25})$$

where we have defined

$$\gamma(r) = \frac{d \ln P}{d \ln \rho} = \frac{\rho}{P} P'(\rho). \quad (\text{B26})$$

Introducing the variable $\xi = \zeta/r$, we can transform Eq. (B25) into

$$\begin{aligned} \frac{d}{dr} \left(\gamma P r^4 \frac{d\xi}{dr} \right) + r^3 \frac{d}{dr} [(3\gamma - 4)P] \xi \\ - \frac{\rho}{m} \Delta Q r^4 \xi - \frac{\rho}{m} r^3 \frac{d\delta Q}{dr} = -\omega^2 \rho r^4 \xi. \end{aligned} \quad (\text{B27})$$

This is the quantum generalization of the equation of pulsations in the form given by Eddington [296].

3. Equivalence between $\omega^2 > 0$ and $\delta^2 E_{\text{tot}}^* > 0$

Taking the scalar product of Eq. (B17) with $\rho \vec{\zeta}$ and integrating over the whole domain we obtain

$$\omega^2 \int \rho \zeta^2 d\mathbf{r} = \int \rho \vec{\zeta} \cdot \nabla \left(\frac{\delta Q}{m} + \delta h + \delta \Phi \right) d\mathbf{r}. \quad (\text{B28})$$

Integrating the second integral by parts and using Eq. (B16), we can rewrite Eq. (B28) as

$$\omega^2 \int \rho \zeta^2 d\mathbf{r} = \int \delta \rho \left(\frac{\delta Q}{m} + \delta h + \delta \Phi \right) d\mathbf{r}. \quad (\text{B29})$$

Comparing the right-hand side of this expression with the second variations of the energy functional from Eq. (B4), we obtain the identity

$$\frac{1}{2} \omega^2 \int \rho \zeta^2 d\mathbf{r} = \delta^2 E_{\text{tot}}^*. \quad (\text{B30})$$

Since the integral is positive, this identity shows that an equilibrium state of the GPP equations is dynamically stable ($\omega^2 > 0$) if, and only if, it is a minimum of energy at fixed mass ($\delta^2 E_{\text{tot}}^* > 0$). Therefore, the stability criteria based on the equation of pulsations and on the energy principle are equivalent. This identity also provides the basis for a quantum generalization of the Chandrasekhar variational principle [294].

Remark:—Since the total energy is conserved, we have $\delta^2 E_{\text{tot}} = 0$ or, equivalently, $\delta^2 \Theta_c + \delta^2 E_{\text{tot}}^* = 0$. Using Eq. (B35) with $\mathbf{u} = \mathbf{0}$ and $\delta \mathbf{u} = -i\omega \vec{\zeta}$, we see that this identity is equivalent to Eq. (B30). On the other hand, since $\delta^2 \Theta_c \geq 0$, the identity $\delta^2 \Theta_c + \delta^2 E_{\text{tot}}^* = 0$ implies the following results: (i) If $\delta^2 E_{\text{tot}}^* > 0$, we cannot have growing modes so the system is stable. (ii) If $\delta^2 E_{\text{tot}}^* < 0$, we can have a growing mode so the system is unstable. This directly establishes the stability result based on the energy principle (see Appendix B 1).

4. Useful identities

The first order variations of the functionals defined by Eqs. (23)–(26) are

$$\delta \Theta_c = \int \delta \rho \frac{\mathbf{u}^2}{2} d\mathbf{r} + \int \rho \mathbf{u} \cdot \delta \mathbf{u} d\mathbf{r}, \quad (\text{B31})$$

$$\delta \Theta_Q = \int \frac{Q}{m} \delta \rho d\mathbf{r}, \quad (\text{B32})$$

$$\delta U = \int V'(\rho) \delta \rho d\mathbf{r} = \int h(\rho) \delta \rho d\mathbf{r}, \quad (\text{B33})$$

$$\delta W = \int \Phi \delta \rho d\mathbf{r}, \quad (\text{B34})$$

where we have used $h(\rho) = V'(\rho)$ (see Appendix H). The second order variations of these functionals are

$$\delta^2 \Theta_c = \int \rho \frac{(\delta \mathbf{u})^2}{2} d\mathbf{r} + \int \delta \rho \mathbf{u} \cdot \delta \mathbf{u} d\mathbf{r}, \quad (\text{B35})$$

$$\delta^2 \Theta_Q = \frac{1}{2} \int \delta \rho \frac{\delta Q}{m} d\mathbf{r}, \quad (\text{B36})$$

$$\begin{aligned} \delta^2 U &= \frac{1}{2} \int V''(\rho) (\delta \rho)^2 d\mathbf{r} = \frac{1}{2} \int h'(\rho) (\delta \rho)^2 d\mathbf{r} \\ &= \frac{1}{2} \int \delta h \delta \rho d\mathbf{r}, \end{aligned} \quad (\text{B37})$$

$$\delta^2 W = \frac{1}{2} \int \delta \Phi \delta \rho d\mathbf{r}. \quad (\text{B38})$$

We also note that δh , $\delta \Phi$, and δQ are related to $\delta \rho$ by

$$\delta h = h'(\rho) \delta \rho = \frac{P'(\rho)}{\rho} \delta \rho, \quad (\text{B39})$$

$$\delta \Phi = -G \int \frac{\delta \rho(\mathbf{r}')}{|\mathbf{r} - \mathbf{r}'|} d\mathbf{r}', \quad (\text{B40})$$

$$\delta Q = \frac{\hbar^2}{4m} \frac{1}{\sqrt{\rho}} \left[\frac{\delta \rho}{\rho} \Delta \sqrt{\rho} - \Delta \left(\frac{\delta \rho}{\sqrt{\rho}} \right) \right], \quad (\text{B41})$$

or

$$\delta Q = \frac{\hbar^2}{4m} \left[\frac{\Delta \rho}{\rho^2} \delta \rho - \frac{\Delta \delta \rho}{\rho} - \frac{1}{\rho^3} (\nabla \rho)^2 \delta \rho + (\nabla \rho \cdot \nabla \delta \rho) \frac{1}{\rho^2} \right], \quad (\text{B42})$$

where we have used $h'(\rho) = P'(\rho)/\rho$ (see Appendix H). Equation (B41) has been obtained by starting from the first equality of Eq. (14), and Eq. (B42) has been obtained by starting from the second equality of Eq. (14). Other

expressions of δQ are provided in Appendix C of [149]. The identities (B31)–(B42) are straightforward except, maybe, Eqs. (B32) and (B36). Therefore, we give a short derivation of these identities below.

Starting from the first equality of Eq. (24), we get at first order

$$\delta\Theta_Q = \frac{\hbar^2}{8m^2} \int \left[-\left(\frac{\nabla\rho}{\rho}\right)^2 \delta\rho + 2\frac{\nabla\rho}{\rho} \cdot \nabla\delta\rho \right] d\mathbf{r}. \quad (\text{B43})$$

Integrating the second term by parts, the foregoing equation can be rewritten as

$$\delta\Theta_Q = -\frac{\hbar^2}{4m^2} \int \left[\frac{\Delta\rho}{\rho} - \frac{1}{2} \left(\frac{\nabla\rho}{\rho}\right)^2 \right] \delta\rho d\mathbf{r}. \quad (\text{B44})$$

Together with Eq. (14), it yields Eq. (B32).

At second order, we have

$$\begin{aligned} \delta^2\Theta_Q &= \frac{\hbar^2}{8m^2} \int \frac{1}{\rho} \left[(\nabla\delta\rho)^2 - 2(\nabla\rho \cdot \nabla\delta\rho) \frac{\delta\rho}{\rho} \right. \\ &\quad \left. + (\nabla\rho)^2 \left(\frac{\delta\rho}{\rho}\right)^2 \right] d\mathbf{r}. \end{aligned} \quad (\text{B45})$$

Integrating the middle term by parts, we can rewrite Eq. (B45) as

$$\delta^2\Theta_Q = \frac{\hbar^2}{8m^2} \int \frac{1}{\rho} \left[(\nabla\delta\rho)^2 + \left(\frac{\Delta\rho}{\rho} - \frac{(\nabla\rho)^2}{\rho^2}\right) (\delta\rho)^2 \right] d\mathbf{r}, \quad (\text{B46})$$

which is the result quoted in Appendix C of Ref. [149]. On the other hand, multiplying Eq. (B42) by $\delta\rho$ and integrating over the whole domain, we get

$$\begin{aligned} \frac{1}{2} \int \delta\rho \frac{\delta Q}{m} d\mathbf{r} &= \frac{\hbar^2}{8m^2} \int \left[\frac{\Delta\rho}{\rho^2} (\delta\rho)^2 - \frac{\Delta\delta\rho}{\rho} \delta\rho \right. \\ &\quad \left. - \frac{1}{\rho^3} (\nabla\rho)^2 (\delta\rho)^2 + (\nabla\rho \cdot \nabla\delta\rho) \frac{1}{\rho^2} \delta\rho \right] d\mathbf{r}. \end{aligned} \quad (\text{B47})$$

Integrating the second term by parts, and comparing the resulting expression with Eq. (B46), we obtain Eq. (B36).

Finally, the identity

$$\nabla\delta\Phi = -4\pi G\rho\vec{\zeta} \quad (\text{B48})$$

needed to establish Eq. (B18) results from the following steps:

$$\begin{aligned} \nabla\delta\Phi &= -G \int \nabla \left(\frac{1}{|\mathbf{r} - \mathbf{r}'|} \right) \delta\rho(\mathbf{r}') d\mathbf{r}' \\ &= G \int \nabla' \left(\frac{1}{|\mathbf{r} - \mathbf{r}'|} \right) \delta\rho(\mathbf{r}') d\mathbf{r}' \\ &= -G \int \nabla' \left(\frac{1}{|\mathbf{r} - \mathbf{r}'|} \right) \nabla' \cdot (\rho\vec{\zeta}) d\mathbf{r}' \\ &= G \int \Delta' \left(\frac{1}{|\mathbf{r} - \mathbf{r}'|} \right) (\rho\vec{\zeta})' d\mathbf{r}' \\ &= -4\pi G \int \delta(\mathbf{r} - \mathbf{r}') (\rho\vec{\zeta})' d\mathbf{r}' \\ &= -4\pi G\rho\vec{\zeta}, \end{aligned} \quad (\text{B49})$$

where we have made use of Eqs. (B16) and (B40).

APPENDIX C: DIMENSIONLESS SELF-INTERACTION CONSTANT λ AND DECAY CONSTANT f

In this appendix, we introduce the dimensionless self-interaction constant λ and decay constant f and regroup in a compact manner the main formulas of the paper for a better visualization. A detailed explanation of these formulas is given in the main text and in Appendixes D and E.

The dimensionless self-interaction constant is defined by (see, e.g., Appendix A of [145])

$$\frac{\lambda}{8\pi} = \frac{a_s mc}{\hbar}. \quad (\text{C1})$$

On the other hand, for bosons with an attractive self-interaction ($a_s < 0$), the decay constant is defined by (see, e.g., [156])

$$f = \left(\frac{\hbar c^3 m}{32\pi |a_s|} \right)^{1/2}. \quad (\text{C2})$$

We have the relation

$$f = \frac{mc^2}{2|\lambda|^{1/2}}. \quad (\text{C3})$$

1. Noninteracting bosons

For noninteracting bosons

$$M = a \frac{\hbar^2}{Gm^2 R} \Rightarrow m = \left(\frac{a\hbar^2}{GMR} \right)^{1/2}. \quad (\text{C4})$$

2. Repulsive self-interaction

In the NI regime,

$$M = a \frac{\hbar^2}{Gm^2 R} \Rightarrow m = \left(\frac{a\hbar^2}{GMR} \right)^{1/2}. \quad (\text{C5})$$

In the TF regime,

$$R = b \left(\frac{a_s \hbar^2}{Gm^3} \right)^{1/2} \Rightarrow \frac{a_s}{m^3} = \frac{GR^2}{b^2 \hbar^2}; \quad (\text{C6})$$

$$R = b \left(\frac{\lambda \hbar^3}{8\pi Gm^4 c} \right)^{1/2} \Rightarrow \frac{\lambda}{8\pi m^4} = \frac{GR^2 c}{b^2 \hbar^3}. \quad (\text{C7})$$

For given (m, a_s) the transition between the NI regime and the TF regime corresponds to

$$M_t = \frac{a}{b} \frac{\hbar}{\sqrt{Gma_s}}, \quad R_t = b \left(\frac{a_s \hbar^2}{Gm^3} \right)^{1/2}; \quad (\text{C8})$$

$$M_t = \frac{a}{b} \left(\frac{8\pi \hbar c}{G\lambda} \right)^{1/2}, \quad R_t = b \left(\frac{\lambda \hbar^3}{8\pi Gm^4 c} \right)^{1/2}. \quad (\text{C9})$$

For given (M, R) the transition between the NI regime and the TF regime corresponds to

$$m_0 = \left(\frac{a \hbar^2}{GMR} \right)^{1/2}, \quad a'_* = \frac{a^{3/2}}{b^2} \left(\frac{\hbar^2 R}{GM^3} \right)^{1/2}, \quad (\text{C10})$$

$$\frac{\lambda'_*}{8\pi} = \frac{a^2 \hbar c}{b^2 GM^2}. \quad (\text{C11})$$

3. Attractive self-interaction

In the NI regime,

$$M = a \frac{\hbar^2}{Gm^2 R} \Rightarrow m = \left(\frac{a \hbar^2}{GMR} \right)^{1/2}. \quad (\text{C12})$$

In the NG regime,

$$M = \frac{a}{b^2} \frac{mR}{|a_s|} \Rightarrow \frac{|a_s|}{m} = \frac{aR}{b^2 M}; \quad (\text{C13})$$

$$M = \frac{a}{b^2} \frac{8\pi m^2 R c}{|\lambda| \hbar} \Rightarrow \frac{|\lambda|}{8\pi m^2} = \frac{a}{b^2} \frac{Rc}{M \hbar}; \quad (\text{C14})$$

$$M = \frac{a}{b^2} \frac{32\pi R f^2}{\hbar c^3} \Rightarrow f^2 = \frac{b^2 M \hbar c^3}{a 32\pi R}. \quad (\text{C15})$$

For given (m, a_s) the transition between the NI regime and the NG regime corresponds to

$$M_t = \frac{a}{b} \frac{\hbar}{\sqrt{Gm|a_s|}}, \quad R_t = b \left(\frac{|a_s| \hbar^2}{Gm^3} \right)^{1/2}; \quad (\text{C16})$$

$$M_t = \frac{a}{b} \left(\frac{8\pi \hbar c}{G|\lambda|} \right)^{1/2}, \quad R_t = b \left(\frac{|\lambda| \hbar^3}{8\pi Gm^4 c} \right)^{1/2}; \quad (\text{C17})$$

$$M_t = \frac{a}{b} \left(\frac{32\pi \hbar f^2}{Gm^2 c^3} \right)^{1/2}, \quad R_t = b \left(\frac{\hbar^3 c^3}{32\pi Gm^2 f^2} \right)^{1/2}. \quad (\text{C18})$$

For given (M, R) the transition between the NI regime and the NG regime corresponds to

$$m_0 = \left(\frac{a \hbar^2}{GMR} \right)^{1/2}, \quad a'_* = \frac{a^{3/2}}{b^2} \left(\frac{\hbar^2 R}{GM^3} \right)^{1/2}, \quad (\text{C19})$$

$$\frac{\lambda'_*}{8\pi} = \frac{a^2 \hbar c}{b^2 GM^2}, \quad f'_* = \left(\frac{b^2 \hbar c^3 M}{a 32\pi R} \right)^{1/2}. \quad (\text{C20})$$

Remark:—We note that the transition scales between the NI regime and the NG regime in the attractive case coincide with the transition scales between the NI regime and the TF regime in the repulsive case provided that a_s is replaced by $|a_s|$. We also note that the formulas expressed in terms of λ and f involve the speed of light c . This is purely artificial since our results apply to nonrelativistic systems. The occurrence of c is due to the definitions of λ and f in Eqs. (C1) and (C2).

APPENDIX D: REFORMULATION OF THE RESULTS OF SEC. II C IN TERMS OF λ AND f

In this appendix, we reformulate the results of Sec. II C in terms of the dimensionless self-interaction constant λ and decay constant f (see Appendix C) instead of the scattering length a_s .

Using Eqs. (48) and (C1), the radius of self-gravitating BECs with a repulsive self-interaction in the TF regime can be written as

$$R_{\text{TF}} = \pi \left(\frac{\lambda \hbar^3}{8\pi Gm^4 c} \right)^{1/2} = 0.627 \sqrt{\lambda} \frac{M_P}{m} \lambda_C, \quad (\text{D1})$$

where $M_P = (\hbar c/G)^{1/2} = 2.18 \times 10^{-5} \text{g}$ is the Planck mass and $\lambda_C = \hbar/mc$ is the Compton wavelength of the particle.

Using Eqs. (49), (50), and (C1), the maximum mass and the corresponding radius of self-gravitating BECs with an attractive self-interaction can be written as

$$M_{\text{max}} = 1.012 \left(\frac{8\pi \hbar c}{G|\lambda|} \right)^{1/2} = 5.073 \frac{M_P}{\sqrt{|\lambda|}}, \quad (\text{D2})$$

$$R_{99}^* = 5.5 \left(\frac{|\lambda| \hbar^3}{8\pi Gm^4 c} \right)^{1/2} = 1.1 \sqrt{|\lambda|} \frac{M_P}{m} \lambda_C. \quad (\text{D3})$$

We note that M_{max} depends only on λ . Using Eq. (C3), we also have

$$M_{\text{max}} = 1.012 \left(\frac{8\pi \hbar c}{G} \right)^{1/2} \frac{2f}{mc^2} = 10.15 \frac{f}{M_P c^2} \frac{M_P^2}{m}, \quad (\text{D4})$$

$$R_{99}^* = 5.5 \left(\frac{\hbar^3}{8\pi G m^4 c} \right)^{1/2} \frac{m c^2}{2f} = 0.55 \frac{M_P c^2}{f} \lambda_c. \quad (\text{D5})$$

Using Eqs. (52), (C1), and (C2), the mass-radius relation of nongravitational BECs with an attractive self-interaction can be written as

$$M = 6.91 \frac{m^2 c}{\hbar |\lambda|} R_{99} = 27.6 \frac{f^2}{\hbar c^3} R_{99}. \quad (\text{D6})$$

We note that it depends only on f .

Remark: According to Eqs. (D2)–(D5) a self-gravitating BEC of mass M can be in equilibrium only if $\lambda > \lambda_{\min}$ or $f > f_{\min}^*$ with

$$\lambda_{\min} = -25.7 \frac{\hbar c}{GM^2} = -25.74 \left(\frac{M_P}{M} \right)^2, \quad (\text{D7})$$

$$\begin{aligned} f_{\min}^* &= 9.86 \times 10^{-2} m M c^2 \left(\frac{G}{\hbar c} \right)^{1/2} \\ &= 9.86 \times 10^{-2} \frac{m M}{M_P^2} M_P c^2. \end{aligned} \quad (\text{D8})$$

APPENDIX E: REFORMULATION OF THE RESULTS OF SEC. IV IN TERMS OF λ AND f

In this appendix, we reformulate the results of Sec. IV in terms of the dimensionless self-interaction constant λ and decay constant f instead of the scattering length a_s .

The dimensionless self-interaction constant is defined by Eq. (C1). This relation may be rewritten as

$$\frac{\lambda}{\lambda'_*} = \frac{a_s}{a'_*} \frac{m}{m_0}, \quad (\text{E1})$$

where we have introduced the scales from Eqs. (85) and (86), and the new scale

$$\frac{\lambda'_*}{8\pi} = \frac{a^2 \hbar c}{b^2 GM^2}. \quad (\text{E2})$$

We note that this scale depends only on the mass M of the minimum halo, not on its radius R .

Using Eqs. (83) and (C1), the relation between the particle mass m and the dimensionless self-interaction constant λ required to match the characteristics of the minimum halo [see Eq. (81)] is given by

$$\lambda = \frac{8\pi a R m^2 c}{b^2 \hbar M} \left(\frac{GMm^2 R}{a \hbar^2} - 1 \right). \quad (\text{E3})$$

Alternatively, using Eqs. (84) and (E1), we obtain in dimensionless form

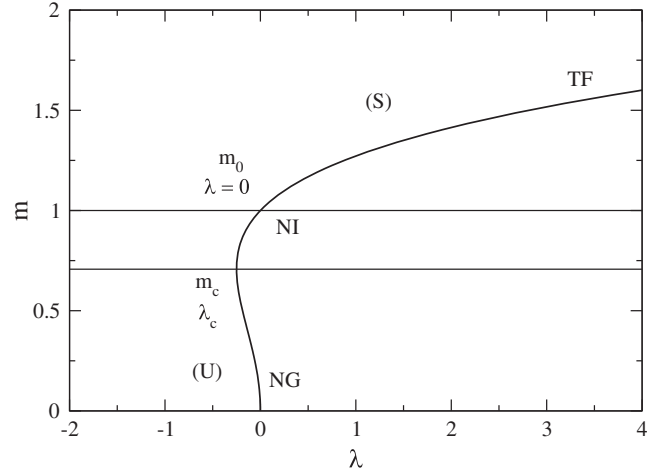


FIG. 10. Mass m of the DM particle as a function of the dimensionless self-interaction constant λ in order to match the characteristics of the minimum halo. The mass is normalized by m_0 and the dimensionless self-interaction constant by λ'_* . The stable part of the curve starts at the critical minimum halo point (λ_c, m_c) which is also the minimum of the curve $\lambda(m)$.

$$\frac{\lambda}{\lambda'_*} = \left(\frac{m}{m_0} \right)^2 \left[\left(\frac{m}{m_0} \right)^2 - 1 \right]. \quad (\text{E4})$$

This is a second degree equation whose solutions are

$$\frac{m}{m_0} = \left(\frac{1 \pm \sqrt{1 + 4\lambda/\lambda'_*}}{2} \right)^{1/2} \quad (\text{E5})$$

with the sign $+$ if $\lambda > 0$ and the signs \pm if $\lambda < 0$. The curve $m(\lambda)$ is plotted in Fig. 10. Taking $a = 9.946$ and $b = \pi$ (see Secs. III A and III B) adapted to bosons with a repulsive self-interaction (or no interaction), we get $m_0 = 2.92 \times 10^{-22}$ eV/ c^2 and $\lambda'_* = 3.02 \times 10^{-90}$. Taking $a = 11.1$ and $b = 5.5$ (see Sec. III C) adapted to bosons with an attractive self-interaction, we get $m_0 = 3.08 \times 10^{-22}$ eV/ c^2 and $\lambda'_* = 1.23 \times 10^{-90}$.

Remark: We note that the characteristic scale $\lambda'_* \sim 10^{-90}$ is extremely small. We will see below that the NI limit is valid for $|\lambda| \ll \lambda'_*$. Therefore, the dimensionless self-interaction constant $|\lambda|$ must be small with respect to 10^{-90} , not with respect to 1. For example, an apparently small value of $|\lambda|$ such as $|\lambda| = 10^{-80}$ actually corresponds to a strong self-interaction. In other words, $|\lambda| = 10^{-80}$ is very different from $\lambda = 0$. The extraordinarily small value of λ'_* was first noted in [108] (see also [145,148,153,156]).

1. Noninteracting bosons

For noninteracting bosons ($\lambda = 0$), we get

$$m_0 = 2.92 \times 10^{-22} \text{ eV}/c^2 \quad (\text{BECNI}). \quad (\text{E6})$$

2. Repulsive self-interaction

For bosons with a repulsive self-interaction ($\lambda > 0$), λ'_* determines the transition between the NI regime ($\lambda \ll \lambda'_*$) where $m \sim m_0$ and the TF regime ($\lambda \gg \lambda'_*$) where

$$\frac{m}{m_0} \sim \left(\frac{\lambda}{\lambda'_*}\right)^{1/4}. \quad (\text{E7})$$

When the self-interaction is repulsive, all the equilibrium states are stable. Therefore, in principle, all the values of $\lambda \geq 0$ and the corresponding masses $m \geq m_0$ are possible. In the TF regime, the $m(\lambda)$ relation (E7) can be written as

$$\frac{\lambda}{8\pi m^4} \sim \frac{GR^2 c}{b^2 \hbar^3}, \quad (\text{E8})$$

which is equivalent to Eq. (90). The minimum halo just determines the ratio

$$\frac{\lambda}{8\pi m^4} = 1.66 \times 10^{-5} (\text{eV}/c^2)^{-4}. \quad (\text{E9})$$

Only the radius R of the minimum halo matters in this determination. In order to determine m and λ individually, we need another equation. Repeating the argument from Sec. IV B, the Bullet Cluster constraint $\sigma/m \leq 1.25 \text{ cm}^2/\text{g}$ implies that λ must lie in the range $0 \leq \lambda \leq \lambda_{\text{max}}$ and that the particle mass must lie in the range $m_0 \leq m \leq m_{\text{max}}$ where³¹

$$m_{\text{max}} = 1.10 \times 10^{-3} \text{ eV}/c^2, \quad \lambda_{\text{max}} = 6.18 \times 10^{-16} \quad (\text{BECTF}). \quad (\text{E10})$$

Although the value of $\lambda_{\text{max}} = 6.18 \times 10^{-16}$ corresponding to the BECTF model may seem small, it is much larger than $\lambda'_* = 3.02 \times 10^{-90}$, implying that we are deep into the TF regime (see the Remark above).

On the other hand, the BECt model corresponding to the transition between the NI limit and the TF limit is obtained by substituting Eq. (E6) into Eq. (E7), or Eq. (E8) into Eq. (E8). This gives

$$m_t = 2.92 \times 10^{-22} \text{ eV}/c^2, \quad \lambda'_* = 3.02 \times 10^{-90} \quad (\text{BECt}). \quad (\text{E11})$$

This corresponds to the scales m_0 and λ'_* defined by Eqs. (85) and (E2).

³¹More generally, if we introduce the parameter $\beta = a_s^2/m = \sigma/(4\pi m)$ which can be constrained by the observations, we obtain $m_{\text{max}} = (\beta\pi^4 \hbar^4/G^2 R^4)^{1/5}$, $(a_s)_{\text{max}} = (\beta^3 \pi^2 \hbar^2/GR^2)^{1/5}$, and $\lambda_{\text{max}}/8\pi = (\beta^4 \pi^6 \hbar c^5/G^3 R^6)^{1/5}$.

3. Attractive self-interaction in terms of λ

For bosons with an attractive self-interaction ($\lambda < 0$), the relation (E4) reveals the existence of a minimum value of the dimensionless self-interaction constant

$$\frac{\lambda_c}{\lambda'_*} = -\frac{1}{4}, \quad \text{at which } \frac{m_c}{m_0} = \frac{1}{\sqrt{2}}. \quad (\text{E12})$$

It turns out that this minimum value also corresponds to the critical point (associated with the maximum mass M_{max}) separating stable from unstable equilibrium states (see Fig. 10). The NI regime corresponds to $|\lambda| \ll \lambda'_*$ and $m \sim m_0$. The NG regime corresponds to $|\lambda| \ll \lambda'_*$ and $m \ll m_0$ such that

$$\frac{m}{m_0} \sim \left(\frac{|\lambda|}{\lambda'_*}\right)^{1/2}. \quad (\text{E13})$$

In the NG regime, the relation (E13) between m and λ can be written as

$$\frac{|\lambda|}{8\pi m^2} = \frac{a}{b^2} \frac{Rc}{M\hbar} = 5.12 \times 10^{-49} (\text{eV}/c^2)^{-2}, \quad (\text{E14})$$

which is equivalent to Eq. (77). The equilibrium states with $m < m_c$ are unstable (they correspond to configurations with $R < R_*$) so that only the equilibrium states with $m > m_c$ are stable (they correspond to configurations with $R > R_*$). Therefore, in the attractive case, the scattering length of the DM boson must lie in the range $\lambda_c < \lambda < 0$ and its mass must lie in the range $m_c < m < m_0$, with

$$m_c = 2.19 \times 10^{-22} \text{ eV}/c^2, \quad \lambda_c = -3.07 \times 10^{-91} \quad (\text{BECcrit}). \quad (\text{E15})$$

There is no equilibrium state with $\lambda < \lambda_c$. Finally, using the constraints from particle physics and cosmology (see Sec. IV D) we find

$$m_{\text{th}} = 2.92 \times 10^{-22} \text{ eV}/c^2, \quad \lambda_{\text{th}} = -1.18 \times 10^{-96} \quad (\text{BECth}). \quad (\text{E16})$$

4. Attractive self-interaction in terms of f

The decay constant is defined by Eq. (C2). This relation may be rewritten as

$$\frac{f}{f'_*} = \left(\frac{m}{m_0}\right)^{1/2} \left(\frac{a'_*}{|a_s|}\right)^{1/2}, \quad (\text{E17})$$

where we have introduced the scales from Eqs. (85) and (86), and the new scale

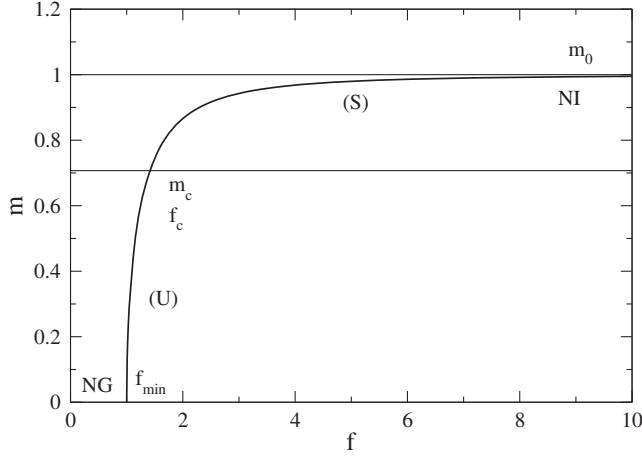


FIG. 11. Mass m of the DM particle as a function of its decay constant f in order to match the characteristics of the minimum halo. The mass is normalized by m_0 and the decay constant by f'_* . The stable part of the curve starts at the critical minimum halo point (f_c, m_c) . It differs from the absolute minimum value f_{\min} of the decay constant.

$$f'_* = \left(\frac{b^2 \hbar c^3 M}{a 32\pi R} \right)^{1/2}. \quad (\text{E18})$$

Using Eqs. (83) and (C2), the relation between the particle mass and the decay constant is given by

$$\frac{1}{f^2} = \frac{32\pi a R}{b^2 \hbar c^3 M} \left(1 - \frac{GMm^2 R}{a \hbar^2} \right). \quad (\text{E19})$$

Alternatively, using Eqs. (84) and (E17), we obtain in dimensionless form

$$\frac{m}{m_0} = \sqrt{1 - \left(\frac{f'_*}{f} \right)^2}. \quad (\text{E20})$$

The curve $m(f)$ is plotted in Fig. 11. Taking $a = 11.1$ and $b = 5.5$ (see Sec. III C) adapted to bosons with an attractive self-interaction, we get $m_0 = 3.08 \times 10^{-22}$ eV/ c^2 and $f'_* = 1.39 \times 10^{14}$ GeV.

The relation from Eq. (E20) reveals the existence of a minimum decay constant $f_{\min} = f'_* = 1.39 \times 10^{14}$ GeV at which $m = 0$.³² However, this minimum scattering length f_{\min} does *not* correspond to the critical point (associated

³²This minimum value arises from the fact that both the mass-radius relation in the NG regime from Eq. (77) and the decay constant from Eq. (C2) present a scaling in $m/|a_s|$ [see Eq. (D6)]. It is interesting to note that our approach predicts a minimum value of f for the existence of DM halos with mass $M \sim 10^8 M_\odot$ and radius $R \sim 1$ kpc. Furthermore, this value turns out to be of the order of the grand unified theory (GUT) scale $f_{\text{GUT}} \sim 10^{15}$ GeV.

with the maximum mass M_{\max}) separating stable from unstable equilibrium states. This latter is located at

$$\frac{f_c}{f'_*} = \sqrt{2}, \quad \frac{m_c}{m_0} = \frac{1}{\sqrt{2}}. \quad (\text{E21})$$

The NI regime corresponds to $f \gg f_{\min}$ and $m \sim m_0$. The NG regime corresponds to $f \sim f_{\min}$ and $m \ll m_0$.

The equilibrium states with $m < m_c$ are unstable (they correspond to configurations with $R < R_*$) so that only the equilibrium states with $m > m_c$ are stable (they correspond to configurations with $R > R_*$). Therefore, the decay constant of the DM boson must lie in the range $f > f_c$ and its mass must lie in the range $m_c < m < m_0$, with³³

$$m_c = 2.19 \times 10^{-22} \text{ eV}/c^2, \quad f_c = 1.97 \times 10^{14} \text{ GeV} \quad (\text{BECcrit}). \quad (\text{E22})$$

There is no equilibrium state with $f < f_{\min}$. On the other hand, the equilibrium states with $f_{\min} \leq f < f_c$ are unstable. Using the constraints from particle physics and cosmology (see Sec. IV D) we find

$$m_{\text{th}} = 2.92 \times 10^{-22} \text{ eV}/c^2, \quad f_{\text{th}} = 1.34 \times 10^{17} \text{ GeV} \quad (\text{BECth}). \quad (\text{E23})$$

The theoretical decay constant $f_{\text{th}} = 1.34 \times 10^{17}$ GeV lies between the GUT scale $f_{\text{GUT}} \sim 10^{15}$ GeV and the Planck scale $M_{\text{Pl}} c^2 = 1.22 \times 10^{19}$ GeV.

APPENDIX F: PULSATION OF A SELF-GRAVITATING BEC

In this appendix, we determine the squared pulsation of the standard self-gravitating BEC described by the equation of state (20).

1. General case

In the general case, the squared pulsation of the standard self-gravitating BEC is approximately given by (see Appendix G 2)

$$\omega^2 = \frac{6\Theta_Q + 12U + 2W}{I}. \quad (\text{F1})$$

This equation can be written in different forms by using the virial theorem $2\Theta_Q + 3U + W = 0$ (see Sec. II B).

With the f -ansatz (see Appendix G 2), the squared pulsation is explicitly given by

³³We note that when the self-interaction is attractive m almost does not change (it is of the order of the mass of noninteracting bosons) while f can change by several orders of magnitude.

$$\omega^2 = \frac{6\sigma}{\alpha} \frac{\hbar^2}{m^2 R^4} - \frac{2\nu}{\alpha} \frac{GM}{R^3} + \frac{24\pi\zeta}{\alpha} \frac{a_s \hbar^2 M}{m^3 R^5}. \quad (\text{F2})$$

On the other hand, the mass-radius relation of the standard self-gravitating BEC writes

$$-2\sigma \frac{\hbar^2 M}{m^2 R^3} + \nu \frac{GM^2}{R^2} - 6\pi\zeta \frac{a_s \hbar^2 M^2}{m^3 R^4} = 0 \quad (\text{F3})$$

or, equivalently,

$$M = \frac{\frac{2\sigma}{\nu} \frac{\hbar^2}{Gm^2 R}}{1 - \frac{6\pi\zeta}{\nu} \frac{a_s \hbar^2}{Gm^3 R^2}}. \quad (\text{F4})$$

If we use a Gaussian ansatz, the values of the coefficients are $\alpha_G = 3/2$, $\sigma_G = 3/4$, $\zeta_G = 1/(2\pi)^{3/2}$, and $\nu_G = 1/\sqrt{2\pi}$ [107]. Furthermore, the relation between the radius R and the radius R_{99} containing 99% of the mass is $R_{99} = 2.38167R$ [107]. The squared pulsation is plotted as a function of the BEC radius R in [107].

2. Noninteracting case

For noninteracting bosons ($a_s = 0$), the squared pulsation from Eq. (F1) reduces to

$$\omega^2 = \frac{6\Theta_Q + 2W}{I} = \frac{2\Theta_Q}{I} = -\frac{W}{I}, \quad (\text{F5})$$

where we have used the virial theorem $2\Theta_Q + W = 0$ to get the last two equalities.

With the f -ansatz, the squared pulsation is given by

$$\omega^2 = \frac{6\sigma}{\alpha} \frac{\hbar^2}{m^2 R^4} - \frac{2\nu}{\alpha} \frac{GM}{R^3}. \quad (\text{F6})$$

On the other hand, the mass-radius relation writes

$$R = \frac{2\sigma}{\nu} \frac{\hbar^2}{GMm^2}. \quad (\text{F7})$$

Combining these two relations we obtain

$$\omega^2 = \frac{\nu}{\alpha} \frac{GM}{R^3} = \frac{2\sigma}{\alpha} \frac{\hbar^2}{m^2 R^4} = \frac{\nu^4}{8\alpha\sigma^3} \frac{G^4 M^4 m^6}{\hbar^6}. \quad (\text{F8})$$

If we use a Gaussian ansatz, the prefactors in Eqs. (F7) and (F8) are 3.76, 0.266, 1, and 5.00×10^{-3} . The first relation of Eq. (F8) shows that the pulsation period $T = 2\pi/\omega$ is equal to about $12.2t_d$, where $t_d = (R^3/GM)^{1/2}$ is the dynamical time. For the minimum halo with $M = 10^8 M_\odot$ and $R = (1/2.38167)$ kpc, we get $t_d = 12.8$ Myrs and $T = 156$ Myrs.

3. TF limit

For bosons with a repulsive self-interaction ($a_s > 0$) in the TF limit ($\hbar = 0$), the squared pulsation from Eq. (F1) reduces to

$$\omega^2 = \frac{12U + 2W}{I} = \frac{6U}{I} = -\frac{2W}{I}, \quad (\text{F9})$$

where we have used the virial theorem $3U + W = 0$ to get the last two equalities.

With the f -ansatz, the squared pulsation is given by

$$\omega^2 = -\frac{2\nu}{\alpha} \frac{GM}{R^3} + \frac{24\pi\zeta}{\alpha} \frac{a_s \hbar^2 M}{m^3 R^5}. \quad (\text{F10})$$

On the other hand, the radius of the BEC is

$$R = \left(\frac{6\pi\zeta}{\nu}\right)^{1/2} \left(\frac{a_s \hbar^2}{Gm^3}\right)^{1/2}. \quad (\text{F11})$$

Combining these two relations we obtain

$$\omega^2 = \frac{2\nu}{\alpha} \frac{GM}{R^3} = \frac{2\nu^{5/2}}{\alpha(6\pi\zeta)^{3/2}} \frac{G^{5/2} M m^{9/2}}{a_s^{3/2} \hbar^3}. \quad (\text{F12})$$

If we use a Gaussian ansatz, the prefactors in Eqs. (F11) and (F12) are 1.73, 0.532, and 0.102. The pulsation period $T = 2\pi/\omega$ is about $8.62t_d$. For the minimum halo with $M = 10^8 M_\odot$ and $R = (1/2.38167)$ kpc, we get $t_d = 12.8$ Myrs and $T = 111$ Myrs.

Remark:—In the TF approximation, the density profile of the BECDM halo is known analytically. In that case, one can obtain the exact expression of the pulsation (see [107] and Appendixes H and I of [163]).

4. Maximum mass and maximum pulsation

For bosons with an attractive self-interaction ($a_s < 0$), the pulsation vanishes at the maximum mass [107]:

$$\omega = 0 \quad \text{at } M = M_{\max}. \quad (\text{F13})$$

With the f -ansatz, the maximum mass and the corresponding radius are given by

$$M_{\max} = \left(\frac{\sigma^2}{6\pi\zeta\nu}\right)^{1/2} \frac{\hbar}{\sqrt{Gm|a_s|}}, \quad (\text{F14})$$

$$R_* = \left(\frac{6\pi\zeta}{\nu}\right)^{1/2} \left(\frac{|a_s| \hbar^2}{Gm^3}\right)^{1/2}. \quad (\text{F15})$$

On the other hand, there is a maximum pulsation at some mass \tilde{M} [107]. With the f -ansatz, we find that

$$\omega_{\max} = 0.4246 \frac{\nu}{6\pi\zeta} \sqrt{\frac{\sigma}{\alpha} \frac{Gm^2}{|a_s|\hbar}} \quad (\text{F16})$$

at

$$\tilde{M} = 0.9717M_{\max}, \quad \tilde{R} = 1.272R_*. \quad (\text{F17})$$

If we use a Gaussian ansatz, the prefactors in Eqs. (F14)–(F16) are 1.085, 1.73, and 0.100.

5. Nongravitational case

For bosons with an attractive self-interaction ($a_s < 0$) in the NG limit ($G = 0$), the squared pulsation from Eq. (F1) reduces to

$$\omega^2 = \frac{6\Theta_Q + 12U}{I} = -\frac{2\Theta_Q}{I} = \frac{3U}{I}, \quad (\text{F18})$$

where we have used the virial theorem $2\Theta_Q + 3U = 0$ to get the last two equalities.

With the f -ansatz, the squared pulsation is given by

$$\omega^2 = \frac{6\sigma}{\alpha} \frac{\hbar^2}{m^2 R^4} + \frac{24\pi\zeta}{\alpha} \frac{a_s \hbar^2 M}{m^3 R^5}. \quad (\text{F19})$$

On the other hand, the mass-radius relation writes

$$M = \frac{\sigma}{3\pi\zeta} \frac{mR}{|a_s|}. \quad (\text{F20})$$

Combining these two relations we obtain

$$\omega^2 = -\frac{2\sigma}{\alpha} \frac{\hbar^2}{m^2 R^4} = -\frac{2\sigma^5}{\alpha(3\pi\zeta)^4} \frac{m^2 \hbar^2}{M^4 a_s^4}. \quad (\text{F21})$$

If we use a Gaussian ansatz, the prefactors in Eqs. (F20) and (F21) are 1.25, 1, and 2.47. We note that these configurations are unstable ($\omega^2 < 0$) so they should not be observed in practice.

APPENDIX G: SIMILARITY BETWEEN THE MASS-RADIUS RELATION OBTAINED FROM THE f -ANSATZ AND FROM THE JEANS INSTABILITY STUDY

In this appendix, we show at a general level that the mass-radius relation $M_J(R_J)$ obtained from the Jeans instability study is similar to the mass-radius relation $M(R)$ of DM halos in their ground state obtained from the minimization of the energy at fixed mass using an f -ansatz. This similarity was first observed in Ref. [107] in a special case (for a $|\psi|^4$ potential of interaction and for a Gaussian ansatz), and it is here generalized to an arbitrary potential of interaction $V(|\psi|^2)$ and an arbitrary ansatz.

1. Mass-radius relation from the Jeans instability study

In this section, we consider the formation of structures in the linear regime from the Jeans instability study (see Sec. II D). The Jeans wave number is determined by the equation [107]

$$\frac{\hbar^2 k_J^4}{4m^2} + c_s^2 k_J^2 - 4\pi G\rho = 0, \quad (\text{G1})$$

where c_s^2 is the squared speed of sound. For a barotropic fluid, this is a function of the density given by Eq. (18). Equation (G1) is a second degree equation for k_J^2 whose physical solution is

$$k_J^2 = \frac{2m^2}{\hbar^2} \left[-c_s^2(\rho) + \sqrt{c_s^4(\rho) + \frac{4\pi G\rho\hbar^2}{m^2}} \right]. \quad (\text{G2})$$

If we define the Jeans radius and the Jeans mass by

$$R_J = \frac{\lambda_J}{2} = \frac{\pi}{k_J}, \quad M_J = \frac{4}{3}\pi\rho R_J^3, \quad (\text{G3})$$

we obtain

$$R_J(\rho) = \frac{\frac{\pi\hbar}{\sqrt{2m}}}{\left[-c_s^2(\rho) + \sqrt{c_s^4(\rho) + \frac{4\pi G\rho\hbar^2}{m^2}} \right]^{1/2}}, \quad (\text{G4})$$

$$M_J(\rho) = \frac{4}{3}\pi\rho R_J(\rho)^3. \quad (\text{G5})$$

These equations determine the Jeans scales $R_J(\rho)$ and $M_J(\rho)$ as a function of the density. They also determine the Jeans mass-radius relation $M_J(R_J)$ in parametric form with parameter ρ .

Remark:—In the nongravitational case, there is a hydrodynamic instability when $c_s^2 < 0$ [76,107].³⁴ In that case, the “Jeans” wave number is determined by the equation

$$\frac{\hbar^2 k_J^2}{4m^2} + c_s^2 = 0, \quad (\text{G6})$$

and the parametric equations (G4) and (G5) reduce to

$$R_J(\rho) = \frac{\pi\hbar}{2m\sqrt{-c_s^2(\rho)}}, \quad (\text{G7})$$

$$M_J(\rho) = \frac{4}{3}\pi\rho R_J(\rho)^3. \quad (\text{G8})$$

³⁴This hydrodynamic instability is also called a tachyonic instability.

2. Mass-radius relation from the f -ansatz

In this section, we consider BECDM halos that appear in the nonlinear regime of structure formation (see Sec. II C). Stable DM halos correspond to minima of energy E_{tot} at fixed mass M . We can obtain an approximate analytical form of the mass-radius relation by making an ansatz for the wave function. A Gaussian ansatz was considered in [107]. To be as general as possible, we consider here an ansatz of the form (that we call f -ansatz)

$$\rho(\mathbf{r}, t) = \frac{M}{R(t)^3} f\left[\frac{\mathbf{r}}{R(t)}\right], \quad (\text{G9})$$

where $f(\mathbf{x})$ is an arbitrary function. We impose $\int f(\mathbf{x}) d\mathbf{x} = 1$ to satisfy the normalization condition (or the conservation of mass). We also assume

$$S(\mathbf{r}, t) = \frac{1}{2} m H(t) r^2 \Rightarrow \mathbf{u}(\mathbf{r}, t) = H(t) \mathbf{r}, \quad (\text{G10})$$

so that the velocity field is proportional to the radial distance. It can be shown (see Appendix J of [149]) that Eqs. (G9) and (G10) yield an exact solution of the continuity equation (10) provided that

$$H = \frac{\dot{R}}{R}. \quad (\text{G11})$$

This function is similar to the Hubble parameter in cosmology. On the other hand, the gravitational potential can be determined from the Poisson equation (13). Using Eq. (G9) we obtain

$$\Phi(\mathbf{r}, t) = \frac{GM}{R(t)} g\left[\frac{\mathbf{r}}{R(t)}\right], \quad (\text{G12})$$

where $g(\mathbf{x})$ is the solution of

$$\Delta g = 4\pi f(\mathbf{x}). \quad (\text{G13})$$

We can now use the ansatz (G9)–(G13) to determine the different functionals that appear in the energy from Eq. (22). We find

$$\Theta_c = \frac{1}{2} \alpha M \left(\frac{dR}{dt}\right)^2 \quad \text{with} \quad \alpha = \int f(\mathbf{x}) x^2 d\mathbf{x}, \quad (\text{G14})$$

$$\Theta_Q = \sigma \frac{\hbar^2 M}{m^2 R^2} \quad \text{with} \quad \sigma = \frac{1}{8} \int \frac{(\nabla f)^2}{f} d\mathbf{x}, \quad (\text{G15})$$

$$U = \frac{\zeta}{\gamma - 1} \frac{KM^\gamma}{R^{3(\gamma-1)}} \quad \text{with} \quad \zeta = \int f^\gamma(\mathbf{x}) d\mathbf{x}, \quad (\text{G16})$$

and

$$W = -\nu \frac{GM^2}{R} \quad \text{with} \quad \nu = -\frac{1}{2} \int f(\mathbf{x}) g(\mathbf{x}) d\mathbf{x}. \quad (\text{G17})$$

The expression (G16) of the internal energy U is valid for a power-law potential associated with a polytropic equation of state (we will see later how to generalize the formalism to an arbitrary potential of interaction or an arbitrary equation of state). The moment of inertia is

$$I = \alpha MR^2. \quad (\text{G18})$$

If we use a Gaussian ansatz $f(\mathbf{x}) = \frac{1}{\pi^{3/2}} e^{-x^2}$, the values of the coefficients are $\alpha_G = 3/2$, $\sigma_G = 3/4$, $\zeta_G = 1/(\gamma\pi^{\gamma-1})^{3/2}$, and $\nu_G = 1/\sqrt{2\pi}$ [107].

With the ansatz from Eqs. (G9) and (G10) the total energy can be written as

$$E_{\text{tot}} = \frac{1}{2} \alpha M \left(\frac{dR}{dt}\right)^2 + V(R) \quad (\text{G19})$$

with

$$V(R) = \sigma \frac{\hbar^2 M}{m^2 R^2} - \nu \frac{GM^2}{R} + \frac{\zeta}{\gamma - 1} \frac{KM^\gamma}{R^{3(\gamma-1)}}. \quad (\text{G20})$$

We have separated the classical kinetic energy Θ_c from the potential energy $V = \Theta_Q + U + W$. From the conservation of energy, $\dot{E}_{\text{tot}} = 0$, we obtain

$$\alpha M \frac{d^2 R}{dt^2} = -V'(R). \quad (\text{G21})$$

This is similar to the equation of motion of a fictive particle of mass αM and position R moving in a potential $V(R)$. At equilibrium, the condition $V'(R) = 0$ (extremum of energy) gives the mass-radius relation

$$-2\sigma \frac{\hbar^2 M}{m^2 R^3} + \nu \frac{GM^2}{R^2} - 3\zeta \frac{KM^\gamma}{R^{3(\gamma-1)+1}} = 0. \quad (\text{G22})$$

For the standard BEC, we get Eq. (F3). The foregoing equations may also be obtained from the virial theorem [107,149] or from the Lagrange equations [145,149].

The pulsation of the self-gravitating BEC is given by [107,149]

$$\omega^2 = \frac{1}{\alpha M} V''(R). \quad (\text{G23})$$

The BEC is stable provided that $\omega^2 > 0$ which is equivalent by Eq. (G23) to the requirement that the equilibrium state is a minimum of energy. Using Eq. (G20) we obtain

$$\omega^2 = \frac{6\sigma}{\alpha} \frac{\hbar^2}{m^2 R^4} - \frac{2\nu}{\alpha} \frac{GM}{R^3} + [3(\gamma - 1) + 1] \frac{3\zeta}{\alpha} \frac{KM^{\gamma-1}}{R^{3(\gamma-1)+2}}. \quad (\text{G24})$$

Using Eqs. (G15)–(G18), the pulsation can also be written in terms of the BEC functionals as

$$\omega^2 = \frac{6\Theta_c + [3(\gamma - 1) + 1]3(\gamma - 1)U + 2W}{I}. \quad (\text{G25})$$

For the usual BEC, we obtain Eqs. (F1) and (F2).

In order to compute the internal energy U for a general self-interaction potential we consider an ansatz based on a uniform (top-hat) density

$$\rho(\mathbf{r}, t) = \frac{3M}{4\pi R(t)^3} \theta(|\mathbf{r}| - R(t)), \quad (\text{G26})$$

where θ is the Heaviside function [$\theta(x) = 1$ if $x < 0$ and $\theta(x) = 0$ if $x > 0$]. In that case, the internal energy is given by

$$U = V \left(\frac{3M}{4\pi R^3} \right) \frac{4}{3} \pi R^3. \quad (\text{G27})$$

We then find that

$$\begin{aligned} U'(R) &= \frac{d}{dR} \left[\frac{V(\rho)}{\rho} M \right] = M \frac{d}{d\rho} \left[\frac{V(\rho)}{\rho} \right] \frac{d\rho}{dR} \\ &= -\frac{9M^2}{4\pi R^4} \frac{d}{d\rho} \left[\frac{V(\rho)}{\rho} \right]. \end{aligned} \quad (\text{G28})$$

Using Eq. (16), which corresponds to the first principle of thermodynamics (see Appendix H)

$$\left[\frac{V(\rho)}{\rho} \right]' = \frac{P(\rho)}{\rho^2} \Leftrightarrow d \left(\frac{V}{\rho} \right) = -P d \left(\frac{1}{\rho} \right), \quad (\text{G29})$$

we obtain

$$U'(R) = -P \left(\frac{3M}{4\pi R^3} \right) 4\pi R^2 \Leftrightarrow dU = -P d\mathcal{V}, \quad (\text{G30})$$

where $\mathcal{V} = (4/3)\pi R^3$ denotes the volume of the BEC. For a power-law self-interaction potential, we recover the expression of U from Eq. (G16) with a coefficient $\zeta_C = (3/4\pi)^{\gamma-1}$. On the other hand, the coefficients entering in the expressions of Θ_c and W from Eqs. (G14) and (G17) are $\alpha_C = 3/5$ and $\nu_C = 3/5$. Unfortunately, we cannot use the constant density ansatz to determine the quantum kinetic energy Θ_c since it is produced by the gradient of the density which is infinite at $r = R$ for the top-hat profile.

For an arbitrary self-interaction potential, we can write the total energy as in Eq. (G19) with an approximate potential energy given by

$$V(R) = \sigma \frac{\hbar^2 M}{m^2 R^2} - \nu \frac{GM^2}{R} + \chi V \left(\frac{3M}{4\pi R^3} \right) \frac{4}{3} \pi R^3, \quad (\text{G31})$$

where χ is a tunable coefficient. For a power-law self-interaction potential, we exactly recover Eq. (G20) with $\chi = \zeta(4\pi/3)^{\gamma-1}$. For an arbitrary self-interaction potential, using Eqs. (G30) and (G31), we get

$$V'(R) = -2\sigma \frac{\hbar^2 M}{m^2 R^3} + \nu \frac{GM^2}{R^2} - \chi P \left(\frac{3M}{4\pi R^3} \right) 4\pi R^2. \quad (\text{G32})$$

The condition of equilibrium $V'(R) = 0$ then yields the mass-radius relation under the form

$$-2\sigma \frac{\hbar^2 M}{m^2 R^3} + \nu \frac{GM^2}{R^2} - \chi P \left(\frac{3M}{4\pi R^3} \right) 4\pi R^2 = 0. \quad (\text{G33})$$

If we work with the variables M and R , it is usually difficult to solve this equation explicitly in the general case. However, if we make the change of variables

$$R = \frac{\pi}{k}, \quad M = \frac{4}{3} \pi \rho R^3, \quad (\text{G34})$$

inspired by Eq. (G3), we get

$$\frac{2\sigma \hbar^2 k^4}{\pi^2 m^2} + 3\chi \frac{P(\rho)}{\rho} k^2 - \frac{4}{3} \pi^3 \nu G \rho = 0. \quad (\text{G35})$$

Remarkably, this equation is similar to the Jeans equation (G1). Therefore, it can be solved easily (this is just a second degree equation for k^2), and the mass-radius relation $M(R)$ can be obtained in parametric form as in Appendix G 1. We get

$$R(\rho) = \frac{\frac{2\sqrt{\sigma}\hbar}{m}}{\left[-3\chi \frac{P(\rho)}{\rho} + \sqrt{9\chi^2 \frac{P(\rho)^2}{\rho^2} + \frac{32\pi}{3} \sigma \nu \frac{G\rho\hbar^2}{m^2}} \right]^{1/2}}, \quad (\text{G36})$$

$$M(\rho) = \frac{4}{3} \pi \rho R(\rho)^3. \quad (\text{G37})$$

This shows in full generality that the Jeans mass-radius relation $M_J(R_J)$ valid in the linear regime of structure formation is formally similar to the mass-radius relation $M(R)$ of DM halos valid in the nonlinear regime of structure formation. Apart from the precise value of the prefactors, we see that the difference with the Jeans study is that the pressure derivative $P'(\rho)$ (equal to c_s^2) is replaced by the ratio $P(\rho)/\rho$. For a polytropic equation of state, the

dependence in the density is the same, i.e., $\rho^{\gamma-1}$, but the prefactor is different.

APPENDIX H: THERMODYNAMICAL IDENTITIES FOR COLD BAROTROPIC GASES

In this appendix, we regroup useful thermodynamical identities valid for cold barotropic gases.

The first principle of thermodynamics can be written under a local form as

$$d\left(\frac{u}{\rho}\right) = -Pd\left(\frac{1}{\rho}\right) + Td\left(\frac{s}{\rho}\right), \quad (\text{H1})$$

where u is the density of internal energy, ρ is the mass density, P is the pressure, T is the temperature, and s is the entropy density. For cold gases ($T = 0$), Eq. (H1) reduces to

$$d\left(\frac{u}{\rho}\right) = -Pd\left(\frac{1}{\rho}\right) = \frac{P}{\rho^2}d\rho. \quad (\text{H2})$$

If we introduce the enthalpy density

$$h = \frac{P + u}{\rho}, \quad (\text{H3})$$

we obtain the relations

$$du = h d\rho \quad \text{and} \quad dh = \frac{dP}{\rho}. \quad (\text{H4})$$

Comparing Eq. (H3) with the Gibbs-Duhem relation for a cold gas ($T = 0$),

$$u = -P + Ts + \frac{\mu}{m}\rho \Rightarrow \frac{\mu}{m} = \frac{P + u}{\rho}, \quad (\text{H5})$$

we see that the enthalpy $h(\mathbf{r})$ coincides with the local chemical potential $\mu(\mathbf{r})$ by unit of mass [$h(\mathbf{r}) = \mu(\mathbf{r})/m$].

1. General barotropic equation of state

For a general barotropic equation of state of the form $P = P(\rho)$, the foregoing relations lead to the identities

$$\left(\frac{u}{\rho}\right)' = \frac{P(\rho)}{\rho^2}, \quad h(\rho) = \frac{P(\rho) + u(\rho)}{\rho}, \quad (\text{H6})$$

$$h(\rho) = u'(\rho), \quad h'(\rho) = \frac{P'(\rho)}{\rho}, \quad (\text{H7})$$

$$P(\rho) = \rho h(\rho) - u(\rho) = \rho u'(\rho) - u(\rho) = \rho^2 \left(\frac{u}{\rho}\right)', \quad (\text{H8})$$

$$P'(\rho) = \rho u''(\rho). \quad (\text{H9})$$

The first principle of thermodynamics for a barotropic gas at $T = 0$ [see Eq. (H2)] provides a general relation between the density of internal energy $u(\rho)$ and the pressure $P(\rho)$. If we know the energy density $u = u(\rho)$, we can obtain the pressure by

$$P = -\frac{d(u/\rho)}{d(1/\rho)} = \rho \frac{du}{d\rho} - u. \quad (\text{H10})$$

Inversely, if we know the equation of state $P = P(\rho)$, we can obtain the energy density by

$$u(\rho) = \rho \int^\rho \frac{P(\rho')}{\rho'^2} d\rho', \quad (\text{H11})$$

which is the solution of the differential equation

$$\rho \frac{du}{d\rho} - u(\rho) = P(\rho). \quad (\text{H12})$$

Remark: Comparing Eqs. (15) and (16) with Eqs. (H8) and (H9), we see that the potential $V(\rho)$ that occurs in the GP equation (1) represents the density of internal energy:

$$u(\rho) = V(\rho). \quad (\text{H13})$$

This justifies the expression of the internal energy in Eqs. (7) and (25).

2. Polytopic equation of state

For a polytopic equation of state of the form $P = K\rho^\gamma$ with $\gamma = 1 + 1/n$, the density of internal energy [see Eq. (H11)] is explicitly given by

$$u = \frac{K}{\gamma - 1} \rho^\gamma = \frac{P}{\gamma - 1} = nP = nK\rho^{1+1/n}, \quad (\text{H14})$$

where we have set the constant of integration to zero. For the standard BEC corresponding to $\gamma = 2$ [see Eq. (3)], we have

$$u = P = \frac{2\pi a_s \hbar^2}{m^3} \rho^2 \Rightarrow U = \frac{2\pi a_s \hbar^2}{m^3} \int \rho^2 d\mathbf{r}. \quad (\text{H15})$$

APPENDIX I: DERIVATION OF THE GPP EQUATIONS IN AN EXPANDING UNIVERSE

In this Appendix, proceeding as in Ref. [114], we derive the GPP equations in an expanding universe starting from their expression in the inertial frame. Alternative derivations starting directly from the KGE equations written with the conformal Newtonian gauge, which is a perturbed form of the Friedmann-Lemaître-Robertson-Walker (FLRW) metric accounting for the expansion of the Universe, and taking the nonrelativistic limit $c \rightarrow +\infty$, can be found in Refs. [133,134,146,156].

1. Homogeneous solution

In the inertial frame, the GPP equations are given by Eqs. (1) and (2). The corresponding hydrodynamic equations, obtained from the Madelung [269] transformation, are given by Eqs. (10)–(13). Let us first show that these equations admit a time-dependent spatially homogeneous solution describing an expanding universe in a Newtonian cosmology.

We consider a spatially homogeneous solution of Eqs. (10)–(13) of the form

$$\rho_b(\mathbf{r}, t) = \rho_b(t), \quad S_b(\mathbf{r}, t) = \frac{1}{2}H(t)mr^2 + S_0(t), \quad (\text{I1})$$

$$\mathbf{u}_b(\mathbf{r}, t) = H(t)\mathbf{r}, \quad \Phi_b(\mathbf{r}, t) = \frac{2}{3}\pi G\rho_b(t)r^2, \quad (\text{I2})$$

where $H = \dot{a}/a$ is the Hubble constant (actually a function of time) and $a(t)$ is the scale factor. The velocity is assumed to be proportional to the distance (Hubble's law), and the gravitational potential has been determined from the Poisson equation $\Delta\Phi_b = 4\pi G\rho_b$. The corresponding wave function is

$$\psi_b(\mathbf{r}, t) = \sqrt{\rho_b(t)}e^{i[\frac{1}{2}H(t)mr^2 + S_0(t)]/\hbar}. \quad (\text{I3})$$

The hydrodynamic equations (10)–(13) then reduce to

$$\frac{d\rho_b}{dt} + 3H\rho_b = 0 \Rightarrow \rho_b \propto a^{-3}, \quad (\text{I4})$$

$$\frac{dS_0}{dt} = -mV'(\rho_b), \quad (\text{I5})$$

$$\dot{H} + H^2 = -\frac{4}{3}\pi G\rho_b \Rightarrow \ddot{a} = -\frac{4}{3}\pi G\rho_b a. \quad (\text{I6})$$

The first equation can be interpreted as the conservation of mass

$$M = \frac{4}{3}\pi\rho_b a^3 \Rightarrow \rho_b = \frac{3M}{4\pi a^3}, \quad (\text{I7})$$

and the third equation as the Newtonian equation of dynamics

$$\ddot{a} = -\frac{GM}{a^2} = -\frac{\frac{4}{3}\pi G\rho_b a^3}{a^2} \quad (\text{I8})$$

for a particle submitted to a gravitational field $-GM/a^2$ created by a mass M . These equations can be justified in a Newtonian cosmology if we view the Universe as a homogeneous sphere of mass M , radius $a(t)$, and density $\rho_b(t)$ evolving under its own gravitation. Equation (18) is then obtained by considering the force experienced by a particle of arbitrary mass m on the surface of this sphere and using Newton's law. The first integral of motion is

$$\frac{1}{2}\left(\frac{da}{dt}\right)^2 - \frac{GM}{a} = E, \quad (\text{I9})$$

implying

$$\left(\frac{da}{dt}\right)^2 = \frac{2GM}{a} + 2E = \frac{8}{3}\pi G\rho_b a^2 + 2E. \quad (\text{I10})$$

We can check that the foregoing equations coincide with the Friedmann equations in the nonrelativistic limit (or for pressureless matter). In the context of general relativity, the term $-2E$ represents the curvature of space κ , where $\kappa = -1, 0, +1$ depending whether the Universe is open, critical, or closed. The theory of inflation and the observations of the CMB favor a flat universe ($\kappa = 0$) so we shall take $E = 0$. In that case, Eq. (I10) reduces to

$$\left(\frac{da}{dt}\right)^2 = \frac{8}{3}\pi G\rho_b a^2 \Rightarrow H^2 = \frac{8}{3}\pi G\rho_b. \quad (\text{I11})$$

Combining Eq. (I11) with Eq. (I4) we obtain the solution

$$a \propto t^{2/3}, \quad H = \frac{\dot{a}}{a} = \frac{2}{3t}, \quad \rho_b = \frac{1}{6\pi G t^2}, \quad (\text{I12})$$

corresponding to the classical pressureless Einstein–de Sitter (EdS) universe (we have assumed a vanishing cosmological constant $\Lambda = 0$). We note that pressure and quantum effects do not change the evolution of the homogeneous background in a nonrelativistic cosmology since they just occur in the form of gradients in Eq. (12) [114].

2. Comoving frame

We now write the GPP equations in the comoving frame. To that purpose, we make the change of variables

$$\mathbf{r} = a(t)\mathbf{x}, \quad \psi(\mathbf{r}, t) = \Psi(\mathbf{x}, t)e^{i\frac{1}{2}mHr^2/\hbar}, \quad (\text{I13})$$

where \mathbf{r} is the proper distance. Equation (I13) is a change of variables from proper locally Minkowski coordinates \mathbf{r} to expanding coordinates \mathbf{x} comoving in the background model [297]. The density is given by $\rho = |\Psi|^2$. Defining the gravitational potential $\phi(\mathbf{x}, t)$ by

$$\Phi(\mathbf{r}, t) = \Phi_b(\mathbf{r}, t) + \phi(\mathbf{x}, t), \quad (\text{I14})$$

we find that the Poisson equation (13) becomes

$$\Delta\phi = 4\pi G a^2(\rho - \rho_b), \quad (\text{I15})$$

where the derivatives are with respect to \mathbf{x} (the same is true for the following equations unless explicitly stated). We see that, in the comoving frame, a sort of neutralizing background appears as in the jellium model of plasma physics. Therefore, the consideration of an expanding Universe allows for spatially homogeneous solutions and avoids the Jeans swindle.

In order to transform the GPP equations (1) and (2) to the comoving frame we first compute

$$\begin{aligned} \left(\frac{\partial \Psi}{\partial t}\right)_{\mathbf{r}} &= \left(\frac{\partial}{\partial t}\right)_{\mathbf{r}} \Psi\left(\frac{\mathbf{r}}{a(t)}, t\right) e^{i\frac{1}{2}mHr^2/\hbar} \\ &= \left(\frac{\partial \Psi}{\partial t} - H\mathbf{x} \cdot \nabla \Psi + \frac{i}{2\hbar} m\dot{H}a^2 x^2 \Psi\right) e^{i\frac{1}{2}mHr^2/\hbar}, \end{aligned} \quad (\text{I16})$$

and

$$\begin{aligned} \Delta_{\mathbf{r}} \Psi &= \left(\frac{1}{a^2} \Delta \Psi + 3\frac{i}{\hbar} mH\Psi + 2\frac{i}{\hbar} mH\mathbf{x} \cdot \nabla \Psi \right. \\ &\quad \left. - \frac{m^2 H^2}{\hbar^2} a^2 x^2 \Psi\right) e^{i\frac{1}{2}mHr^2/\hbar}. \end{aligned} \quad (\text{I17})$$

Substituting the foregoing relations into Eq. (1) we find after simplification [using Eq. (I6)] that

$$i\hbar \frac{\partial \Psi}{\partial t} + \frac{3}{2} i\hbar H\Psi = -\frac{\hbar^2}{2ma^2} \Delta \Psi + m \frac{dV}{d|\Psi|^2} \Psi + m\phi\Psi. \quad (\text{I18})$$

On the other hand, using Eq. (I11), the Poisson equation (I15) can be written as

$$\frac{\Delta \phi}{4\pi G a^2} = |\Psi|^2 - \frac{3H^2}{8\pi G}. \quad (\text{I19})$$

We can similarly transform the hydrodynamic equations (10)–(13) to the comoving frame. The wave function can be written as

$$\Psi(\mathbf{x}, t) = \sqrt{\rho(\mathbf{x}, t)} e^{i\mathcal{S}(\mathbf{x}, t)/\hbar}, \quad (\text{I20})$$

where $\rho(\mathbf{x}, t)$ is the mass density and $\mathcal{S}(\mathbf{x}, t)$ is the action in the comoving frame. Making the Madelung [269] transformation

$$\rho(\mathbf{x}, t) = |\Psi|^2 \quad \text{and} \quad \mathbf{v} = \frac{\nabla \mathcal{S}}{ma}, \quad (\text{I21})$$

where $\mathbf{v}(\mathbf{x}, t)$ is the velocity field in the comoving frame, and comparing Eqs. (8), (I13), and (I20), we get

$$S(\mathbf{r}, t) = \mathcal{S}(\mathbf{x}, t) + \frac{1}{2} mHr^2 \Rightarrow \mathbf{u}(\mathbf{r}, t) = \mathbf{v}(\mathbf{x}, t) + H\mathbf{r}, \quad (\text{I22})$$

where \mathbf{u} is the velocity field in the inertial frame and $H\mathbf{r}$ is the Hubble flow.³⁵ Then, we compute

$$\left(\frac{\partial \rho}{\partial t}\right)_{\mathbf{r}} = \left(\frac{\partial}{\partial t}\right)_{\mathbf{r}} \rho\left(\frac{\mathbf{r}}{a(t)}, t\right) = \frac{\partial \rho}{\partial t} - H\mathbf{x} \cdot \nabla \rho \quad (\text{I23})$$

and

³⁵This result can also be obtained as follows. Taking the derivative with respect to time of the relation $\mathbf{r} = a(t)\mathbf{x}$, we get $d\mathbf{r}/dt = \dot{a}\mathbf{x} + a d\mathbf{x}/dt$. This can be written as $\mathbf{u} = H\mathbf{r} + \mathbf{v}$, with $\mathbf{u} = d\mathbf{r}/dt$ and $\mathbf{v} = a d\mathbf{x}/dt$, where \mathbf{u} is the proper velocity and \mathbf{v} is the peculiar velocity.

$$\nabla_{\mathbf{r}}(\rho \mathbf{u}) = \frac{1}{a} \nabla \cdot (\rho \mathbf{v}) + H\mathbf{x} \cdot \nabla \rho + 3H\rho. \quad (\text{I24})$$

With these relations, the continuity equation (10) becomes

$$\frac{\partial \rho}{\partial t} + 3H\rho + \frac{1}{a} \nabla \cdot (\rho \mathbf{v}) = 0. \quad (\text{I25})$$

Similarly, using

$$\begin{aligned} \left(\frac{\partial \mathbf{u}}{\partial t}\right)_{\mathbf{r}} &= \left(\frac{\partial}{\partial t}\right)_{\mathbf{r}} \mathbf{v}\left(\frac{\mathbf{r}}{a(t)}, t\right) + \dot{H}\mathbf{r} \\ &= \frac{\partial \mathbf{v}}{\partial t} - H(\mathbf{x} \cdot \nabla) \mathbf{v} + \dot{H}a\mathbf{x}, \end{aligned} \quad (\text{I26})$$

and

$$\begin{aligned} (\mathbf{u} \cdot \nabla_{\mathbf{r}}) \mathbf{u} &= [(H\mathbf{r} + \mathbf{v}) \cdot \nabla_{\mathbf{r}}] (H\mathbf{r} + \mathbf{v}) \\ &= H^2 a \mathbf{x} + H(\mathbf{x} \cdot \nabla) \mathbf{v} + H\mathbf{v} + \frac{1}{a} (\mathbf{v} \cdot \nabla) \mathbf{v}, \end{aligned} \quad (\text{I27})$$

the quantum Euler equation (12) becomes

$$\frac{\partial \mathbf{v}}{\partial t} + \frac{1}{a} (\mathbf{v} \cdot \nabla) \mathbf{v} + H\mathbf{v} = -\frac{1}{\rho a} \nabla P - \frac{1}{a} \nabla \phi - \frac{1}{ma} \nabla Q \quad (\text{I28})$$

with the quantum potential

$$Q = -\frac{\hbar^2}{2ma^2} \frac{\Delta \sqrt{\rho}}{\sqrt{\rho}} = -\frac{\hbar^2}{4ma^2} \left[\frac{\Delta \rho}{\rho} - \frac{1}{2} \frac{(\nabla \rho)^2}{\rho^2} \right], \quad (\text{I29})$$

where we have used Eq. (I6) to simplify some terms. These transformations can also be made at the level of the action. Using

$$\begin{aligned} \left(\frac{\partial S}{\partial t}\right)_{\mathbf{r}} &= \left(\frac{\partial}{\partial t}\right)_{\mathbf{r}} S\left(\frac{\mathbf{r}}{a(t)}, t\right) + \frac{1}{2} m\dot{H}r^2 \\ &= \frac{\partial S}{\partial t} - H\mathbf{x} \cdot \nabla S + \frac{1}{2} m\dot{H}r^2 \end{aligned} \quad (\text{I30})$$

and

$$\nabla_{\mathbf{r}} S = \frac{1}{a} \nabla S + mH\mathbf{r}, \quad (\text{I31})$$

the Hamilton-Jacobi equation (11) becomes after simplification

$$\frac{\partial S}{\partial t} + \frac{(\nabla S)^2}{2ma^2} = -Q - m\phi - mV'(\rho). \quad (\text{I32})$$

We can check that the above results return the equations of Refs. [114,133,134,146,156] up to an obvious change of notations.

- [1] WMAP Collaboration, *Astrophys. J. Suppl.* **180**, 225 (2009).
- [2] Planck Collaboration, *Astron. Astrophys.* **571**, A66 (2014).
- [3] Planck Collaboration, *Astron. Astrophys.* **594**, A13 (2016).
- [4] B. Moore, T. Quinn, F. Governato, J. Stadel, and G. Lake, *Mon. Not. R. Astron. Soc.* **310**, 1147 (1999).
- [5] G. Kauffmann, S. D. M. White, and B. Guiderdoni, *Mon. Not. R. Astron. Soc.* **264**, 201 (1993).
- [6] A. Klypin, A. V. Kravtsov, and O. Valenzuela, *Astrophys. J.* **522**, 82 (1999).
- [7] M. Kamionkowski and A. R. Liddle, *Phys. Rev. Lett.* **84**, 4525 (2000).
- [8] M. Boylan-Kolchin, J. S. Bullock, and M. Kaplinghat, *Mon. Not. R. Astron. Soc.* **415**, L40 (2011).
- [9] J. S. Bullock and M. Boylan-Kolchin, *Annu. Rev. Astron. Astrophys.* **55**, 343 (2017).
- [10] D. N. Spergel and P. J. Steinhardt, *Phys. Rev. Lett.* **84**, 3760 (2000).
- [11] P. Bode, J. P. Ostriker, and N. Turok, *Astrophys. J.* **556**, 93 (2001).
- [12] E. Romano-Díaz, I. Shlosman, Y. Hoffman, and C. Heller, *Astrophys. J.* **685**, L105 (2008).
- [13] A. Pontzen and F. Governato, *Nature (London)* **506**, 171 (2014).
- [14] J. Oñorbe *et al.*, *Mon. Not. R. Astron. Soc.* **454**, 2092 (2015).
- [15] D. Marsh, *Phys. Rep.* **643**, 1 (2016).
- [16] M. A. Markov, *Phys. Lett.* **10**, 122 (1964).
- [17] R. Cowsik and J. McClelland, *Phys. Rev. Lett.* **29**, 669 (1972).
- [18] R. Cowsik and J. McClelland, *Astrophys. J.* **180**, 7 (1973).
- [19] S. Tremaine and J. E. Gunn, *Phys. Rev. Lett.* **42**, 407 (1979).
- [20] R. Ruffini, *Lett. Nuovo Cimento* **29**, 161 (1980).
- [21] J. G. Gao and R. Ruffini, *Phys. Lett.* **97B**, 388 (1980).
- [22] J. G. Gao and R. Ruffini, *Acta Astrophysica Sinica* **1**, 19 (1981).
- [23] C.-G. Källman, *Phys. Lett.* **83A**, 179 (1981).
- [24] A. Crollalanza, J. G. Gao, and R. Ruffini, *Lett. Nuovo Cimento* **32**, 411 (1981).
- [25] R. Fabbri, R. T. Jantzen, and R. Ruffini, *Astron. Astrophys.* **114**, 219 (1982).
- [26] J. L. Zhang, W. Y. Chau, K. Lake, and J. Stone, *Astrophys. Space Sci.* **96**, 417 (1983).
- [27] M. R. Baldeschi, G. B. Gelmini, and R. Ruffini, *Phys. Lett.* **122B**, 221 (1983).
- [28] R. Ruffini and L. Stella, *Astron. Astrophys.* **119**, 35 (1983).
- [29] W. Y. Chau, K. Lake, and J. Stone, *Astrophys. J.* **281**, 560 (1984).
- [30] W. Y. Chau and K. Lake, *Phys. Lett.* **134B**, 409 (1984).
- [31] G. Ingrosso and R. Ruffini, *Nuovo Cimento* **101**, 369 (1988).
- [32] J. G. Gao, M. Merafina, and R. Ruffini, *Astron. Astrophys.* **235**, 1 (1990).
- [33] M. Merafina, *Nuovo Cimento* **105**, 985 (1990).
- [34] G. Ingrosso, M. Merafina, R. Ruffini, and F. Strafella, *Astron. Astrophys.* **258**, 223 (1992).
- [35] R. D. Viollier, F. R. Leimgruber, and D. Trautmann, *Phys. Lett. B* **297**, 132 (1992).
- [36] R. D. Viollier, D. Trautmann, and G. B. Tupper, *Phys. Lett. B* **306**, 79 (1993).
- [37] R. D. Viollier, *Prog. Part. Nucl. Phys.* **32**, 51 (1994).
- [38] N. Bilic and R. D. Viollier, *Phys. Lett. B* **408**, 75 (1997).
- [39] D. Tsiklauri and R. D. Viollier, *Astrophys. J.* **501**, 486 (1998).
- [40] N. Bilic, F. Munyaneza, and R. D. Viollier, *Phys. Rev. D* **59**, 024003 (1998).
- [41] P. H. Chavanis and J. Sommeria, *Mon. Not. R. Astron. Soc.* **296**, 569 (1998).
- [42] P. H. Chavanis, *Mon. Not. R. Astron. Soc.* **300**, 981 (1998).
- [43] R. Robert, *Classical Quantum Gravity* **15**, 3827 (1998).
- [44] N. Bilić and R. D. Viollier, *Gen. Relativ. Gravit.* **31**, 1105 (1999).
- [45] N. Bilic and R. D. Viollier, *Eur. Phys. J. C* **11**, 173 (1999).
- [46] F. De Paolis, G. Ingrosso, A. A. Nucita, D. Orlando, S. Capozziello, and G. Iovane, *Astron. Astrophys.* **376**, 853 (2001).
- [47] N. Bilic, F. Munyaneza, G. B. Tupper, and R. D. Viollier, *Prog. Part. Nucl. Phys.* **48**, 291 (2002).
- [48] P. H. Chavanis, *Phys. Rev. E* **65**, 056123 (2002).
- [49] P. H. Chavanis, The self-gravitating Fermi gas, in *Dark Matter in Astro- and Particle Physics*, edited by H. V. Klapdor-Kleingrothaus and R. D. Viollier (Springer, New York, 2002).
- [50] P. H. Chavanis and I. Ispolatov, *Phys. Rev. E* **66**, 036109 (2002).
- [51] N. Bilic, G. B. Tupper, and R. D. Viollier, *Lect. Notes Phys.* **616**, 24 (2003).
- [52] P. H. Chavanis and M. Rieutord, *Astron. Astrophys.* **412**, 1 (2003).
- [53] P. H. Chavanis, *Phys. Rev. E* **69**, 066126 (2004).
- [54] T. Nakajima and M. Morikawa, arXiv:astro-ph/0506623.
- [55] P. H. Chavanis, *Int. J. Mod. Phys. B* **20**, 3113 (2006).
- [56] F. Munyaneza and P. L. Biermann, *Astron. Astrophys.* **458**, L9 (2006).
- [57] G. Narain, J. Schaffner-Bielich, and I. N. Mishustin, *Phys. Rev. D* **74**, 063003 (2006).
- [58] J. Ren, X. Q. Li, and H. Shen, *Commun. Theor. Phys.* **49**, 212 (2008).
- [59] G. Kupa, *Phys. Rev. D* **77**, 023001 (2008).
- [60] C. Destri, H. J. de Vega, and N. G. Sanchez, *New Astron.* **22**, 39 (2013).
- [61] C. Destri, H. J. de Vega, and N. G. Sanchez, *Astropart. Phys.* **46**, 14 (2013).
- [62] H. J. de Vega, P. Salucci, and N. G. Sanchez, *Mon. Not. R. Astron. Soc.* **442**, 2717 (2014).
- [63] C. R. Argüelles and R. Ruffini, *Int. J. Mod. Phys. D* **23**, 1442020 (2014).
- [64] C. R. Argüelles, R. Ruffini, and B. M. O. Fraga, *J. Korean Phys. Soc.* **65**, 809 (2014).
- [65] I. Siutsou, C. R. Argüelles, and R. Ruffini, *Astronomy Reports* **59**, 656 (2015).
- [66] R. Ruffini, C. R. Argüelles, and J. A. Rueda, *Mon. Not. R. Astron. Soc.* **451**, 622 (2015).
- [67] V. Domcke and A. Urbano, *J. Cosmol. Astropart. Phys.* **01** (2015) 002.

- [68] P. H. Chavanis, M. Lemou, and F. Méhats, *Phys. Rev. D* **91**, 063531 (2015).
- [69] P. H. Chavanis, M. Lemou, and F. Méhats, *Phys. Rev. D* **92**, 123527 (2015).
- [70] H. J. de Vega and N. G. Sanchez, *Int. J. Mod. Phys. A* **31**, 1650073 (2016).
- [71] H. J. de Vega and N. G. Sanchez, *Eur. Phys. J. C* **77**, 81 (2017).
- [72] L. Randall, J. Scholtz, and J. Unwin, *Mon. Not. R. Astron. Soc.* **467**, 1515 (2017).
- [73] H. J. de Vega and N. G. Sanchez, [arXiv:1705.05418](https://arxiv.org/abs/1705.05418).
- [74] C. R. Argüelles, A. Krut, J. A. Rueda, and R. Ruffini, *Phys. Dark Universe* **21**, 82 (2018).
- [75] M. R. Baldeschi, G. B. Gelmini, and R. Ruffini, *Phys. Lett.* **122B**, 221 (1983).
- [76] M. Yu. Khlopov, B. A. Malomed, and Ya. B. Zeldovich, *Mon. Not. R. Astron. Soc.* **215**, 575 (1985).
- [77] M. Membrado, A. F. Pacheco, and J. Sanudo, *Phys. Rev. A* **39**, 4207 (1989).
- [78] M. Membrado, J. Abad, A. F. Pacheco, and J. Sañudo, *Phys. Rev. D* **40**, 2736 (1989).
- [79] M. Bianchi, D. Grasso, and R. Ruffini, *Astron. Astrophys.* **231**, 301 (1990).
- [80] S. J. Sin, *Phys. Rev. D* **50**, 3650 (1994).
- [81] S. U. Ji and S. J. Sin, *Phys. Rev. D* **50**, 3655 (1994).
- [82] J. W. Lee and I. Koh, *Phys. Rev. D* **53**, 2236 (1996).
- [83] F. E. Schunck, [arXiv:astro-ph/9802258](https://arxiv.org/abs/astro-ph/9802258).
- [84] T. Matos and F. S. Guzmán, *F. Astron. Nachr.* **320**, 97 (1999).
- [85] V. Sahni and L. Wang, *Phys. Rev. D* **62**, 103517 (2000).
- [86] F. S. Guzmán and T. Matos, *Classical Quantum Gravity* **17**, L9 (2000).
- [87] W. Hu, R. Barkana, and A. Gruzinov, *Phys. Rev. Lett.* **85**, 1158 (2000).
- [88] P. J. E. Peebles, *Astrophys. J.* **534**, L127 (2000).
- [89] J. Goodman, *New Astron.* **5**, 103 (2000).
- [90] T. Matos and L. A. Ureña-López, *Phys. Rev. D* **63**, 063506 (2001).
- [91] A. Arbey, J. Lesgourgues, and P. Salati, *Phys. Rev. D* **64**, 123528 (2001).
- [92] M. P. Silverman and R. L. Mallett, *Classical Quantum Gravity* **18**, L103 (2001).
- [93] M. Alcubierre, F. S. Guzmán, T. Matos, D. Núñez, L. A. Ureña-López, and P. Wiederhold, *Classical Quantum Gravity* **19**, 5017 (2002).
- [94] M. P. Silverman and R. L. Mallett, *Gen. Relativ. Gravit.* **34**, 633 (2002).
- [95] J. Lesgourgues, A. Arbey, and P. Salati, *New Astron. Rev.* **46**, 791 (2002).
- [96] A. Arbey, J. Lesgourgues, and P. Salati, *Phys. Rev. D* **68**, 023511 (2003).
- [97] T. Fukuyama and M. Morikawa, *Prog. Theor. Phys.* **115**, 1047 (2006).
- [98] C. G. Böhrer and T. Harko, *J. Cosmol. Astropart. Phys.* **06** (2007) 025.
- [99] T. Fukuyama, M. Morikawa, and T. Tatekawa, *J. Cosmol. Astropart. Phys.* **06** (2008) 033.
- [100] A. Bernal, T. Matos, and D. Núñez, *Rev. Mex. Astron. Astrofis.* **44**, 149 (2008).
- [101] T. Fukuyama and M. Morikawa, *Phys. Rev. D* **80**, 063520 (2009).
- [102] P. Sikivie and Q. Yang, *Phys. Rev. Lett.* **103**, 111301 (2009).
- [103] T. Matos, A. Vázquez-González, and J. Magaña, *Mon. Not. R. Astron. Soc.* **393**, 1359 (2009).
- [104] J. W. Lee, *Phys. Lett. B* **681**, 118 (2009).
- [105] T. P. Woo and T. Chiueh, *Astrophys. J.* **697**, 850 (2009).
- [106] J. W. Lee and S. Lim, *J. Cosmol. Astropart. Phys.* **01** (2010) 007.
- [107] P. H. Chavanis, *Phys. Rev. D* **84**, 043531 (2011).
- [108] P. H. Chavanis and L. Delfini, *Phys. Rev. D* **84**, 043532 (2011).
- [109] P. H. Chavanis, *Phys. Rev. D* **84**, 063518 (2011).
- [110] F. Briscese, *Phys. Lett. B* **696**, 315 (2011).
- [111] T. Harko, *Mon. Not. R. Astron. Soc.* **413**, 3095 (2011).
- [112] T. Harko, *J. Cosmol. Astropart. Phys.* **05** (2011) 022.
- [113] A. Suárez and T. Matos, *Mon. Not. R. Astron. Soc.* **416**, 87 (2011).
- [114] P. H. Chavanis, *Astron. Astrophys.* **537**, A127 (2012).
- [115] H. Velten and E. Wamba, *Phys. Lett. B* **709**, 1 (2012).
- [116] M. O. C. Pires and J. C. C. de Souza, *J. Cosmol. Astropart. Phys.* **11** (2012) 024.
- [117] C.-G. Park, J.-C. Hwang, and H. Noh, *Phys. Rev. D* **86**, 083535 (2012).
- [118] V. H. Robles and T. Matos, *Mon. Not. R. Astron. Soc.* **422**, 282 (2012).
- [119] T. Rindler-Daller and P. R. Shapiro, *Mon. Not. R. Astron. Soc.* **422**, 135 (2012).
- [120] V. Lora, J. Magaña, A. Bernal, F. J. Sánchez-Salcedo, and E. K. Grebel, *J. Cosmol. Astropart. Phys.* **02** (2012) 011.
- [121] J. Magaña, T. Matos, A. Suárez, and F. J. Sánchez-Salcedo, *J. Cosmol. Astropart. Phys.* **10** (2012) 003.
- [122] G. Manfredi, P. A. Hervieux, and F. Haas, *Classical Quantum Gravity* **30**, 075006 (2013).
- [123] A. X. González-Morales, A. Diez-Tejedor, L. A. Ureña-López, and O. Valenzuela, *Phys. Rev. D* **87**, 021301(R) (2013).
- [124] F. S. Guzmán, F. D. Lora-Clavijo, J. J. González-Avilés, and F. J. Rivera-Paleo, *J. Cosmol. Astropart. Phys.* **09** (2013) 034.
- [125] H. Y. Schive, T. Chiueh, and T. Broadhurst, *Nat. Phys.* **10**, 496 (2014).
- [126] H. Y. Schive, M.-H. Liao, T.-P. Woo, S.-K. Wong, T. Chiueh, T. Broadhurst, and W.-Y. Pauchy Hwang, *Phys. Rev. Lett.* **113**, 261302 (2014).
- [127] B. Li, T. Rindler-Daller, and P. R. Shapiro, *Phys. Rev. D* **89**, 083536 (2014).
- [128] D. Bettoni, M. Colombo, and S. Liberati, *J. Cosmol. Astropart. Phys.* **02** (2014) 004.
- [129] V. Lora and J. Magaña, *J. Cosmol. Astropart. Phys.* **09** (2014) 011.
- [130] P. H. Chavanis, *Eur. Phys. J. Plus* **130**, 181 (2015).
- [131] E. J. M. Madarassy and V. T. Toth, *Phys. Rev. D* **91**, 044041 (2015).
- [132] D. J. E. Marsh, *Phys. Rev. D* **91**, 123520 (2015).
- [133] A. Suárez and P. H. Chavanis, *Phys. Rev. D* **92**, 023510 (2015).
- [134] A. Suárez and P. H. Chavanis, *J. Phys. Conf. Ser.* **654**, 012008 (2015).

- [135] P. H. Chavanis, *Phys. Rev. D* **92**, 103004 (2015).
- [136] J. C. C. de Souza and M. Ujevic, *Gen. Relativ. Gravit.* **47**, 100 (2015).
- [137] R. C. de Freitas and H. Velten, *Eur. Phys. J. C* **75**, 597 (2015).
- [138] J. Alexandre, *Phys. Rev. D* **92**, 123524 (2015).
- [139] K. Schroven, M. List, and C. Lämmerzahl, *Phys. Rev. D* **92**, 124008 (2015).
- [140] D. Marsh and A. R. Pop, *Mon. Not. R. Astron. Soc.* **451**, 2479 (2015).
- [141] J. A. R. Cembranos, A. L. Maroto, and S. J. Núñez Jareño, *J. High Energy Phys.* 03 (2016) 013.
- [142] B. Schwabe, J. Niemeyer, and J. Engels, *Phys. Rev. D* **94**, 043513 (2016).
- [143] J. Fan, *Phys. Dark Universe* **14**, 84 (2016).
- [144] E. Calabrese and D. N. Spergel, *Mon. Not. R. Astron. Soc.* **460**, 4397 (2016).
- [145] P. H. Chavanis, *Phys. Rev. D* **94**, 083007 (2016).
- [146] P. H. Chavanis and T. Matos, *Eur. Phys. J. Plus* **132**, 30 (2017).
- [147] L. Hui, J. Ostriker, S. Tremaine, and E. Witten, *Phys. Rev. D* **95**, 043541 (2017).
- [148] A. Suárez and P. H. Chavanis, *Phys. Rev. D* **95**, 063515 (2017).
- [149] P. H. Chavanis, *Eur. Phys. J. Plus* **132**, 248 (2017).
- [150] B. Li, T. Rindler-Daller, and P. R. Shapiro, *Phys. Rev. D* **96**, 063505 (2017).
- [151] P. Mocz, M. Vogelsberger, V. H. Robles, J. Zavala, M. Boylan-Kolchin, A. Fialkov, and L. Hernquist, *Mon. Not. R. Astron. Soc.* **471**, 4559 (2017).
- [152] J. Zhang, Y. L. Sming Tsai, J. L. Kuo, K. Cheung, and M. C. Chu, *Astrophys. J.* **853**, 51 (2018).
- [153] A. Suárez and P. H. Chavanis, *Phys. Rev. D* **98**, 083529 (2018).
- [154] J. Veltmaat, J. C. Niemeyer, and B. Schwabe, *Phys. Rev. D* **98**, 043509 (2018).
- [155] P. Mocz, L. Lancaster, A. Fialkov, F. Becerra, and P. H. Chavanis, *Phys. Rev. D* **97**, 083519 (2018).
- [156] P. H. Chavanis, *Phys. Rev. D* **98**, 023009 (2018).
- [157] N. Bar, D. Blas, K. Blum, and S. Sibiryakov, *Phys. Rev. D* **98**, 083027 (2018).
- [158] J. A. R. Cembranos, A. L. Maroto, S. J. Núñez Jareño, and H. Villarrubia-Rojo, *J. High Energy Phys.* 08 (2018) 073.
- [159] V. Poulin, T. L. Smith, D. Grin, T. Karwal, and M. Kamionkowski, *Phys. Rev. D* **98**, 083525 (2018).
- [160] F. Edwards, E. Kendall, S. Hotchkiss, and R. Easther, *J. Cosmol. Astropart. Phys.* 10 (2018) 027.
- [161] A. A. Avilez, L. E. Padilla, T. Bernal, and T. Matos, *Mon. Not. R. Astron. Soc.* **477**, 3257 (2018).
- [162] D. G. Levkov, A. G. Panin, and I. I. Tkachev, *Phys. Rev. Lett.* **121**, 151301 (2018).
- [163] P. H. Chavanis, *Eur. Phys. J. Plus* **134**, 352 (2019).
- [164] A. A. Avilez and F. S. Guzman, *Phys. Rev. D* **99**, 043542 (2019).
- [165] X. Li, L. Hui, and G. L. Bryan, *Phys. Rev. D* **99**, 063509 (2019).
- [166] M. Nori, R. Murgia, V. Irsic, M. Baldi, and M. Viel, *Mon. Not. R. Astron. Soc.* **482**, 3227 (2019).
- [167] J. Zhang, H. Liu, and M.-C. Chu, *Front. Astron. Space Sci.* **5**, 48 (2019).
- [168] S. Alexander, J. J. Bramburger, and E. McDonough, *Phys. Lett. B* **797**, 134871 (2019).
- [169] P. H. Chavanis, *Phys. Rev. D* **100**, 083022 (2019).
- [170] B. Bar-Or, J. B. Fouvry, and S. Tremaine, *Astrophys. J.* **871**, 28 (2019).
- [171] N. Bar, K. Blum, T. Lacroix, and P. Panci, *J. Cosmol. Astropart. Phys.* 07 (2019) 045.
- [172] V. Desjacques and A. Nusser, *Mon. Not. R. Astron. Soc.* **488**, 4497 (2019).
- [173] N. Bar, K. Blum, J. Eby, and R. Sato, *Phys. Rev. D* **99**, 103020 (2019).
- [174] P. Brax, P. Valageas, and J. A. R. Cembranos, *Phys. Rev. D* **100**, 023526 (2019).
- [175] M. A. Amin and P. Mocz, *Phys. Rev. D* **100**, 063507 (2019).
- [176] T. Matos, A. Avilez, T. Bernal, and P. H. Chavanis, *Gen. Relativ. Gravit.* **51**, 159 (2019).
- [177] F. S. Guzmán, J. A. González, and I. Alvarez-Ríos, *Rev. Mex. Fis.* **67**, 75 (2021).
- [178] P. Mocz *et al.*, *Phys. Rev. Lett.* **123**, 141301 (2019).
- [179] P. H. Chavanis, *Phys. Rev. D* **100**, 123506 (2019).
- [180] T. Harko, *Eur. Phys. J. C* **79**, 787 (2019).
- [181] P. H. Chavanis, *Phys. Rev. D* **101**, 063532 (2020).
- [182] M. Reig, J. W. F. Valle, and M. Yamada, *J. Cosmol. Astropart. Phys.* 09 (2019) 029.
- [183] E. Y. Davies and P. Mocz, *Mon. Not. R. Astron. Soc.* **492**, 5721 (2020).
- [184] A. Arvanitaki, S. Dimopoulos, M. Galanis, L. Lehner, J. O. Thompson, and K. Van Tilburg, *Phys. Rev. D* **101**, 083014 (2020).
- [185] P. Mocz *et al.*, *Mon. Not. R. Astron. Soc.* **494**, 2027 (2020).
- [186] A. K. Verma, R. Pandit, and M. E. Brachet, [arXiv:1912.10172](https://arxiv.org/abs/1912.10172).
- [187] P. Brax, J. A. R. Cembranos, and P. Valageas, *Phys. Rev. D* **101**, 023521 (2020).
- [188] L. Lancaster, C. Giovanetti, P. Mocz, Y. Kahn, M. Lisanti, and D. N. Spergel, *J. Cosmol. Astropart. Phys.* 01 (2020) 001.
- [189] P. H. Chavanis, *Phys. Rev. D* **102**, 083531 (2020).
- [190] P. H. Chavanis, *Universe* **6**, 226 (2020).
- [191] J. W. Lee, *EPJ Web Conf.* **168**, 06005 (2018).
- [192] A. Suárez, V. H. Robles, and T. Matos, *Astrophys. Space Sci. Proc.* **38**, 107 (2014).
- [193] T. Rindler-Daller and P. R. Shapiro, *Astrophys. Space Sci. Proc.* **38**, 163 (2014).
- [194] P. H. Chavanis, Self-gravitating Bose-Einstein condensates, in *Quantum Aspects of Black Holes*, edited by X. Calmet (Springer, New York, 2015).
- [195] J. C. Niemeyer, *Prog. Part. Nucl. Phys.* **113**, 103787 (2020).
- [196] E. Ferreira, [arXiv:2005.03254](https://arxiv.org/abs/2005.03254).
- [197] J. Barranco and A. Bernal, *Phys. Rev. D* **83**, 043525 (2011).
- [198] J. Eby, P. Suranyi, C. Vaz, and L. C. R. Wijewardhana, *J. High Energy Phys.* 03 (2015) 080.
- [199] A. H. Guth, M. P. Hertzberg, and C. Prescod-Weinstein, *Phys. Rev. D* **92**, 103513 (2015).
- [200] J. Eby, C. Kouvaris, N. G. Nielsen, and L. C. R. Wijewardhana, *J. High Energy Phys.* 02 (2016) 028.

- [201] E. Braaten, A. Mohapatra, and H. Zhang, *Phys. Rev. Lett.* **117**, 121801 (2016).
- [202] E. Braaten, A. Mohapatra, and H. Zhang, *Phys. Rev. D* **94**, 076004 (2016).
- [203] S. Davidson and T. Schwetz, *Phys. Rev. D* **93**, 123509 (2016).
- [204] J. Eby, M. Leembruggen, P. Suranyi, and L. C. R. Wijewardhana, *J. High Energy Phys.* **12** (2016) 066.
- [205] Y. Bai, V. Barger, and J. Berger, *J. High Energy Phys.* **12** (2016) 127.
- [206] J. Eby, P. Suranyi, and L. C. R. Wijewardhana, *Mod. Phys. Lett.* **31**, 1650090 (2016).
- [207] E. Cotner, *Phys. Rev. D* **94**, 063503 (2016).
- [208] J. Eby, M. Leembruggen, J. Leeney, P. Suranyi, and L. C. R. Wijewardhana, *J. High Energy Phys.* **04** (2017) 099.
- [209] J. Eby, M. Leembruggen, P. Suranyi, and L. C. R. Wijewardhana, *J. High Energy Phys.* **06** (2017) 014.
- [210] D. G. Levkov, A. G. Panin, and I. I. Tkachev, *Phys. Rev. Lett.* **118**, 011301 (2017).
- [211] T. Helfer, D. J. E. Marsh, K. Clough, M. Fairbairn, E. A. Lim, and R. Becerril, *J. Cosmol. Astropart. Phys.* **03** (2017) 055.
- [212] F. Kling and A. Rajaraman, *Phys. Rev. D* **97**, 063012 (2018).
- [213] S. Sarkar, C. Vaz, and L. C. R. Wijewardhana, *Phys. Rev. D* **97**, 103022 (2018).
- [214] L. Visinelli, S. Baum, J. Redondo, K. Freese, and F. Wilczek, *Phys. Lett. B* **777**, 64 (2018).
- [215] F. Michel and I. G. Moss, *Phys. Lett. B* **785**, 9 (2018).
- [216] J. Eby, P. Suranyi, and L. C. R. Wijewardhana, *J. Cosmol. Astropart. Phys.* **04** (2018) 038.
- [217] J. Eby, M. Leembruggen, P. Suranyi, and L. C. R. Wijewardhana, *J. Cosmol. Astropart. Phys.* **10** (2018) 058.
- [218] J. Eby, M. Ma, P. Suranyi, and L. C. R. Wijewardhana, *J. High Energy Phys.* **01** (2018) 066.
- [219] M. H. Namjoo, A. H. Guth, and D. I. Kaiser, *Phys. Rev. D* **98**, 016011 (2018).
- [220] J. Eby, M. Leembruggen, L. Street, P. Suranyi, and L. C. R. Wijewardhana, *Phys. Rev. D* **98**, 123013 (2018).
- [221] E. D. Schiappacasse and M. P. Hertzberg, *J. Cosmol. Astropart. Phys.* **01** (2018) 037.
- [222] M. P. Hertzberg and E. D. Schiappacasse, *J. Cosmol. Astropart. Phys.* **08** (2018) 028.
- [223] G. Choi, H. J. He, and E. D. Schiappacasse, *J. Cosmol. Astropart. Phys.* **10** (2019) 043.
- [224] D. Croon, J. Fan, and C. Sun, *J. Cosmol. Astropart. Phys.* **04** (2019) 008.
- [225] J. Eby, K. Mukaida, M. Takimoto, L. C. R. Wijewardhana, and M. Yamada, *Phys. Rev. D* **99**, 123503 (2019).
- [226] J. Eby, M. Leembruggen, L. Street, P. Suranyi, and L. C. R. Wijewardhana, *Phys. Rev. D* **100**, 063002 (2019).
- [227] D. Guerra, C. F. B. Macedo, and P. Pani, *J. Cosmol. Astropart. Phys.* **09** (2019) 061.
- [228] I. I. Tkachev, *Sov. Astron. Lett.* **12**, 305 (1986).
- [229] I. I. Tkachev, *Phys. Lett. B* **261**, 289 (1991).
- [230] E. W. Kolb and I. I. Tkachev, *Phys. Rev. D* **49**, 5040 (1994).
- [231] E. Braaten and H. Zhang, *Rev. Mod. Phys.* **91**, 041002 (2019).
- [232] J. R. Oppenheimer and G. M. Volkoff, *Phys. Rev.* **55**, 374 (1939).
- [233] D. J. Kaup, *Phys. Rev.* **172**, 1331 (1968).
- [234] R. Ruffini and S. Bonazzola, *Phys. Rev.* **187**, 1767 (1969).
- [235] M. Colpi, S. L. Shapiro, and I. Wasserman, *Phys. Rev. Lett.* **57**, 2485 (1986).
- [236] P. H. Chavanis and T. Harko, *Phys. Rev. D* **86**, 064011 (2012).
- [237] J. Jeans, *Phil. Trans. R. Soc. A* **199**, 1 (1902).
- [238] M. Sasaki, *Prog. Theor. Phys.* **70**, 394 (1983).
- [239] M. Sasaki, *Prog. Theor. Phys.* **72**, 1266 (1984).
- [240] V. F. Mukhanov, *JETP Lett.* **41**, 493 (1985).
- [241] B. Ratra and P. J. E. Peebles, *Phys. Rev. D* **37**, 3406 (1988).
- [242] Y. Nambu and M. Sasaki, *Phys. Rev. D* **42**, 3918 (1990).
- [243] B. Ratra, *Phys. Rev. D* **44**, 352 (1991).
- [244] V. F. Mukhanov, H. A. Feldman, and R. H. Brandenberger, *Phys. Rep.* **215**, 203 (1992).
- [245] J. Hwang, *Phys. Lett. B* **401**, 241 (1997).
- [246] P. Jetzer and D. Scialom, *Phys. Rev. D* **55**, 7440 (1997).
- [247] W. Hu, *Astrophys. J.* **506**, 485 (1998).
- [248] P. G. Ferreira and M. Joyce, *Phys. Rev. D* **58**, 023503 (1998).
- [249] C. P. Ma, R. R. Caldwell, P. Bode, and L. Wang, *Astrophys. J.* **521**, L1 (1999).
- [250] F. Perrotta and C. Baccigalupi, *Phys. Rev. D* **59**, 123508 (1999).
- [251] P. Brax, J. Martin, and A. Rizuelo, *Phys. Rev. D* **62**, 103505 (2000).
- [252] T. Matos and L. A. Ureña-López, *Phys. Rev. D* **63**, 063506 (2001).
- [253] J. Hwang and H. Noh, *Phys. Rev. D* **64**, 103509 (2001).
- [254] L. A. Boyle, R. R. Caldwell, and M. Kamionkowski, *Phys. Lett. B* **545**, 17 (2002).
- [255] M. C. Johnson and M. Kamionkowski, *Phys. Rev. D* **78**, 063010 (2008).
- [256] J. Hwang and H. Noh, *Phys. Lett. B* **680**, 1 (2009).
- [257] K. A. Malik and D. Wands, *Phys. Rep.* **475**, 1 (2009).
- [258] A. Arvanitaki, S. Dimopoulos, S. Dubovsky, N. Kaloper, and J. March-Russell, *Phys. Rev. D* **81**, 123530 (2010).
- [259] D. Marsh and P. G. Ferreira, *Phys. Rev. D* **82**, 103528 (2010).
- [260] R. Easther, R. Flauger, and J. B. Gilmore, *J. Cosmol. Astropart. Phys.* **04** (2011) 027.
- [261] J. Magaña, T. Matos, A. Suárez, and F. J. Sánchez-Salcedo, *J. Cosmol. Astropart. Phys.* **10** (2012) 003.
- [262] H. Noh, C. G. Park, and J. Hwang, *Phys. Lett. B* **726**, 559 (2013).
- [263] H. Noh, J. Hwang, and C. G. Park, *J. Cosmol. Astropart. Phys.* **12** (2015) 016.
- [264] R. Hlozek, D. Grin, D. Marsh, and P. G. Ferreira, *Phys. Rev. D* **91**, 103512 (2015).
- [265] M. Alcubierre, A. de la Macorra, A. Diez-Tejedor, and J. M. Torres, *Phys. Rev. D* **92**, 063508 (2015).
- [266] L. A. Ureña-López and A. X. Gonzalez-Morales, *J. Cosmol. Astropart. Phys.* **07** (2016) 048.
- [267] E. Seidel and W. M. Suen, *Phys. Rev. Lett.* **72**, 2516 (1994).
- [268] D. Lynden-Bell, *Mon. Not. R. Astron. Soc.* **136**, 101 (1967).
- [269] E. Madelung, *Z. Phys.* **40**, 322 (1927).

- [270] J. Binney and S. Tremaine, *Galactic Dynamics*, Princeton Series in Astrophysics (Princeton, NJ, 1987).
- [271] H. Poincaré, *Acta Math.* **7**, 259 (1885).
- [272] J. Katz, *Mon. Not. R. Astron. Soc.* **183**, 765 (1978).
- [273] B. K. Harrison, K. S. Thorne, M. Wakano, and J. A. Wheeler, *Gravitation Theory and Gravitational Collapse* (University of Chicago Press, Chicago, 1965).
- [274] S. Chandrasekhar, *An Introduction to the Study of Stellar Structure* (Dover, New York, 1958).
- [275] A. Ritter, *Wiedemann's Ann.* **11**, 332 (1880).
- [276] P. S. Laplace, *Traité de Mécanique Céleste*, Vol. V, livre XI (Paris, Bachelier, 1825).
- [277] P. H. Chavanis, *Eur. Phys. J. B* **85**, 229 (2012).
- [278] S. Weinberg, *Gravitation and Cosmology* (John Wiley & Sons, New York, 1972).
- [279] S. W. Randall, M. Markevitch, D. Clowe, A. H. Gonzalez, and M. Bradac, *Astrophys. J.* **679**, 1173 (2008).
- [280] M. Craciun and T. Harko, *Eur. Phys. J. C* **80**, 735 (2020).
- [281] J. E. Kim and G. Carosi, *Rev. Mod. Phys.* **82**, 557 (2010).
- [282] J. Kormendy, K. C. Freeman, S. D. Ryder, D. J. Pisano, M. A. Walker, and K. C. Freeman, in *Proc. IAU Symp. 220, Dark Matter in Galaxies* (Astron. Soc. Pac., San Francisco, 2004), p. 377.
- [283] M. Spano, M. Marcelin, P. Amram, C. Carignan, B. Epinat, and O. Hernandez, *Mon. Not. R. Astron. Soc.* **383**, 297 (2008).
- [284] F. Donato, G. Gentile, P. Salucci, C. Frigerio Martins, M. I. Wilkinson, G. Gilmore, E. K. Grebel, A. Koch, and R. Wyse, *Mon. Not. R. Astron. Soc.* **397**, 1169 (2009).
- [285] S. Gillessen, F. Eisenhauer, T. K. Fritz, H. Bartko, K. Dodds-Eden, O. Pfuhl, T. Ott, and R. Genzel, *Astrophys. J.* **707**, L114 (2009).
- [286] D. Lynden-Bell and R. Wood, *Mon. Not. R. Astron. Soc.* **138**, 495 (1968).
- [287] S. Balberg, S. L. Shapiro, and S. Inagaki, *Astrophys. J.* **568**, 475 (2002).
- [288] C. J. Hogan and M. J. Rees, *Phys. Lett. B* **205**, 228 (1988).
- [289] E. W. Kolb and I. I. Tkachev, *Astrophys. J.* **460**, L25 (1996).
- [290] L. Nottale, *Scale Relativity and Fractal Space-Time* (Imperial College Press, London, 2011).
- [291] P. H. Chavanis, *Eur. Phys. J. Plus* **132**, 286 (2017).
- [292] E. Nelson, *Phys. Rev.* **150**, 1079 (1966).
- [293] D. D. Holm, J. E. Marsden, T. Ratiu, and A. Weinstein, *Phys. Rep.* **123**, 1 (1985).
- [294] S. Chandrasekhar, *Astrophys. J.* **139**, 664 (1964).
- [295] P. H. Chavanis, *Astron. Astrophys.* **451**, 109 (2006).
- [296] A. S. Eddington, *Mon. Not. R. Astron. Soc.* **79**, 2 (1918).
- [297] P. J. E. Peebles, *The Large-Scale Structure of the Universe* (Princeton University Press, Princeton, NJ, 1980).